

**Synthetic Stratagem, Characterization and Potential
Applications of Main group/Heteronuclear Transition
Metal Complexes derived from N, O containing Ligands**



by

Mehwish Mehmood

Department of Chemistry
Quaid-i-Azam University
Islamabad

2022

**Synthetic Stratagem, Characterization and Potential
Applications of Main group/Heteronuclear Transition
Metal Complexes derived from N, O containing Ligands**



A dissertation submitted to the Department of Chemistry,
Quaid-i-Azam University, Islamabad, in partial fulfillment
of the requirements for the degree of

Doctor of Philosophy
in
Inorganic/Analytical Chemistry

by

Mehwish Mehmood

Department of Chemistry
Quaid-i-Azam University
Islamabad

2022



بِسْمِ اللَّهِ الرَّحْمَنِ الرَّحِيمِ

In the name of Allah, the most gracious, the most merciful





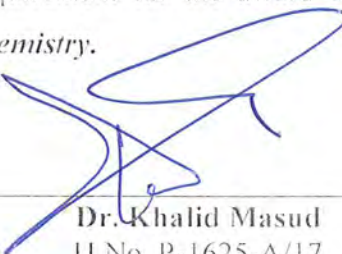
Dedication

*I dedicate this thesis to my
"WORLD'S BEST PARENTS"
for raising me to believe that
anything was possible*

DECLARATION

This is to certify that this dissertation entitled "*Synthesis Stratagem, Characterization and Potential Applications of Main Group/Heteronuclear Transition Metal Complexes Derived from N,O Containing Ligands*" submitted by *Ms. Mehwish Mehmood*, is accepted in its present form by the Department of Chemistry, Quaid-i-Azam University, Islamabad, Pakistan, as satisfying the partial requirement for the award of degree of *Doctor of Philosophy in Analytical/Inorganic Chemistry*.

External Examiner (I):



Dr. Khalid Masud
H.No. P-1625-A/17
Near Government College
Asghar Mall Road, Rawalpindi

External Examiner (II):



Dr. Shafqat Nadeem
General Manager Technical PQAS-12,
DDG (PS&PP) NDC
P.O Box 2216
Islamabad

Supervisor :



Prof. Dr. Imtiaz-ud-Din
Department of Chemistry
Quaid-i-Azam University
Islamabad.

Head of Section:



Prof. Dr. Mrs. Zareen Akhter
Department of Chemistry
Quaid-i-Azam University
Islamabad.

Chairman:



Prof. Dr. Aamer Saeed Bhatti
Department of Chemistry
Quaid-i-Azam University
Islamabad.


AUTHOR'S DECLARATION

I, Ms. Mehwish Mehmood hereby state that my Ph.D. thesis titled "Synthesis Stratagem, Characterization and Potential Applications of Main Group/Heteronuclear Transition Metal Complexes Derived from N,O Containing Ligands" is my own work and has not been submitted previously by me for taking any degree from this University (Quaid-i-Azam University Islamabad) or anywhere else in the country/world.

At anytime if my statement is found to be incorrect even after my Graduation the University has the right to withdraw my Ph.D. degree.

Name of student: Ms. Mehwish Mehmood

Signature



Dated: _____


PLAGIARISM UNDERTAKING

I solemnly declare that, the research work presented in the thesis titled "Synthesis Stratagem, Characterization and Potential Applications of Main Group/Heteronuclear Transition Metal Complexes Derived from N,O Containing Ligands" is solely my research work with no significant contribution from any other person. Small contribution/help wherever taken has been duly acknowledged and that complete thesis has been written by me.

I understand the zero tolerance policy of the HEC and Quaid-i-Azam University Islamabad towards plagiarism. Therefore, I as an Author of the above titled thesis declare that no portion of my thesis has been plagiarized and any material used as reference is properly referred/cited.

I undertake that if I am found guilty of any formal plagiarism in the above titled thesis even after award of Ph.D. degree, the university reserves the rights to withdraw/revoke my Ph.D. degree and that HEC and the University has the right to publish my name on the HEC/University website on which names of students are placed who submitted plagiarized thesis.

Student/Author Signature: _____



Name: Ms. Mehwish Mehmood

Table of Contents

Acknowledgements	v
List of Tables	vi
List of Figures	vii
List of Abbreviations	ix
Abstract	xi
CHAPTER-1	1-42
INTRODUCTION	1
1. Bismuth complexes.....	2
1.1. Bismuth(III) derivatives	2
1.1.1. Derivatives containing Bi-O linkage.....	3
1.1.2. Derivatives containing Bi-S linkage	7
1.1.3. Derivatives containing Bi-N linkage.....	10
1.2. Bismuth(V) derivatives.....	11
1.2.1. Derivatives containing Bi-O linkage.....	11
1.2.2. Derivatives containing Bi-S linkage	13
1.3. Heterometallic transition metal complexes	15
1.4. Schiff bases and their significance in synthetic chemistry	16
1.4.1. Synthetic approaches to Schiff bases	17
1.4.2. Synthetic approaches to heterometallic complexes.....	19
1.5. Characterization techniques.....	26
1.5.1. FT-IR spectroscopy	26

1.5.2.	NMR spectroscopy	28
1.5.3.	X-ray crystallography	30
1.5.3.1.	Crystal structure for organobismuth derivatives.....	30
1.5.3.2.	Crystal structure for dinuclear Zn/Nd complex.....	32
1.5.3.3.	Crystal structure for trinuclear Zn/Nd/Zn complex.....	33
1.6.	Applications.....	34
1.6.1.	Biological applications of bismuth complexes.....	34
1.6.1.1.	Gastrointestinal activity	34
1.6.1.2.	Antileishmanial activity.....	36
1.6.2.	Biological studies of heteronuclear complexes.....	36
1.6.3.	Non-biological applications of bismuth complexes	37
1.6.4.	Non-biological studies of heteronuclear complexes	37
1.6.4.1.	Magnetic properties.....	38
1.6.4.2.	Photoluminescence properties	40
1.7.	Aims and objectives.....	40
1.8.	Plan of work.....	41
CHAPTER-2.....	43-66	
EXPERIMENTAL	43	
2.1.	Materials	43
2.2.	Instrumentation.....	43
2.3.	Synthesis.....	44
2.3.1.	Preparation of bismuth derivatives.....	44
2.3.2.	Bi-compartmental Schiff base ligands	55

2.3.3.	Heterodi-/trinuclear 3d/4f complexes.....	56
2.4.	Applications.....	63
2.4.1.	Antibacterial activity.....	63
2.4.2.	Antifungal activity.....	63
2.4.3.	Alpha amylase inhibition assay.....	64
2.4.4.	Protein kinase inhibition assay.....	64
2.4.5.	Brine shrimp lethality assay (Cytotoxicity)	64
2.4.6.	Computational studies.....	65
2.5.	Photoluminescence studies.....	65
2.6.	Magnetic studies.....	66
CHAPTER-3.....-67-100	
RESULTS AND DISCUSSION67	
3.1.	Chemistry.....	67
3.2.	FT-IR spectroscopic data.....	67
3.3.	NMR spectroscopic data.....	69
3.4.	X-rays crystallographic data.....	69
3.4.1.	Bis(2-methylbenzoato)triphenylbismuth(V) (7).....	70
3.4.2.	Bis(2-napthoato)tris(p-tolyl)bismuth(V) (17).....	71
3.4.3.	Bis(4-chlorobenzoato)tris(p-tolyl)bismuth(V) (18).....	73
3.4.4.	Bis(2-methylbenzoato)tris(p-tolyl)bismuth(V) (19).....	74
3.4.5.	[ZnNd(L ₁)(NO ₃) ₃ H ₂ O] (27).....	75
3.4.6.	[Zn ₂ Dy(L ₄) ₂ (NO ₃) ₃ H ₂ O].CH ₃ CN.H ₂ O (45).....	77
3.5.	Biological applications	80

3.5.1.	Antimicrobial activity	80
3.5.2.	Alpha amylase inhibition assay	83
3.5.3.	Protein kinase inhibition assay	85
3.5.4.	Brine shrimp lethality assay	87
3.5.5.	Computational studies	89
3.5.5.1.	<i>H. pylori</i> Urease.....	89
3.5.5.2.	Tyrosine kinase.....	92
3.5.5.3.	Human pancreatic alpha amylase	93
3.6.	Structure -to-activity relationship (SAR)	95
3.7.	Non-biological applications.....	96
3.7.1.	Photoluminescence data	96
3.7.2.	Magnetic susceptibility data.....	98
References.....	101-132
Conclusions.....	133
Future Plan.....	134
List of Publications.....	135
Appendix.....	136-145

Acknowledgement

All praises be to **Almighty Allah**, who is the most gracious, the most compassionate and the most kind. He has bestowed human with intelligence, wisdom and guided them through His **Holy Prophet Muhammad**, who is the source of knowledge and guidance for the entire humankind.

I am highly thankful to my research supervisor, **Prof. Dr. Imtiaz-ud-Din**, for his guidance, encouragement and valuable discussions and for providing all the requisite research facilities. His guidance helped me in the obscurity and escorted me to the light of success. I would always be obliged to him.

I am grateful to the respected, **Prof. Dr. Aamer Saeed**, Chairperson, Department of Chemistry, Quaid-i-Azam University, Islamabad, for providing all the necessary space and instruments for current studies on time. I am also indebted to **Prof. Dr. Zareen Akhter**, head of inorganic/analytical section. I am much obliged to **Prof. Dr. Nawaz Tahir**, Department of Physics, University of Sargodha, for arranging single crystal XRD data for certain compounds, which provided edge to my research work.

I would like to extend my gratitude to my research fellows: **Ms. Anham Zafar**, **Ms. Sumaira Abbas**, **Ms. Sadia Batool** and **Ms. Haseeba Sadaf** for the conversations we shared, both creative and hilarious.

My love goes to my **parents, husband, siblings, daughter (Zoha Jahanzaib)** and all my close family relatives who provided me their unconditional love and encouraged me, prayed for my success and backed me morally, financially and spiritually for the completion of this project. Last but not least, I am thankful to staff for their technical support and to all those who assisted and guided me in the completion of this work.

MEHWISH MEHMOOD

List of Tables

Table #	Title	Page #
Table 1.1	Comparative study of magnetic susceptibility at various temperatures with respect to nuclearity	39
Table 3.1	Selected bond lengths (Å) and bond angles (°) for (7)	71
Table 3.2	Selected bond lengths (Å) and bond angles (°) for (17)	72
Table 3.3	Selected bond lengths (Å) and bond angles (°) for (18)	74
Table 3.4	Selected bond lengths (Å) and bond angles (°) for (19)	75
Table 3.5	Selected bond lengths (Å) and bond angles (°) for (27)	77
Table 3.6	Selected hydrogen bond parameters for (27)	77
Table 3.7	Selected bond lengths (Å) and bond angles (°) for (45)	79
Table 3.8	Selected hydrogen bond parameters for (45)	80
Table 3.9	Antibacterial activity data for (1-25)	81
Table 3.10	Antifungal activity data for (1-25)	82
Table 3.11	Alpha amylase inhibition data for (1-25)	84
Table 3.12	Protein kinase inhibition data for (1-25)	86
Table 3.13	Brine shrimp lethality data for (1-25)	88
Table 3.14	GOLD fitness score against various enzymes* for selected compounds	90
Table 3.15	Photoluminescence parameters for the selected compounds	97
Table 3.16	A comparative study of magnetic susceptibility data for some selected compounds ^(a,b)	100
Table A1	Crystallographic data and refinement details for (7, 17)	136
Table A2	Crystallographic data and refinement details for (18, 19)	137
Table A3	Crystallographic data and refinement details for (27, 45)	138

List of Figures

Figure #	Title	Page #
Figure 1.1	Coordination geometries around Bi center	3
Figure 1.2	Chemical structure for tetradentate [N ₂ O ₂] salen type Schiff bases	16
Figure 1.3	Variation in the binding modes of bismuth(V) carboxylates	27
Figure 1.4	¹ H NMR spectrum of [Bi(C ₆ H ₅) ₃ (O ₂ CC ₆ H ₃ -2-OH-5-Cl) ₂] in CDCl ₃ at 25 °C at t = 0 h and t = 6 months	29
Figure 1.5	Crystal structure for [Bi(O ₂ CC ₆ H ₄ -o-OCH ₃) ₂ (C ₆ H ₅) ₃]	31
Figure 1.6	Crystal structure for [Bi(O ₂ CC ₆ H ₄ -2-NH-(C ₆ H ₃ -2-CH ₃ -3-Cl)) ₂ (C ₆ H ₅) ₃]	31
Figure 1.7	Crystal structure for [Bi(o-Tol) ₃ (dif) ₂]	32
Figure 1.8	Crystal structure for [ZnNdL(OAc)(NO ₃) ₂ (DMF)]	33
Figure 1.9	Crystal structure for [Zn ₂ L ₂ (OAc) ₂ Nd] ⁺¹	34
Figure 1.10	Urease-The ultimate therapeutic target for <i>H. pylori</i>	35
Figure 1.11	Design of luminescent Ln(III)-based single molecular magnets	38
Figure 3.1	ORTEP diagram for (7)	71
Figure 3.2	ORTEP diagram for (17)	72
Figure 3.3	ORTEP diagram for (18)	72
Figure 3.4	ORTEP diagram for (19)	74
Figure 3.5	ORTEP diagram for (27)	76
Figure 3.6	ORTEP diagram for (45)	79
Figure 3.7	Bar graph showing antibacterial activity for (1-25)	83
Figure 3.8	Bar graph showing antifungal activity for (1-25)	83
Figure 3.9	Bar graph showing antidiabetic activity for (1-25)	85
Figure 3.10	Bar graph showing protein kinase inhibition activity for (1-25)	87
Figure 3.11	Bar graph showing brine shrimp lethality assay for (1-25)	89

Figure 3.12	Preferred binding mode for (20) in the active site of <i>H. pylori</i> urease	91
Figure 3.13	The 2-D depiction of docked ‘lead’ compound within the binding pocket of urease protein through DS Visualizer	91
Figure 3.14	Preferred binding mode for (5) in the active site of receptor tyrosine kinase	92
Figure 3.15	The 2-D representation of docked ‘lead complex’ within the binding pocket of tyrosine kinase protein through DS Visualizer	93
Figure 3.16	Preferred binding modes for (7) in active sites of human pancreatic alpha amylase	94
Figure 3.17	The 2-D presentation for (7) showing interactions within the binding pocket of alpha amylase protein through DS Visualizer	94
Figure 3.18	UV-vis spectra for L4, ZnL4, 43 and 45	97
Figure 3.19	Steady state photoluminescence spectra for L4, ZnL4, 43 and 45 [in methanol (2×10^{-5} M)]	98
Figure 3.20	Time resolved photoluminescence spectra for L4, ZnL4, 43 and 45 [in methanol (2×10^{-5} M)]	98
Figure 3.21	FT-IR spectrum for (8)	139
Figure 3.22	^1H NMR spectrum for (8)	140
Figure 3.23	^{13}C NMR spectrum for (8)	141
Figure 3.24	^1H NMR spectrum for (20)	142
Figure 3.25	^{13}C NMR spectrum for (20)	143
Figure 3.26	FT-IR spectrum for (L4)	144
Figure 3.27	FT-IR spectrum for (30)	145

List of Abbreviations

ATCC	American type culture collection
bipy	Bipyridine
BSLA	Brine shrimp lethality assay
CBS	Bismuth subcitrate
CFSE	Crystal field stabilization energy
CFU	Colony forming unit
DMSO	Dimethyl sulphoxide
EGFR	Epidermal growth factor receptor
FCBP	Fungal culture bank of Pakistan
FT-IR	Fourier transform infrared
GOLD	Genetic optimization for ligand docking
MIC	Minimum inhibitory concentration
NIR	Near infrared
NMR	Nuclear magnetic resonance
NSAIDs	Non-steroidal anti-inflammatory drug
ORTEP	Oak Ridge thermal-ellipsoid plot program
OLED	Organic light emitting diode
PDB	Protein data bank
phen	Phenanthroline
ppm	Parts per million
ROP	Ring opening polymerization
SAR	Structure-to-activity relationship
SHAB	Soft and hard acid base
SMM	Single molecular magnet
SSPL	Steady-state photoluminescence
TCSPT	Time-correlated single-photon counting technique
THF	Tetrahydrofuran

TMS	Tetramethyl silane
TRPL	Time-resolved photoluminescence
XRD	X-ray diffraction

DRSML QAU

Abstract

This dissertation comprises two parts; the first deals with the synthesis of heteroleptic triorganobismuth(V) carboxylate whereas the second pertains to the preparation of heterodi- and trinuclear 3d/4f complexes derived from bi-compartmental ligands.

A series of heteroleptic triorganobismuth(V) carboxylates (**1-25**) of general formula $\text{Ar}_3\text{Bi}(\text{COOR})_2$; where Ar = C_6H_5 (**1-12**), $p\text{-CH}_3\text{C}_6\text{H}_4$ (**13-25**) was synthesized by stoichiometric reaction between the precursor, Ar_3BiBr_2 , and the respective carboxylic acid in dry toluene. The synthesized compounds were characterized by FT-IR, NMR spectroscopy and single crystal X-ray technique to get unequivocal evidence for their structural motifs. The XRD data for (**7, 17 & 18**) depict the existence of five-coordinated bismuth center having distorted trigonal bipyramidal molecular geometry, whereas (**19**) described weakly hexacoordinated bismuth including a unique bidentate interaction of one of the carboxylate ligands, assuming a distorted octahedral molecular geometry. The molecular docking studies demonstrate that compounds (**5, 7 & 20**) give significant GOLD (Genetic optimization for ligand docking) fitness scores of 60.09, 56.30 and 62.65 against epidermal growth factor receptor tyrosine kinase, *H. pylori* urease and human pancreatic alpha amylase, respectively. The antibacterial activity profile looks good with MIC value range from 50 to 6.25 $\mu\text{g}/\text{mL}$ against various bacterial and fungal strains and the values are comparable to the reference drug(s). The compounds (**2 & 14**) display significant % alpha amylase inhibition of around 62.3%, whereas (**7**) exhibits 30 mm bald zone of inhibition for alpha amylase and protein kinase inhibition studies, thus, proving their worth as moderate enzyme inhibitors.

The second part of the dissertation involves the formation of transition metal complexes. The heterodi- and trinuclear complexes of general formula $[(\text{M}_1)_n(\text{H}_2\text{O})(\text{L})_n\text{M}_2(\text{NO}_3)_n]$ (**26-45**) were synthesized by reacting bi-compartmental ligands with the specific 3d metal (Zn) and various 4f metals (La, Nd, Sm, Gd and Dy).

Four hexadentate and tetradentate Schiff base ligands (**L1-L4**) were prepared by the condensation of 2-hydroxy-3-methoxybenzaldehyde and 2-hydroxybenzaldehyde with ethylenediamine, o-phenylenediamine and propane 1, 2-diamine in 2:1 mole ratio. The characterization of these complexes were carried out by using elemental analysis, FT-IR, multinuclear NMR spectroscopy and single crystal XRD analysis. The X-ray structures for (**27** & **45**) have also been obtained which completely describe the coordination behavior around each metal center and the respective geometric shape of the synthesized heteronuclear compound. In dinuclear complex (**27**), Zn(II) and Nd(III) are coordinated through N, O and O, O sites, respectively. The Zn(II) center is pentacoordinated having distorted square pyramidal geometry, whereas Nd(III) is decacoordinated, while in trinuclear complex (**45**), Dy(III) is octacoordinated. The results of photoluminescence properties (PL) show that the synthesized 3d/4f heteronuclear complexes correspond to strong and characteristic luminescence properties with emissive lifetimes in the nanosecond range, due to the effective intramolecular energy transfer. The present research approach relates a favorable methodology to build up proficient 3d/4f luminescence as well as magnetic properties and may serve as photoluminescent single molecular magnets.

CHAPTER-1

INTRODUCTION

Bismuth compounds have been used in medicine for the treatment of various infections including skin and gastrointestinal ailments for the last many years [1]. The use of metal-incorporated drugs can be traced back to primordial times due to their varied and rich history [2]. The word bismuth itself is derived from German language which is “Wismuth” that means white mass and relatively rare metal, having least abundance of about 0.008 ppm in the Earth’s crust among pnicogens which is twice as abundant as gold [3-5]. It was found primarily as bismuth sulfide (bismuthinite) and bismuth oxide (bismite) ores which are byproducts produced during mining of tin, copper and lead [6, 7]. ^{209}Bi is naturally occurring isotope which is considered to be stable heavy element with half-life of 1.9×10^9 years. In contrast to natural monoisotopic form, bismuth also exists in radioactive isotopic form as ^{212}Bi and ^{213}Bi with theoretical half-life of 60.6 and 45.6 minutes, respectively. These radioisotopes play vital role in radiopharmaceutics as radiometal [8]. Despite its heavy-metal nature, it is considered to be non-toxic, non-carcinogenic and harmless for environment, due to which it qualifies a status of green element [9, 10]. Due to their less toxicity (even less than that of table salt, NaCl) bismuth salts are being used in medicines and cosmetic, however, poisoning may occur due to overuse [11-13].

There are a variety of fields where bismuth (III/V) derivatives can extensively be employed like biocidal applications such as gastrointestinal [11, 14-16], antitumor/antiproliferative [17-19], antimicrobial [20, 21], anticancer [22-24] antileishmanial agent [25, 26]. Bismuth compounds have long been applied in medicines by physicians due to their lowest solubilities, hence exploiting their least toxicity and highest activity. The first account for intake of bismuth compound is trailed by Odier who treated dyspepsia in 1786 [27]. During 19th century various compounds including subgallate, subcarbonate, subsalicylate, subnitrate and subcitrate tartrate, were utilized to cure hypertension, skin infections, gastrointestinal ailments and syphilis [9]. Later in 20th

century, two most commonly taken medicines were synthesized and used worldwide as bismuth subcitrate (CBS, De-NoI[®]) and bismuth subsalicylate (BSS, Pepto-Bismole[®]) to cure peptic ulcers and diarrhea respectively [28, 29]. Recently, the bioeffectiveness of newly synthesized bismuth derivatives have been attributed to their bactericidal and bacteriostatic action against *Helicobacter pylori* [30].

1. Bismuth Complexes

The oxidation states of bismuth range from three to ten, but the most common oxidation states are +3 and +5. Bismuth(III) is predominantly more stable than Bi(V) due to an inert pair effect [27].

1.1. Bismuth(III) Derivatives

Bismuth(III) compounds have gained enormous interest due to their vital applications in materials, medicines, catalysts and organic chemistry. Because of the Lewis acidity of Bi⁺³ center, additional intra- and intermolecular forces of attraction are developed that lead to the construction of extended coordination compounds with coordination number three to ten. For instance, [Bi(NO₃)₃.5H₂O] bismuth nitrate pentahydrate displays a coordination number ten around the bismuth(III) moiety with four water molecules and three bidentate NO₃⁻¹ ligands [31]. According to Pearson's SHAB concept, Bi⁺³ is a borderline metal which shows high affinity towards O-, N- and S- containing multidentate ligands [32]. In this respect, following binding possibilities arise as appeared in the literature.

- 1) Bi(III)-Amide derivatives
- 2) Bi(III)-Carboxylate derivatives
- 3) Bi(III)-Dithiocarbamate derivatives
- 4) Bi(III)-Thiocarboxylate derivatives
- 5) Bi(III)-Thiolates and thioxoketonate derivatives
- 6) Bi(III)-Semicarbazone and thiosemicarbazone derivatives
- 7) Bi(III)-Hydrazones derivatives

1.1.1. Derivatives containing Bi-O linkage

The Bi-O linkage has been extensively studied in literature among various functionalities owing to its versatile utilities in biological domain. The chemical diversity in these types of complexes arises when modification in Bi-C bond is performed that brought a variety of structural motifs. The reaction of triorganobismuth precursor with a variety of carboxylic acids is discussed in the literature owing to its capability to form series of compounds ranging from simple coordination compounds to complex molecular cages and polymers. Loss of one or two phenyl/tolyl moieties may be eliminated under specific conditions. The diarylation of one or two phenyl/tolyl moieties will yield diverse molecular geometries as depicted in Fig. 1.1.

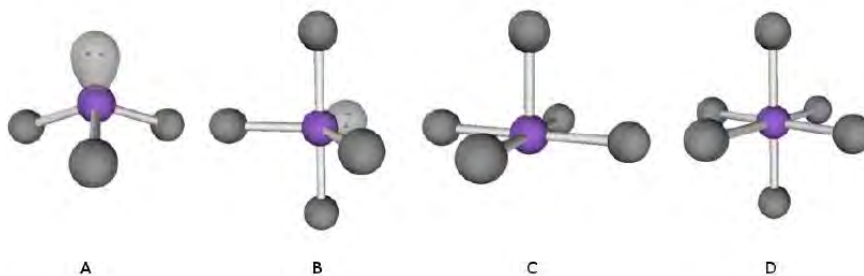
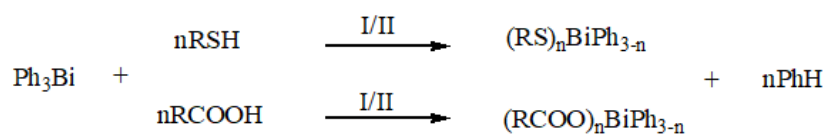


Figure 1.1: Coordination geometries around Bi center (A) trigonal pyramidal, (B) trigonal bipyramidal, (C) square pyramidal and (D) octahedral

All the compounds of type RBiX_2 , R_2BiX and R_3Bi (where R is aliphatic and X is halogen group), are highly unstable and inflammable in nature that causes decomposition of most of them. Hence, major attempts were focused to synthesize triaryl bismuth derivatives, whereas traces of trialkyl bismuthines were also focused. The most suitable method adopted for the preparation of triaryl bismuth compounds was first described by Pietsch and Pfeiffer and then by Challenger using bismuth halides and the Grignard reagent. A trivial change was made to isolate the product in its pure form and extraction was executed applying chloroform and carbon tetrachloride [33].

Andrews *et al.* used thermally-induced solvent free synthesis that involved ball milling Ph_3Bi with series of carboxylic acids and thiols such as salicylic acid, 2-

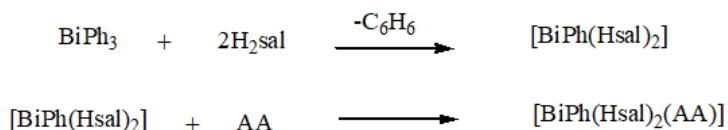
ethoxybenzoic acid, 2-marceptooxazole, 2-marceptobenzothiazole and 1-marceptopropanol in varying ratios of 1:3, 1:2 and 1:1. However, this technique was ruled out as it gave powdered product with almost 40% yield, which mainly includes mixture of fully substituted bismuth product. Later, they attempted an experiment involving premixed crystalline Ph_3Bi and substituted carboxylic acids/thiols. The heating of mixture at about 110-130°C (without inert atmosphere) brought about to the visible release of benzene from the reaction mixture resulting in the formation of crystalline product as shown in Scheme 1.1 [34].



I-Ball milling; time=1-12 hrs., **II**-Heating; time=1-12 hrs., Temp=110-130°C

Scheme 1.1

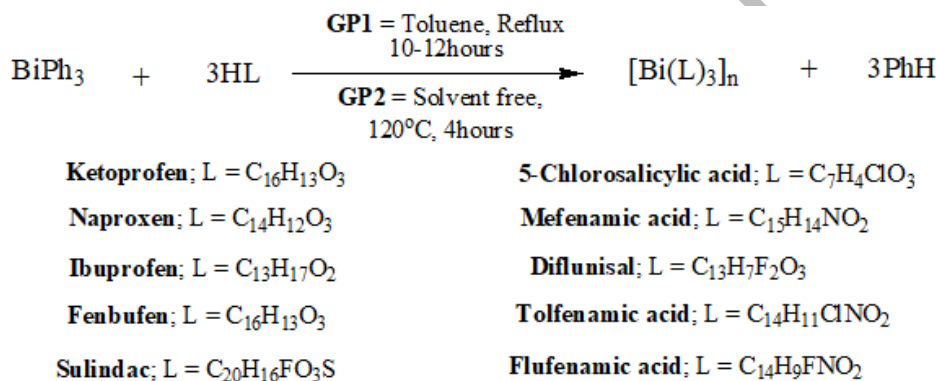
In continuation to the above work Stavila prepared $[\text{Bi}(\text{sal})_3]$ by refluxing salicylic acid and BiPh_3 via acidolysis, besides incorporating 1,10-phenanthroline and 2,2'-bipyridine to yield $[\text{Bi}(\text{sal})(\text{Hsal})(\text{phen})]$ and $[\text{Bi}(\text{bipy})(\text{Hsal})_3]$, respectively as major products, however, $[\text{BiPh}(\text{phen})(\text{Hsal})_2]$ and $[\text{BiPh}(\text{bipy})(\text{Hsal})_2]$ were also obtained. So, in order to obtain the targeted compounds, first step was effected in boiling acetone while second step was marked by the addition of heterocyclic amines as depicted in Scheme 1.2 [35].



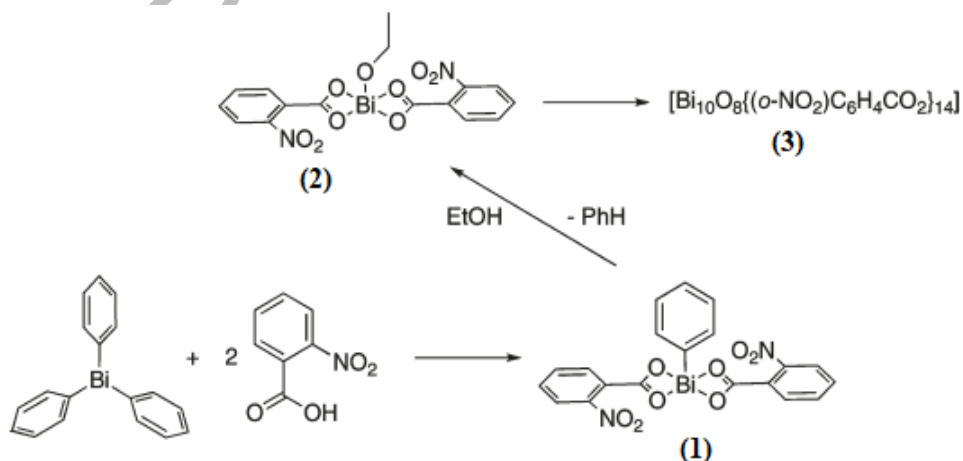
Where, **AA** = bipy, phen **H₂sal** = 4-methyl-2-hydroxybenzoic acid, 2-hydroxybenzoic acid

Scheme 1.2

Andrews *et al.* demonstrated solvent-mediated and solvent-free methods for the synthesis of trisubstituted homoleptic bismuth(III) derivatives by incorporating commercially available non-steroidal anti-inflammatory drugs and products were isolated in good yield [36]. The reaction conditions for both the methods are mentioned in Scheme 1.3. In another approach, Andrews [37] proposed that refluxing triaryl bismuth(III) and o-nitrobenzoic acid in dry ethanol yield monoaryl substituted bismuth derivative (1) which upon alcoholysis replaced its phenyl group with ethoxy group of the solvent and produced (2). This varying degree of substitution around Bi nuclei ultimately formed Bi oxo cluster $[\text{Bi}_{10}\text{O}_8\text{L}_{14}(\text{EtOH})(\text{H}_2\text{O})_z]_\infty$ (Scheme 1.4).

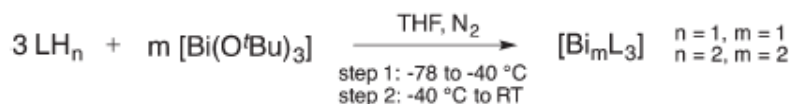


Scheme 1.3



Scheme 1.4

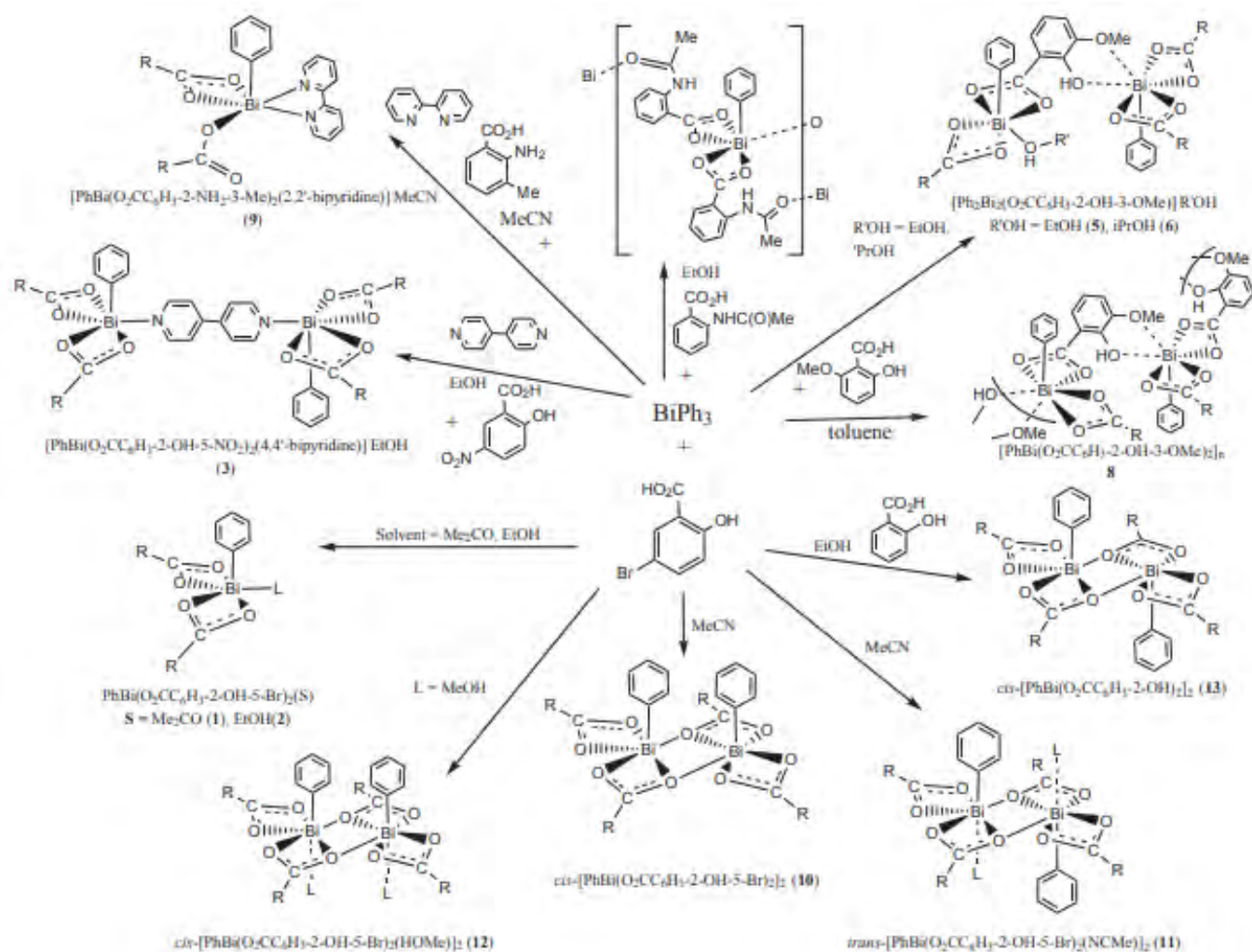
Busse *et al.* [38] synthesized Bi(III) complexes from α -amino acids, based on four different routes employing BiPh₃ under solvent-mediated (SM) and solvent-free (SF) metathesis reactions using Ag(I) salts of amino acids and bismuth salt of tertiary butyl, i.e., [Bi(O^tBu)₃]. All these approaches were considered unsuccessful with BiPh₃ due to the formation of zwitterion of α -amino acids while facile decomposition of Ag(I) led to the formation of black precipitates. As such, these stratagems were not viable whereas best results were achieved when [Bi(O^tBu)₃] was added at controlled temperature of about -78°C and the temperature was raised to -40°C, subsequently slowly allowing it to evaporate at room temperature to achieve the targeted products. In this way, four monoprotic [BiL₃] and three polyprotic [Bi₂L₃] α -amino acids derivatives of Bi(III) were obtained as shown in Scheme 1.5.



Scheme 1.5

Andrews *et al.* [39] characterized two complexes which were proved to be tetrameric [PhBi(2-(C₃H₄N)CO₂)₂]₄ and polymeric [Bi(o-MeOC₆H₄CO₂)₃]_∞, having five membered ring that involved pyridyl moiety (rather than carboxylate which is less stable) and tridentate unsymmetrical bridging carboxylate groups, respectively. Later on, Anjaneyulu *et al.* [40, 41] synthesized various coordination monomers and polymers using diverse pyridine carboxylates by means of aqueous-mediated reaction which were environmentally benign like Bi(O₂CC₉H₆NH)(O₃N)(O₂CC₉H₆N)₂·2H₂O and [Bi(2-OOC-C₅NH₄)₃]_n. Anjaneyulu and coworkers [42] also prepared oligomers by reacting triphenyl bismuth(III) with 3-hydroxypicolinic acid in 1:3 employing ethanol as a solvent at room temperature that led to the target product as [BiPh(2-O₂C-3-(OH)(2-O₂C-3-(OH)C₅H₃N)₂C₅H₃NH)]. Kumar *et al.* [43] made an extensive effort to elaborate the reaction stratagem for thirteen Bi(III) complexes derived from BiPh₃ and ArCOOH in

mole ratio 1:2 that caused to the formation of various monoaryl complexes $[\text{PhBi}(\text{O}_2\text{CR})_2]$ in various organic solvents. The reaction conditions are mentioned in Scheme 1.6.

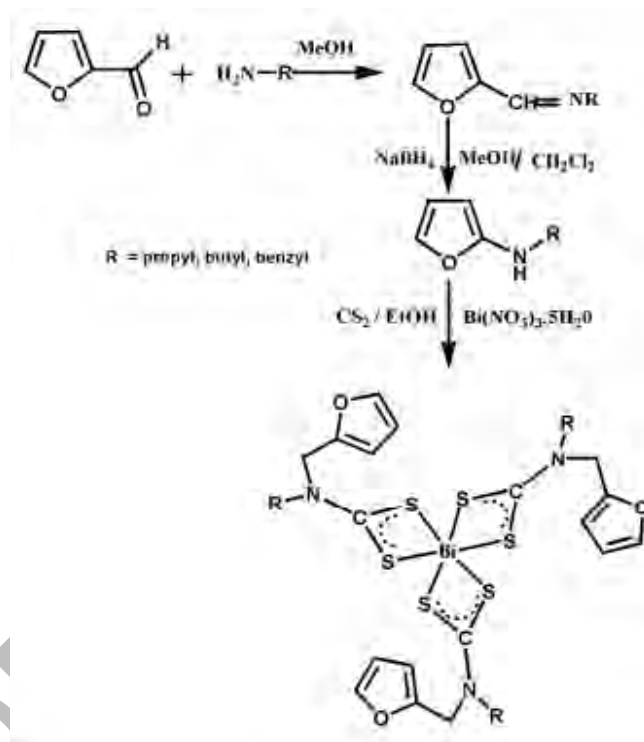


Scheme 1.6

1.1.2. Derivatives containing Bi-S linkage

Bismuth compounds having Bi-S linkage mainly include dithiocarbamates, thiocarboxylates, thiolates and β -thioxoketonates as ligating moieties due to their less labile nature and extra thermodynamic stability in comparison to carboxylate counterparts, which in turn, enhance their hydrolytic stability, reproducibility, purity, and biological applications [44]. Sivasekar *et al.* [45] synthesized series of Bi(III) complexes having dithiocarbamate moiety incorporating acidified $\text{Bi}(\text{NO}_3)_3$ solution into the ethanolic

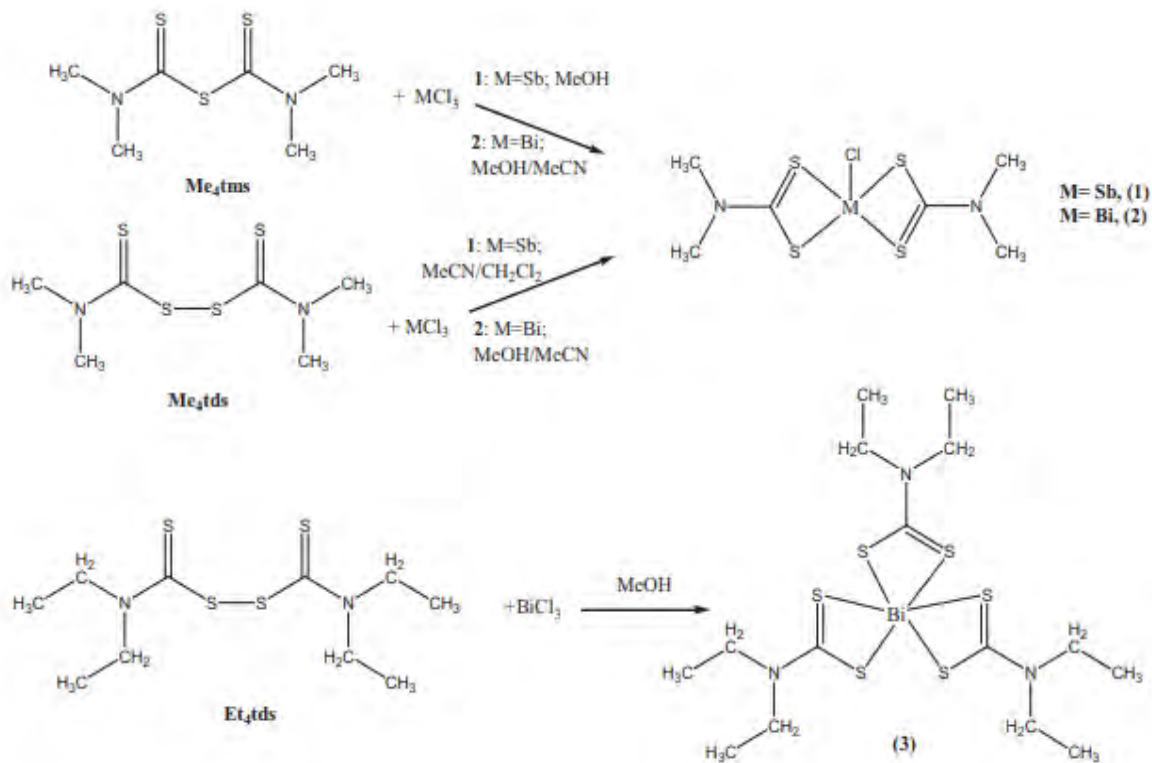
solution of dithiocarbamate which was prepared *in-situ* to achieve target complexes such as; $\text{Bi}(\text{chedtc})_3$, $[\text{Bi}(\text{chmdtc})_3]$ and $[\text{Bi}(\text{dchdtc})_3]$ where, chedtc = cyclohexylethylthiocarbamate, dchdtc = dicyclohexylthiocarbamate), chmdtc = cyclohexylmethylthiocarbamate. Further to this work, Tamilvanan and his coworkers employed comparable scheme in order to synthesize Bi(III) complexes of dithiocarbamate derived from furfural group utilizing $\text{Bi}(\text{NO}_3)_3$ as a metal source as presented in scheme 1.7 [46].



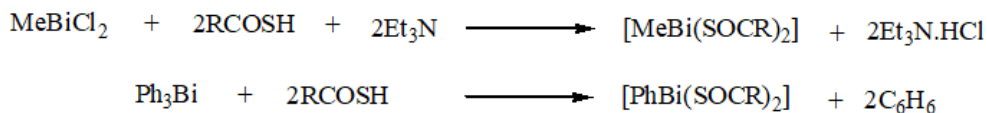
Scheme 1.7

In another study, Ozturk and coworkers synthesized bismuth and antimony complexes having Bi-S direct linkage using dithiocarbamates obtained by degradation of thiuram such as; $[\text{BiCl}(\text{Me}_2\text{dtc})_2]_n$, $[\text{SbCl}(\text{Me}_2\text{dtc})_2]_n$ and $[\text{Bi}(\text{Et}_2\text{dtc})_3]_2$ (where, Me_2dtc = dimethyldithiocarbamate and Et_2dtc = diethyldithiocarbamate) as given in scheme 1.8. In the first approach, tetramethylthiuram monosulfide was reacted with BiCl_3 in 1:1 metal to ligand ratio in dichloromethane/acetonitrile solvent system to achieve the polymorph, while in the second strategy, bismuth complex was isolated by reacting methanolic solution

of tetraethyl thiuram disulfide in 1:1 as shown in Scheme 1.8. In this scheme, C-S or S-S bonds were clipped and, in this way, thiocarboxamide and dithiocarbamate coordinated with Bi(III) ion to get the targeted complex [47].



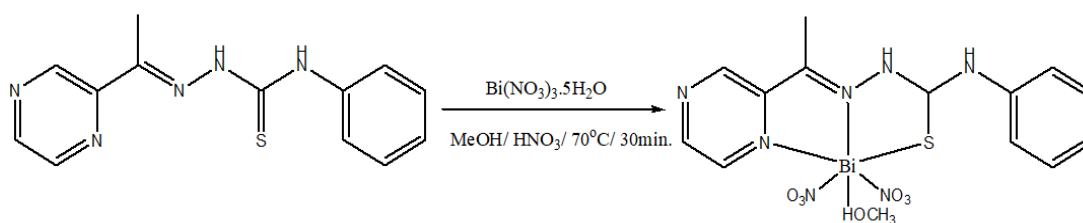
Chaudhari et al. [48] developed a facile route for the synthesis of monoaryl bismuth(III) thiocarboxylates by treating methyl and phenyl bismuth dichloride with substituted thiocarboxylic acid in the presence of triethylamine to achieve $[\text{MeBi}(\text{SOCR})_2]$ and $[\text{PhBi}(\text{SOCR})_2]$ as mentioned in Scheme 1.9.



Where R = Me and Ph

Scheme 1.9

Li *et al.* [50] developed Bi(III)-N and Bi(III)-S linkage in one complex using thiosemicarbazone moieties. They synthesized 2-acetylpyrazine N(4)-phenylthiosemicarbazone as a potential ligand and refluxed it with $\text{Bi}(\text{NO}_3)_3 \cdot 5\text{H}_2\text{O}$ in dry methanol to yield target product as demonstrated in Scheme 1.11. Similarly, Ferrera [51] and Ferraz *et al.* [52] brought further bismuth and antimony complexes employing 2,6 diacetylpyridine bis(benzoylhydrazone) and 2-benzoylpyridine-derived hydrazones, respectively.



Scheme 1.11

1.2. Bismuth(V) Derivatives

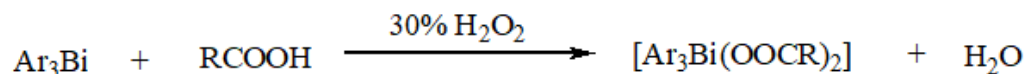
Bi^{+5} is less stable than Bi^{+3} owing to inert pair effect [27]. The inert pair effect increases down the group in pnictogens which is responsible for the penetration of s-orbital (closer to the nucleus) and leaves three electrons in p-orbitals available for bonding with the ligating moieties. For this reason, a few Bi(V) complexes are not with in the literature as compared to Bi(III), making Bi^{+5} even more unique. Some of these reports are discussed here.

1.2.1. Derivatives containing Bi-O linkage

Ong *et al.* [53, 54] did remarkable work regarding the formation of triaryl substituted benzoates of bismuth(V) complexes and synthesized eleven triphenyl and twenty nine ortho-, meta- and para-substituted derivatives by oxidative addition reaction utilizing Ar_3Bi , benzoic acid and 30% hydrogen peroxide in 1:2:1 molar ratio (Scheme 1.12). Ong and coworkers also compared this synthetic route with salt metathesis reaction incorporating Et_3N as a base and found out that in the former case yeild was affected to some extent. Kumar *et al.* [55] followed the Ong startegy in order to develop five

coordinated $[\text{Ph}_3\text{Bi}(\text{OOCR})_2]$ complexes having distorted pentagonal bipyramidal molecular geometry but this research group employed 2-propanol as solvent and results were comparable with the as the previous reports manifested.

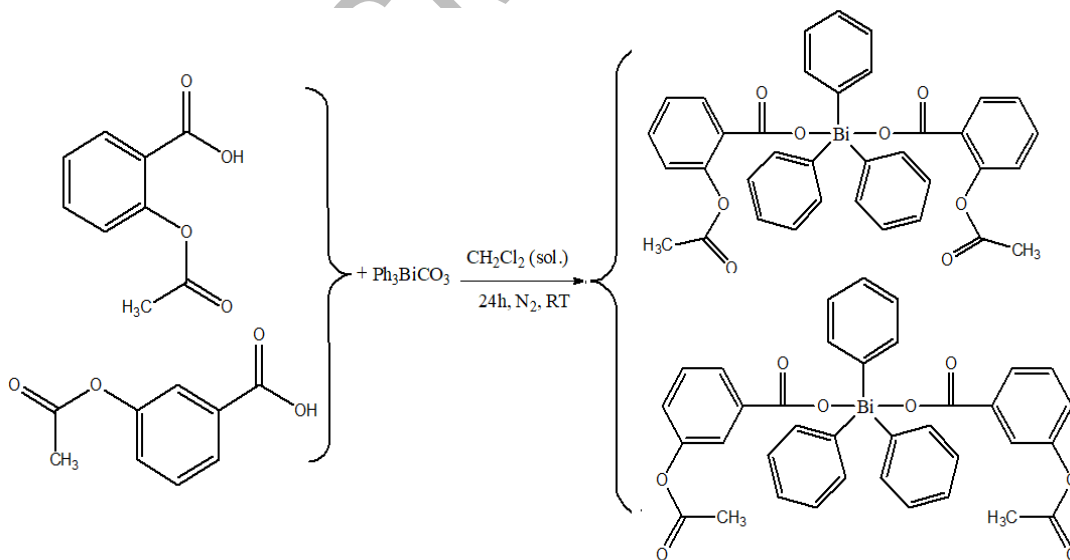
Sharutin *et al.* [56-58] worked on the same strategy and synthesized triphenylbismuth bis(2,3,4,5,6-pentachlorobenzoate) from Ph_3Bi and pentachlorobenzoic acid in the presence of 37% hydrogen peroxide solution and found comparable results.



Ar = Phenyl, Tollyl (ortho-, meta-, para-)

Scheme 1.12

Islam *et al.* [25] synthesized two novel organobismuth(V) complexes derived from substituted acetylbenzoic acid and triphenylbismuth(V) carbonate and compared these bismuth derivatives with antimonials. The schematic representation for this complexation is given in Scheme 1.13.



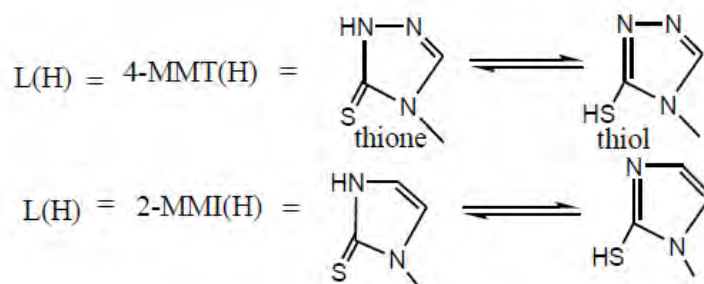
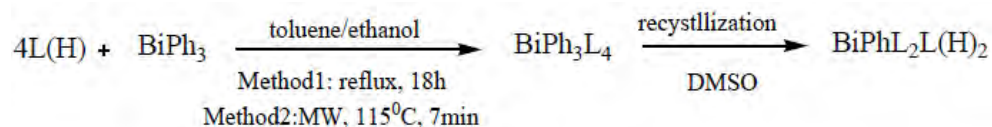
Scheme 1.13

Cui [24] and coworkers synthesized three novel organobismuth(V) complexes $\text{Ph}_3\text{Bi}(\text{OOC}\text{C}_4\text{H}_3\text{S})_2$, $\text{Ph}_3\text{Bi}(\text{OOC}\text{C}_6\text{H}_4\text{CF}_3)_2$ and $\text{Ph}_3\text{Bi}(\text{OOC}\text{C}_6\text{H}_3\text{F}_2)_2$ by stirring substituted-benzoic acids and sodium methoxide in methanol to prepare sodium salt then stirred along with triphenylbismuth to obtain the clear product allowing it to evaporate to achieve crystals. Later Zhang [59] and coworkers continued with the same scheme synthesizing fluoro-substituted benzoates of Bi(V) using sodium methoxide and studying their photodegradation properties in detail.

1.2.2. Derivatives containing Bi-S linkage

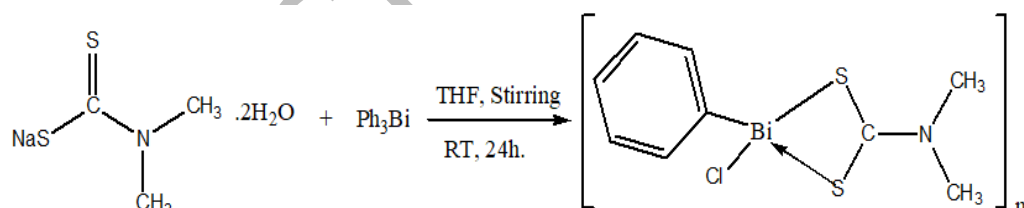
Bismuth is considered to be a typical heavy metal that is generally capable of forming thermodynamically stable and less labile Bi-S bond in comparison to Bi-O bond [8]. Thus, bismuth thiolates and dithiocarbamates are stable species that make them a successful candidate for medicine and biology [60, 61].

For exploiting the unusual biological potential of bismuth thiolates, Luqman and coworkers developed a route to synthesize monoaryl bismuth(V) derivatives of thiolates i.e., 2-mercapto-1-methylimidazole and 4-methyl-4H-1,2,4-triazole-3-thiol. The synthesis involved microwave irradiation (MWI) of BiPh_3 with preceding thiolates in ethanol/toluene solvent or by refluxing this mixture as contained in Scheme 1.14. This study revealed that thiol form was converted into more stable thiolate form upon deprotonation that give rise to the development of Bi-S bond which was in nature and thermodynamically more stable in nature resulting in the formation of $[\text{BiPh}(2\text{-MMIH})_2(2\text{-MMI})_2]$ and $[\text{BiPh}(4\text{-MTTH})_2(4\text{-MTT})_2]$ as rare homometallic complexes [62].



Scheme 1.14

Cui *et al.* [63] produced a Bi(V) coordination polymer, i.e., $[PhBiClS_2CN(CH_3)_2]_n$ by stirring sodium dimethyldithiocarbamate dihydrate in methanol and triphenylbismuth(III) dissolved in THF for 24h at 25°C (Scheme 1.15). Single crystal XRD study revealed 1D spiral chain structure bridged through chlorine atom that linked two Bi ions and appeared as a double helical structure.



Scheme 1.15

1.3. Heterometallic transition metal complexes

Here introductory remarks about the bi-compartmental Schiff base ligands and their respective transition metal complexes along with their literature reviews are being presented. Bi-compartmental hexadentate and tetradentate Schiff base ligands have been synthesized by condensation reaction to develop 3d/4f heteronuclear complexes for the last few decades [64, 65]. This is due to the fact that the inner core of these ligands are equipped with 'N' and 'O' chelating sites responsible for the incorporation of 3d ion (with ionic radii 0.60-0.75 Å), while the outer coordination site contains four oxygens providing enough space to incorporate large 4f ions (with ionic radii 0.85-1.06 Å) [66]. In order to develop discrete magnetic and optical devices, heteronuclear lanthanide metal complexes have gained massive interest owing to their potential applications as contrasting agents in magnetic resonance imaging [67-69], as a luminescent probe in bioimaging and biosensing [64, 70, 71], in light conversion devices [72, 73] and catalytic applications in various fields [74]. The photoluminescence studies of Ln(III) complexes such as those of Er, Pr, Nd and Yb etc. display efficient photophysical properties because these ions reveal long emission/luminescent life-times, ligand-induced large Stokes shift, narrow emission lines, luminescence sensitization and high quantum yields [75]. They are also employed in various potential applications like, optical telecommunication [76], organic light emitting diodes (OLED) [77], fluoro-immunoassay and imaging [78, 79]. However, the absorption coefficient of lanthanides is considerably low which makes these complexes weak absorber, due to parity/Laporte forbidden f-f transition. In order to surmount this difficulty the researchers manipulated well-designed ligands (chromophores) and d-block metal complexes for sensitization of lanthanide ions that provided necessary antenna effect [80]. Keeping this in view, three effective strategies have been adopted to improve the photoluminescence (PL) of the synthesized compounds, i.e. extended conjugation on the flanking phenyl ring, exploitation of rigid spacers and functional bridges like -OH and various anion groups [75]. Considering the magnetic properties of lanthanides and their compounds, the Ln⁺³ ion is expected to possess large magnetic anisotropy and sufficient magnetic moment for achieving luminescent single molecular magnet (SMM) with long lifetime emission spectra and high energy barrier for the reversal of magnetization [81, 82].

1.4. Schiff bases and their significance in synthetic chemistry

Schiff base synthesis is one of the oldest known reaction in chemistry materialized by the condensation reaction of substituted aldehyde and amine [83-86]. Salen type of bi-compartmental Schiff base ligands which drew attention owing to their multidentate nature, are usually obtained by condensation of 2 mole of salicylaldehyde and o-vanillin with 1 mole of 1,2-diamine [87-89]. Salen ligands are like other well-known tetradentate ligands, e.g., porphyrin, based on the formation of two coordinate covalent and two covalent bonds with a variety of metal ions leaving two axial positions open for additional ligands [90-92]. However, bi-compartmental Schiff bases, unlike porphyrin ligands are inexpensive, easy to synthesize, of reasonable stability, loaded with rich photophysical and biocidal application [89]. The metal complexes of such type of ligands also attracted attention in a variety of fields like catalysis [84, 85, 87, 89], optical materials [83, 86, 93], supramolecular materials [94-97], chemical probes [98-100], DNA cleavage [101, 102] and cell imaging [103, 104].

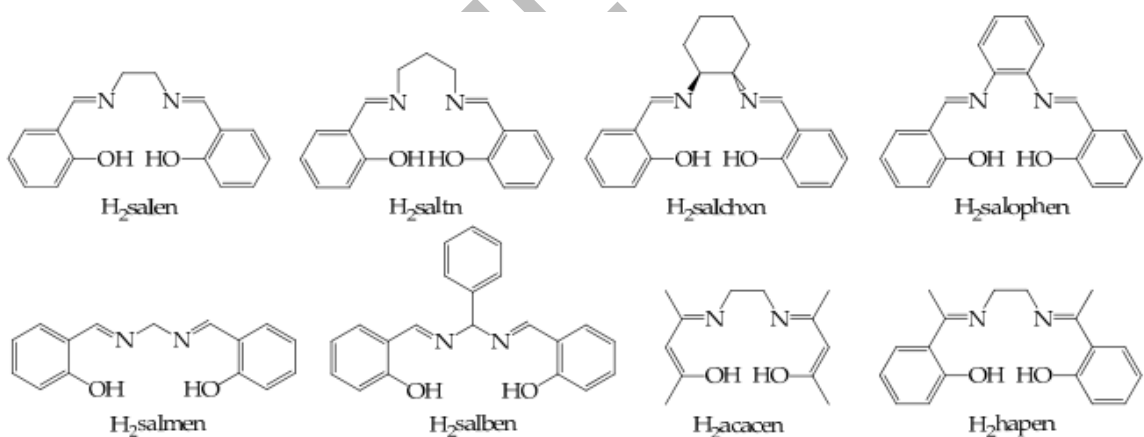


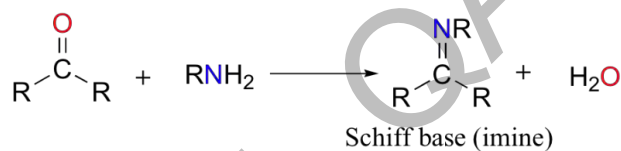
Figure 1.2 Chemical structure for tetradentate [N₂O₂] salen type Schiff bases

Recently, bi-compartmental Schiff bases, their Al(III) [105-107], B(III) [108-110], Pt(II) [111-113] and Zn(II) [114-117] derivatives have displayed good quantum yield (Φ) with good stability, facilitating these compounds to be used as OLEDs. Moreover, salen ligands have pi-conjugated tetradentate and hexadentate chelating system which firmly interacts with metal ions and ligands, thus, they can be utilized as an optical probe for

several metal ions, like Mg(II) [118], Zn(II) [114-117], Cu(II) [100, 119], Al(III) [120], La(III) [121] and Pt(II) [122].

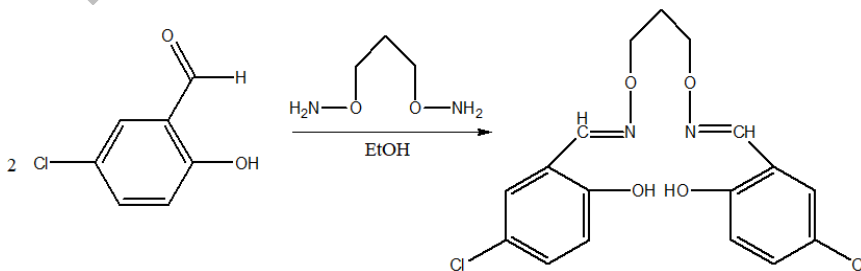
1.4.1. Synthetic approaches to Schiff bases

Schiff base ligands are prepared using conventional and microwave assisted methods that leads to the varieties in molecular architecture. The general synthetic strategy is given in Scheme 1.16, where reaction proceeds through acid-catalyzed nucleophilic route followed by the reflux for about 2-3 hours. In the same way, bi-compartmental Schiff base ligands are synthesized that may affect to both symmetrical and unsymmetrical type of azomethine Schiff bases as the case may be. Some of these synthetic stratagems are depicted in the following scheme:



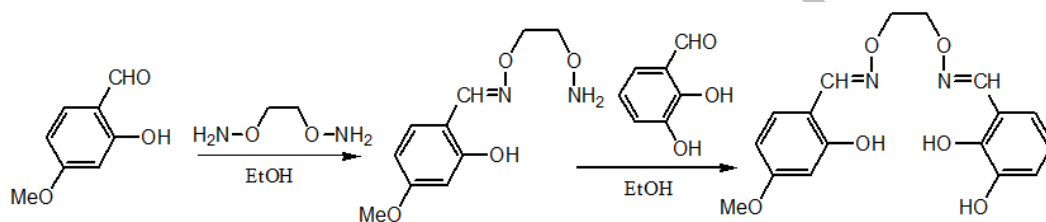
Scheme 1.16

Li *et al.* synthesized one trinuclear Co(II) and one mononuclear Ni(II) complex using symmetrical salamo type of bi-compartmental ligand; the salamo ligand 4,4'-dichloro-2,2' -[(propane-1,3-diyldioxy)bis(nitrilomethylidyne)]diphenol was synthesized by refluxing two equivalent of 5-chlorosalicylaldehyde and one equivalent of diamine in ethanol (Scheme 1.17) [123, 124].



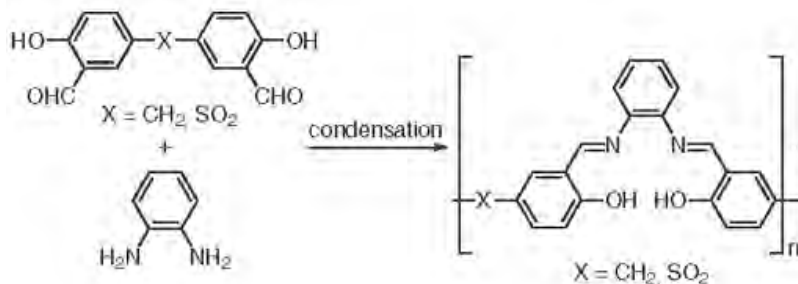
Scheme 1.17

Owing to the fact that salen and salamo-type bi-compartmental ligands have tremendous chelating and luminescent properties, they are widely used in coordination chemistry and organometallics. Moreover, drastic alteration in characteristic features, advanced ideal structural modifications and novel properties can be induced by synthesizing asymmetric configurations. Peng *et al.* synthesized salamo-based asymmetrical ligand by first preparing its counterpart as 2-[O-(1-ethoxyamide)]oxime-5-methoxyphenol as depicted in Scheme 1.3. To the same ethanolic solution, 2,3-dihydroxybenzaldehyde was added and, upon constant stirring for 6 hours, required asymmetric bi-compartmental salamo ligand resulted as shown in Scheme 1.18 [125].



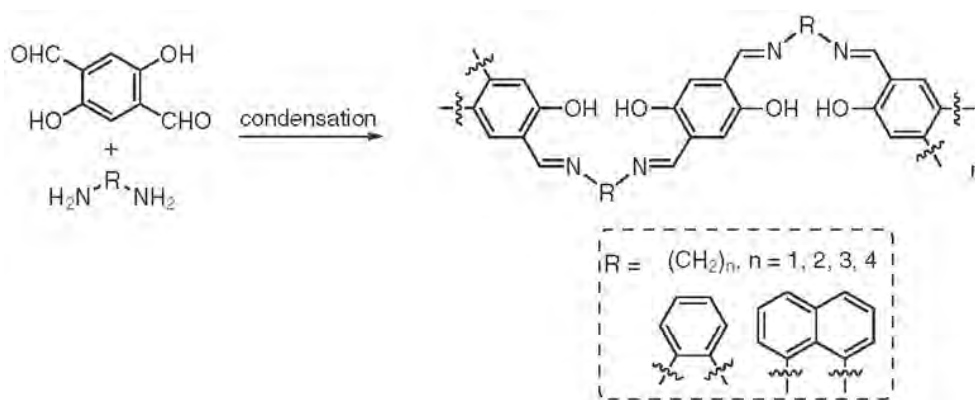
Scheme 1.18

Marvel *et al.* prepared first polysalphen derivatives by condensation reaction between ortho-phenylene diamine with sulfone and methylene-bridged salicylaldehyde in late 1950s (Scheme 1.19) [126, 127]. They also successfully obtained metal containing salphen polymeric derivatives in a large variety by treating them with free metal [Cd(II), Ni(II), Cu(II), Zn(II) and Co(II)] salts. According to elemental analysis, these polymers had a chain length of about 45 monomeric units. Furthermore, sulphone and methylene linkages caused to the enhancement of thermal stability in such type of metal derivatives.



Scheme 1.19

Manecke *et al.* also presented the same approach based upon 2,5-dihydroxyterephthalaldehyde in the early 1970s. This approach mainly focused on varying different diamine rather than altering the aldehyde for condensation that ultimately prompted 1D polymeric backbone capable of incorporating a variety of free metal ions as well (Scheme 1.20). They tabled the conductivity data of the synthesized target compounds and found out that the metal-incorporated polymers were five times more conductive than free ligands [128-130].

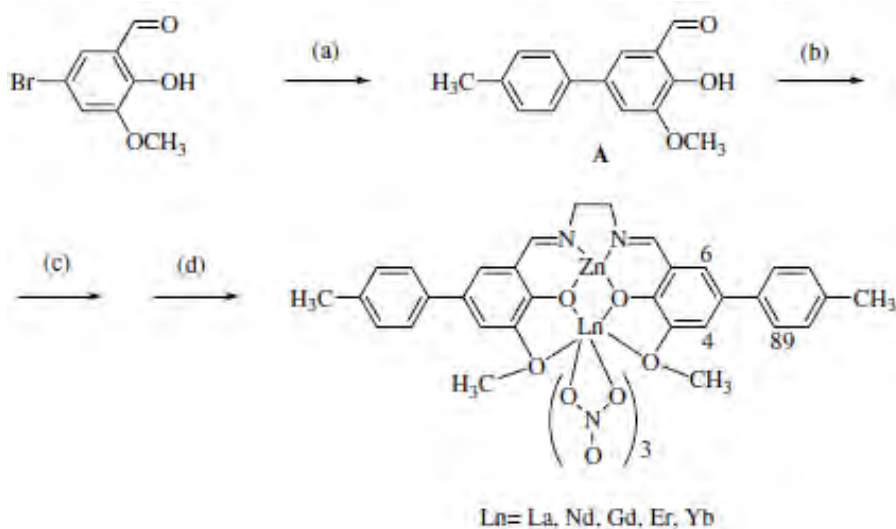


Scheme 1.20

1.4.2. Synthetic approaches to heterometallic complexes

There is currently some growing concerns in the synthesis of salen based bi-compartmental azomethine ligands having 3d and 4f nucleus leading to the simultaneous incorporation of magnetic and photophysical properties. The production of heterometallic 3d/4f complexes having variable nuclearity is quite a challenging task that follows assorted strategies, some of which are explained in the subsequent paragraphs.

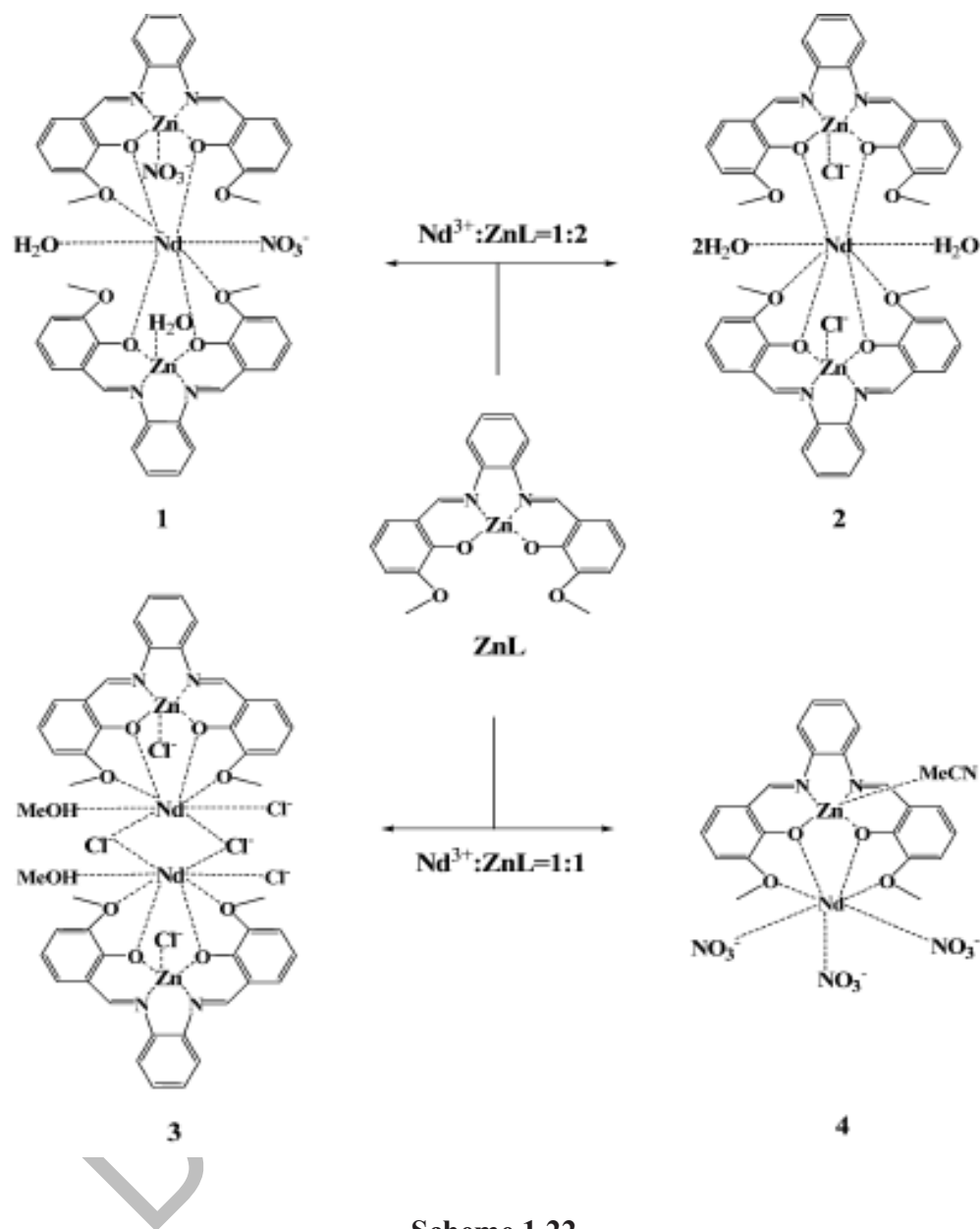
Lo *et al.* synthesized heterobimetallic 3d/4f complexes through substituted aldehyde refluxing 5-bromo-3-methoxysalicylaldehyde with 4-methylboronic acid and $\text{Pd}(\text{OAc})_2$ in deionized water to extract 5-(4'-methylphenyl)-3-methoxysalicylaldehyde as indicated in Scheme 1.21. The compartmental Schiff base was made by refluxing it with ethylenediamine, which was later reacted with $\text{Zn}(\text{OAc})_2$ and $\text{Ln}(\text{NO}_3)_3$ in acetonitrile to yield binuclear complex [131, 132].



Where, (a) = Pd(OAc)₂, 4-Methylboronic acid (b) Ethylenediamine, reflux (c) Zinc acetate, ethanol. Reflux, (d) Ln(NO₃)₃, acetonitrile, reflux

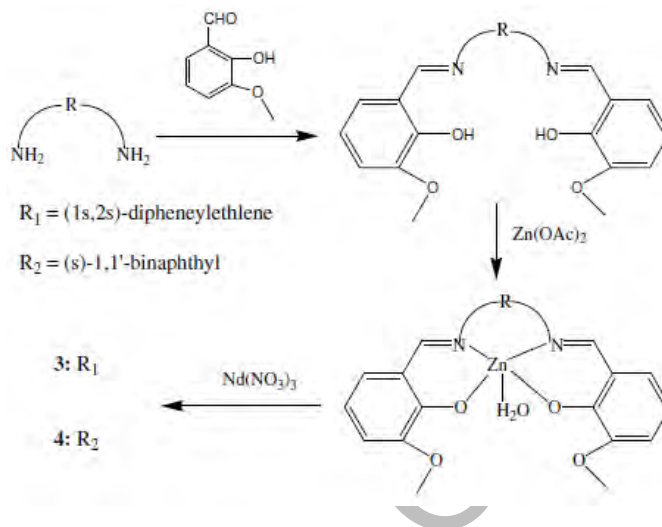
Scheme 1.21

Wong and coworkers prepared four di- and trinuclear Zn-Nd complexes derived from o-phenylene diamine based compartmental Schiff base, where two of these compounds were extracted in double decker fashion having novel pi-stacked structure and rest of the two complexes were obtained in binuclear manner exhibiting luminescent properties. The outcome of this study provides evidence that structure and stoichiometry of these complexes is completely dependent upon Nd : Zn ratio and the nature of anions incorporated (Cl or NO₃) as shown in Scheme 1.22 [133, 134].

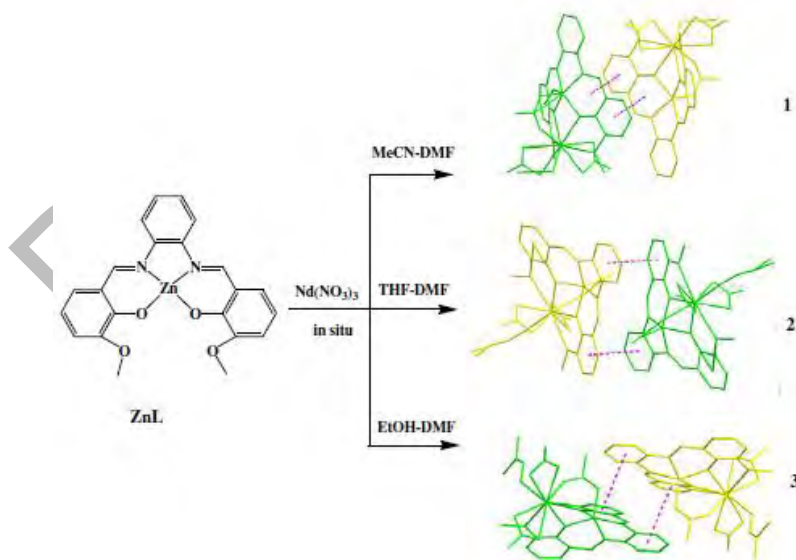


Bi and coworkers synthesized two chiral bicompartmental salen Schiff bases incorporating 1,1'-binaphthyl and (1s,2s)-diphenylethylene diamines to feature different electronic and steric effect in target 3d/4f complexes (Scheme 1.23). These chiral moieties acted as spacer groups and were responsible to improve photophysical properties in Zn-Nd dinuclear complexes [64]. Later on, they also incorporated a heavy atom like bromine in order to enhance the quantum yield and suitable energy transfer from ligands to 4f Ln⁺³ ion [75]. Bi *et al.* also reported some distinguishing optical characteristics of these solvent-

induced pseudo-polymorphic complexes established by π - π intermolecular interaction in crystal lattice. The *in situ* synthesis of ZnL complex was allowed to mix with $\text{Nd}(\text{NO}_3)_3$ in equimolar ratio and refluxed in DMF mixed solvents like ethanol, THF and acetonitrile to yield $[\text{Zn}(\text{OAc})\text{NdL}(\text{NO}_3)_2(\text{DMF})]$ solvate as drawn in Scheme 1.24 [65, 135].



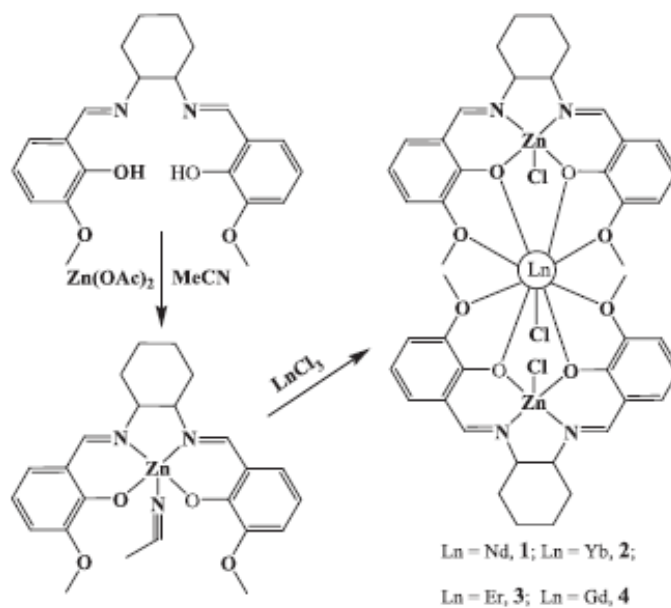
Scheme 1.23



Scheme 1.24

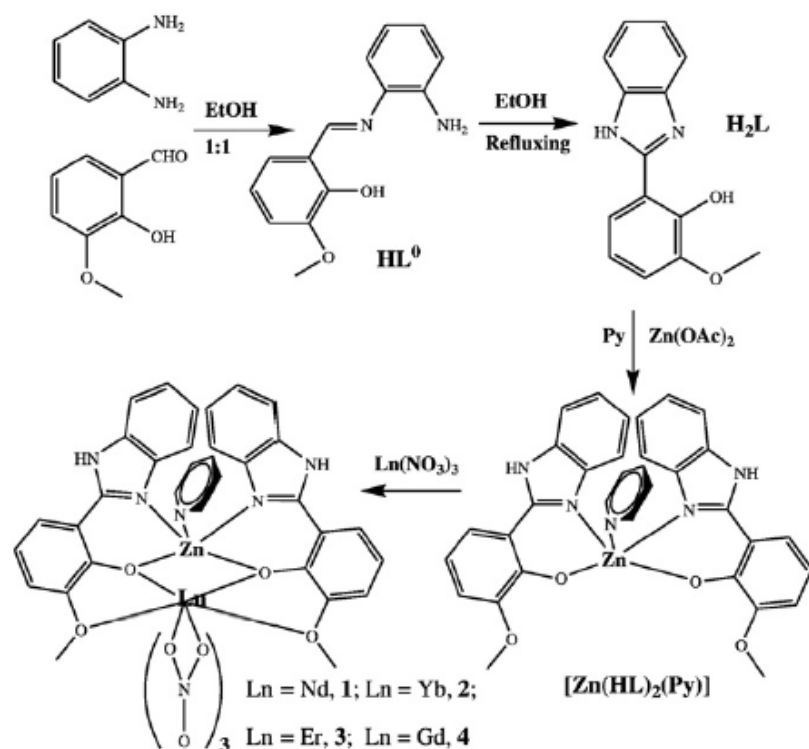
In order to facilitate NIR sensitization Feng and coworker synthesized series of trinuclear complexes with general formula $[\text{Zn}_2\text{Ln}(\text{L})_2(\text{Cl})_3]$ employing mononuclear zinc

precursor $[\text{ZnL}(\text{MeCN})]$ and $\text{LnCl}_3 \cdot 6\text{H}_2\text{O}$ in 2:1 that resulted in the formation of target heterotrimeric complex. In these complexes, Cl anions also served to enhance photophysical properties and emission lifetime in microsecond range (Scheme 1.25) [71, 80, 136].



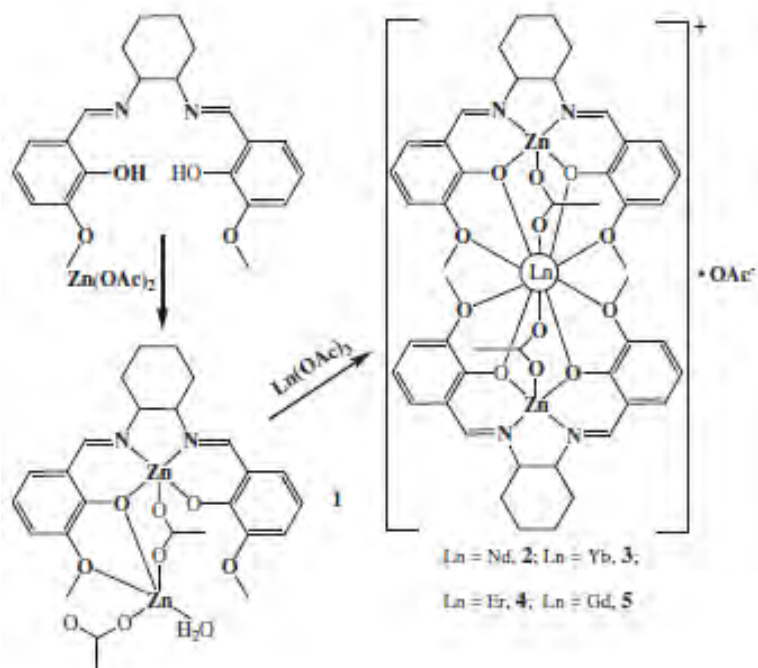
Scheme 1.25

Ding *et al.* synthesized monometallic Ni(II) complex, which was further complexed with $\text{Ln}(\text{NO}_3)_3$ salts in ethanol/DMF mixture to yield bimetallic Ni(II)-Ln(III) complexes that were successfully employed to catalyze solvent-free ring opening polymerization (ROP) reaction of L-lactide [74]. Later Shi and coworker prepared benzimidazole-based ligand as a starting material to make heterodinuclear complexes $[\text{ZnLn}(\text{NO}_3)_3(\text{HL})_2(\text{Py})]$ ($\text{Ln} = \text{Nd}, \text{Yb}, \text{Er}$ or Gd) with two energy donor groups around Ln(III) ion as mentioned in Scheme 1.26 [137].

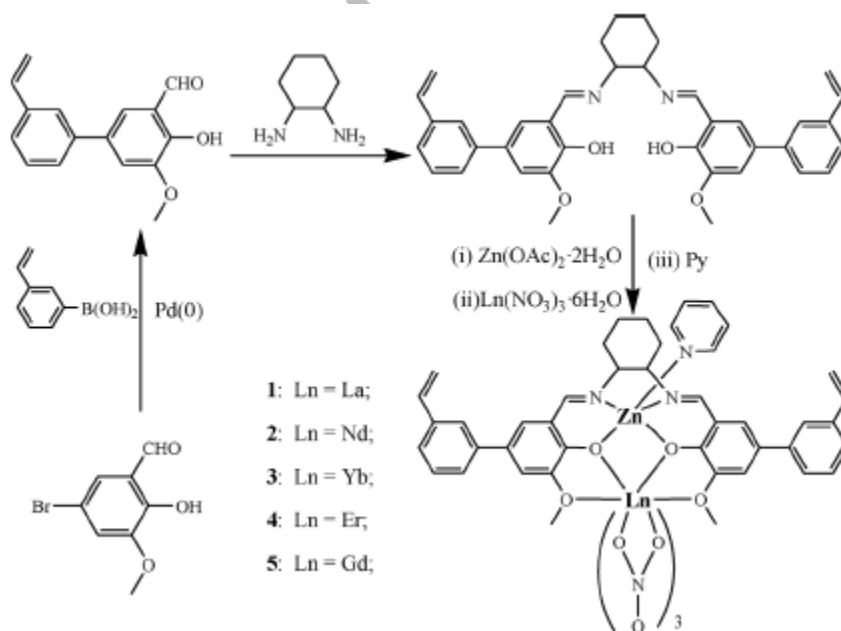


Scheme 1.26

Zhang *et al.* formed series of heterotrimeric complexes having general formula $[\text{Zn}_2\text{LnL}_2(\text{OAc})_2] \cdot \text{OAc}$ ($\text{Ln} = \text{Nd}, \text{Gd}, \text{Er}, \text{Yb}$) by reacting $[\text{Zn}_2\text{L}(\text{H}_2\text{O})(\text{OAc})_2]$ with $\text{Ln}(\text{OAc})_3 \cdot 6\text{H}_2\text{O}$ (Scheme 1.27). The solubility of these complexes was enhanced by the presence of charged components as $([\text{Zn}_2\text{LnL}_2(\text{OAc})_2]^{+1} \text{ and } \text{OAc}^{-1})$ in each of the target complexes [138]. In continuation to this work, they synthesized divinylphenyl based salen Schiff base and incorporated Zn and Ln metals to prepare 3d-4f complex $[\text{ZnLn}(\text{L})(\text{NO}_3)_3]$ (Scheme 1.28). The target complexes were grafted into polymer matrices of polymethylmethacrylate, polystyrene and polyvinylcarbazole to obtain Wolf type II metallopolymers [139].



Scheme 1.27



Scheme 1.28

1.5. Characterization techniques

Organobismuth derivatives and heteronuclear 3d/4f complexes with a variety of organic moieties are structurally characterized by a number of sophisticated analytical techniques like CHN analysis, FT-IR, multinuclear NMR spectroscopy, mass spectrometry and single crystal X-ray diffraction. During past few years NMR studies were conducted for both quantitative and qualitative investigation, whereas most accurate and precise information about the structure of these compounds come from single crystal XRD data.

1.5.1. FT-IR spectroscopy

FT-IR spectroscopy is employed as a fundamental interpretation technique to distinguish distinct functional groups present in the targeted complexes. IR spectral range 4000-250 cm^{-1} encompasses both fingerprint as well as functional group regions. Various researchers gave tabulated data for vibrational frequencies and found that position of vibrational bands was altered not only by the nature of ligand moiety but also by the masses of atoms involved in metal derivatives [140]. This technique is considered to be the most adaptable analytical procedure in which absorption of IR radiation leads to the transfer of photon and excitation is produced in sample from ground state to excited state. This excitation is responsible for molecular vibrations in the bond at different wavenumbers [141]. The FT-IR data provide reasonable information regarding coordination to the metal center and basic functionalities present in the complex. The spectral range of IR data comprises of some common functionalities like $\nu(\text{C-H}_{\text{aromatic}})$, $\nu(\text{C-H}_{\text{aliphatic}})$, $\nu(\text{COO}_{\text{asym}})$, $\nu(\text{COO}_{\text{sym}})$, $\nu(\text{Bi-C})$, $\nu(\text{Bi-O})$. In IR spectra of non-coordinated carboxylic acid, broad bands in the regions 3300–2500 cm^{-1} and 3500–3000 cm^{-1} are correlated with presence or absence of dimer in solid state, respectively [142]. In IR spectra of free ligand, a typical band for O-H stretching vibrations (ν_{OH}) is observed around 3500-3000 cm^{-1} which is clearly absent in IR spectra of metal complex, hence, absence of this band is a clear indication of successful complexation of metal with the oxygen of carboxyl moiety [143-145].

The carbonyl vibrational band for $\nu(\text{C}=\text{O})$ occur around $1700\text{-}1600\text{ cm}^{-1}$, whereas the symmetric $\nu(\text{COO}_{\text{sym}})$ and asymmetric stretch $\nu(\text{COO}_{\text{asym}})$ bands appear in the range of $1320\text{-}1450$ and $1659\text{-}1724\text{ cm}^{-1}$, respectively. Moreover, it has been observed that due to the presence of pentafluorophenyl moiety in the target complex, the $\nu(\text{COO}_{\text{asym}})$ arises at slightly higher frequency [146, 147]. Carboxylic group in organobismuth(V) complexes may act as monodentate, anionic bidentate and bidentate having coordination number five (trigonal bipyramidal), six (octahedral) and seven (pentagonal bipyramidal), respectively. The coordination behavior can be inferred from the difference between $\nu(\text{COO}_{\text{sym}})$ and $\nu(\text{COO}_{\text{asym}})$ stretching bands [$\Delta\nu = \nu(\text{COO}_{\text{asym}}) - \nu(\text{COO}_{\text{sym}})$]. If the value is greater than 250 cm^{-1} then it corresponds to monodentate binding mode, if less than 200 cm^{-1} then it show bidentate mode of chelation [53, 54, 148]. Kumar *et al.* synthesized variety of bismuth(V) carboxylates and proposed binding modes for the carboxyl moiety as delineated in Fig. 1.3 [55].

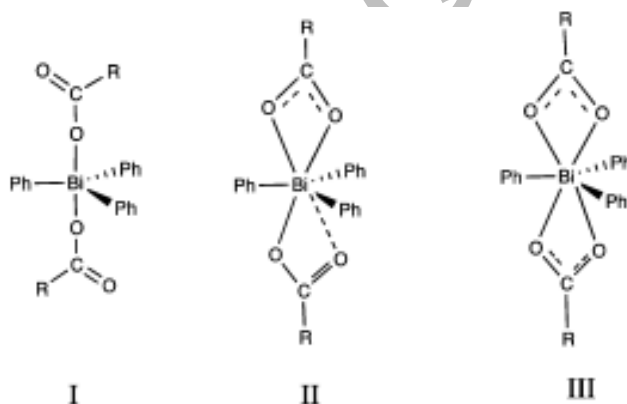


Figure 1.3: Variation in the binding modes of bismuth(V) carboxylates

FT-IR spectroscopy is mainly applied to qualitative and quantitative analyses of structural motifs of heteronuclear metal complexes. Nearly all functional groups including $\nu(\text{O-H})$, $\nu(\text{C}=\text{N})$, $\nu(\text{C-O})$, $\nu(3\text{d-N})$, $\nu(3\text{d-O})$ and $\nu(\text{Ln-O})$, present in heteronuclear 3d/4f complexes, necessary for complete structural elucidation are observed in spectral range $4000\text{-}250\text{ cm}^{-1}$. The structure of a new complex can be advanced in comparison with the spectral data of Schiff base or mononuclear 3d complex [149].

Bi et al. reported a detailed overview of the FT-IR spectra for two heterodinuclear 3d/4f complexes in comparison to the salen-based schiff base. The data explicitly unfolded two absorption bands around 1319-1316 and 1454-1452 cm^{-1} , which directly corresponded to bidentate chelation of nitrate moiety in two target complexes. The bands emerging around 2260, 759 or 761 cm^{-1} are generally assigned to $\nu_{(\text{C}\equiv\text{N})}$ vibrations in acetonitrile solvate molecule, $\nu_{(\text{C}-\text{Br})}$ vibrations in target complex and salen-based Schiff base, respectively. The absorption band for $\nu_{(\text{C}=\text{N})}$ at 1614 cm^{-1} in binuclear complex is blue-shifted (7 cm^{-1}) relative to salen-based Schiff base (1607 cm^{-1}) upon coordination with Nd metal [75]. Some additional bands also appear around 500-540 and 350-500 cm^{-1} that correspond to vibrational bands $\nu_{(3\text{d}-\text{O})}$ and $\nu_{(\text{Ln}-\text{O})}$, respectively [150, 151]. Hence, IR spectral data clearly indicate the successful synthesis of final product having particular functionalities as the previous reports manifested.

1.5.2. NMR spectroscopy

NMR can provide comprehensive information on the chemical and molecular structure, which is not surpassed by any other analytical technique. Substantial evidence for the synthesis of triarylbi(bismuth(V) carboxylates is available in literature as for tri(phenyl)bi(bismuth(V) bis(3-acetoxybenzoate) and tri(phenyl)bi(bismuth(V) bis(acetylsalicylate)), the coordination of bismuth to the carboxylate moiety taking place through deprotonation of proton around 11.14 and 10.7 ppm, respectively. In addition, the resonances for aromatic proton appear around 8.30-6.80 ppm with slight change in position as compared to free carboxylic acid. The ^1H NMR data also depict that the signals for the methyl group appear in their usual positions that give clear indication that metal center is not coordinated to the ester oxygen [25].

Ong *et al.* used ^1H NMR spectroscopy as a tool to determine the stability of triphenyl and tritolybi(bismuth(V) derivatives in solution by comparing the ^1H NMR spectra of these derivatives at $t = 0$ and $t = 6$ months in D_6 -DMSO as a solvent. These two spectra presented a clear difference in resonances that were related to benzoate moiety of the complex and after the lapse of six months, it split into two signals, maintaining the same integration value as compared to phenyl protons [54]. During this time interval, the melting

points of these complexes remained same which correlates with the stability of these derivatives. This prominent difference in two spectra was attributed to the thermodynamically more favored geometry that brought the interconversion of trigonal bipyramidal to square pyramidal geometry [152].

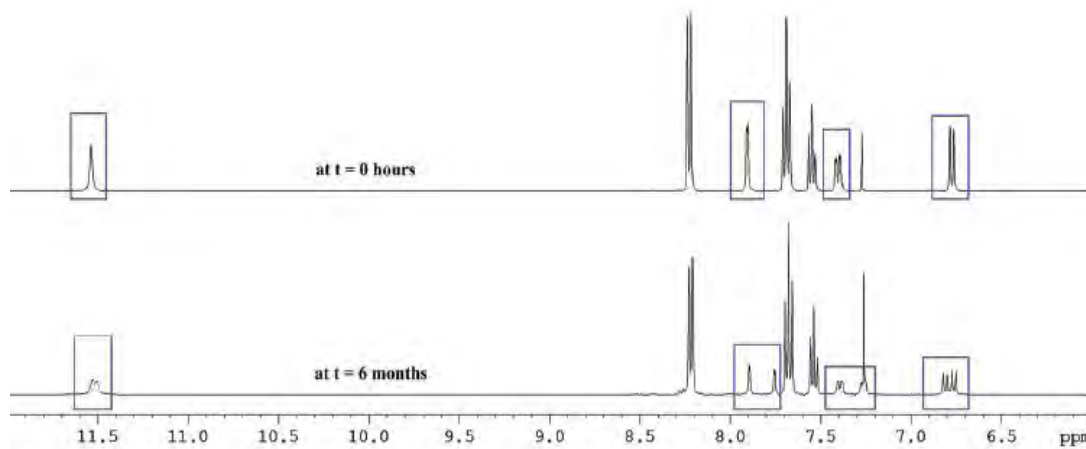


Figure 1.4: ^1H NMR spectrum of $[\text{Bi}(\text{O}_2\text{CC}_6\text{H}_3\text{-2-OH-5-Cl})_2(\text{C}_6\text{H}_5)_3]$ at $t = 0$ h and $t = 6$ months [54]

Islam *et al.* synthesized bismuth(V) derivatives and characterized them using ^{13}C NMR spectroscopy where prominent resonance was obtained at about 170 ppm in both ligands and metal complexes that corresponded to the carbon of carboxylic acid. The signals for methyl carbon were observed around 21 ppm, and no significant change was observed after complexation that correlates to the non-involvement of methyl upon coordination. The signals for aromatic carbons appeared in the range of 151.3-122.2 ppm, whereas upon coordination they shifted in the range of 160.3-122.9 ppm indicating shielded or deshielded up to 1.93-0.68 ppm as compared to free ligand [25].

Ample evidence for the synthesis of salen-based ligands comes from the spectroscopic studies, where chemical shift values of 7.58-6.98, 8.58 and 12.75 ppm correspond to aromatic as well as pyridine proton, azomethine and phenolic moieties respectively [153]. Bi and coworkers prepared three target complexes having heterodinuclear moieties and their unchanged ^1H NMR results manifested that these complexes were stable up to one month in CD_3OD solution. Almost similar ^1H NMR

spectra were observed for all the complexes with a considerable change in chemical shift values both for deshielded (δ 15.35-5.08 ppm) and shielded regions corresponding to the lanthanide induced shift, whereas for free H₂L ligand and Zn precursor (ZnL), the values were observed at 8.77-3.88ppm and 9.09-3.77 ppm, respectively [64, 65]. A detailed explanation of ¹³C NMR spectrum for one of the salen-based ligand is given in many articles, where CH₂-CH₂ moiety is found around 61.9 ppm. The signal for these sp³ hybridized carbons is deshielded in these ligands (usually arises at 30 ppm) due to the presence of pi bond and electronegative nitrogen atom in adjacent position. The signals for sp² hybridized CH appear around 140 ppm, which are also slightly deshielded in these ligands. The signal for phenolic carbon is generally observed at 161 ppm, whereas rest of the aromatic carbons are resonated around 120-130 ppm. The meta carbon of phenol moiety remains unchanged [154].

1.5.3. X-ray crystallography

Single crystal XRD analysis reveals molecular and structural characterization of a metal complex including bond angles, bond lengths, hydrogen bonding parameters, exact position of metal and ligating atoms and various thermal displacement parameters. Here a few mm crystal mounted on the glass fiber of goniometer of spectrometer helps to determine three dimensional structure of a metal complex [155].

1.5.3.1. Crystal structure for organobismuth derivatives

Ong *et al.* several triphenyl and o-tritolylbismuth(V) carboxylates and successfully resolved their crystal structure to find out their characteristic features as depicted in Figs. 1.5-1.7. All these frameworks emerge as isostructural adopting trigonal bipyramidal geometry in case of o-tritolylbismuth(V) dicarboxylates with coordination number five and pentagonal bipyramidal geometry for triphenylbismuth(V) dicarboxylate with coordination number seven. The three phenyl and o-tolyl moieties occupy equatorial position in a propeller like fashion, whereas the oxygen atom of substituted-benzoic acids takes axial position around Bi(V) metal center [54]. The Bi-C bond lengths in phenyl and o-tritolylbismuth moieties lie in the range of 2.210-2.177 Å and 2.223-2.208 Å, respectively.

In phenyl derivatives, all the deprotonated benzoate moieties are coordinated to bismuth center through bidentate fashion with bite angle (O-Bi-O) ranging from 51.47°-46.22° [53, 54].

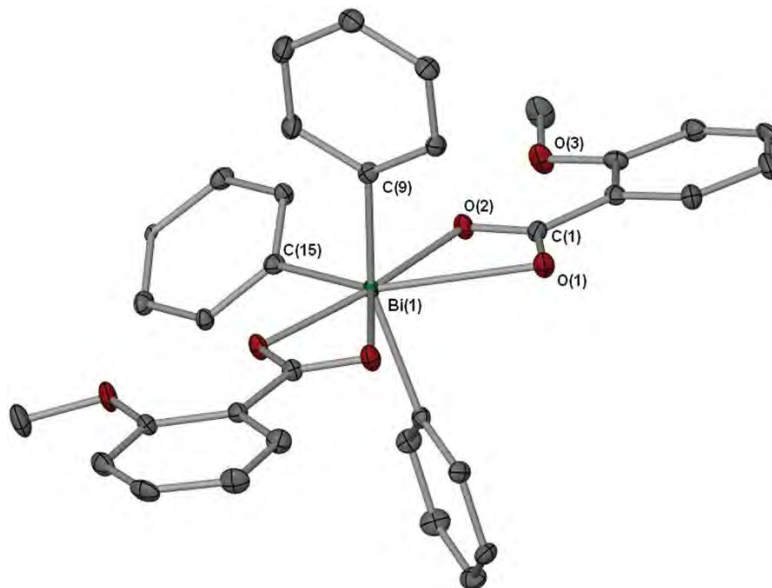


Figure 1.5: Crystal structure for $[\text{Bi}(\text{O}_2\text{CC}_6\text{H}_4\text{-o-OCH}_3)_2(\text{C}_6\text{H}_5)_3]$ [54]

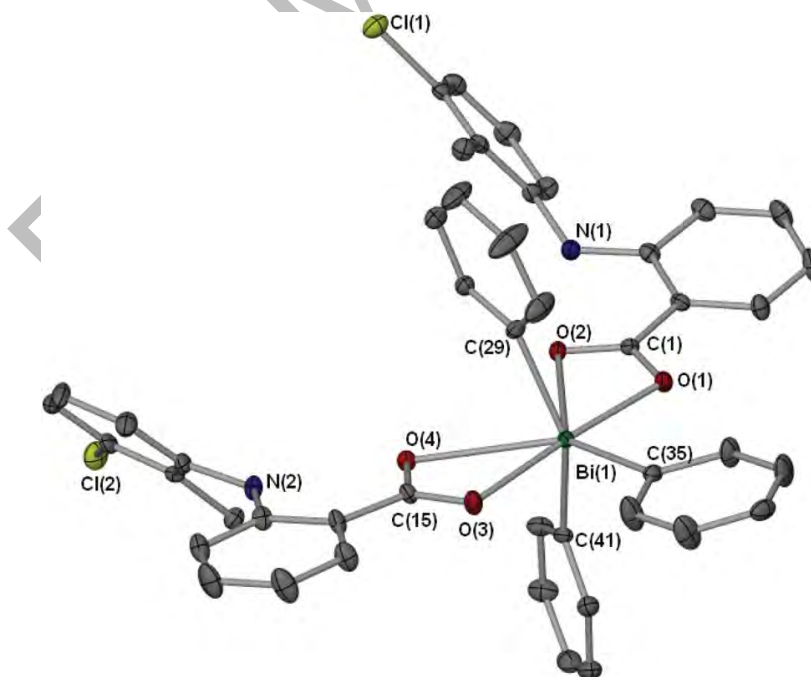


Figure 1.6: Crystal structure for $[\text{Bi}(\text{O}_2\text{CC}_6\text{H}_4\text{-2-NH-(C}_6\text{H}_3\text{-2-CH}_3\text{-3-Cl)})_2(\text{C}_6\text{H}_5)_3]$ [54]

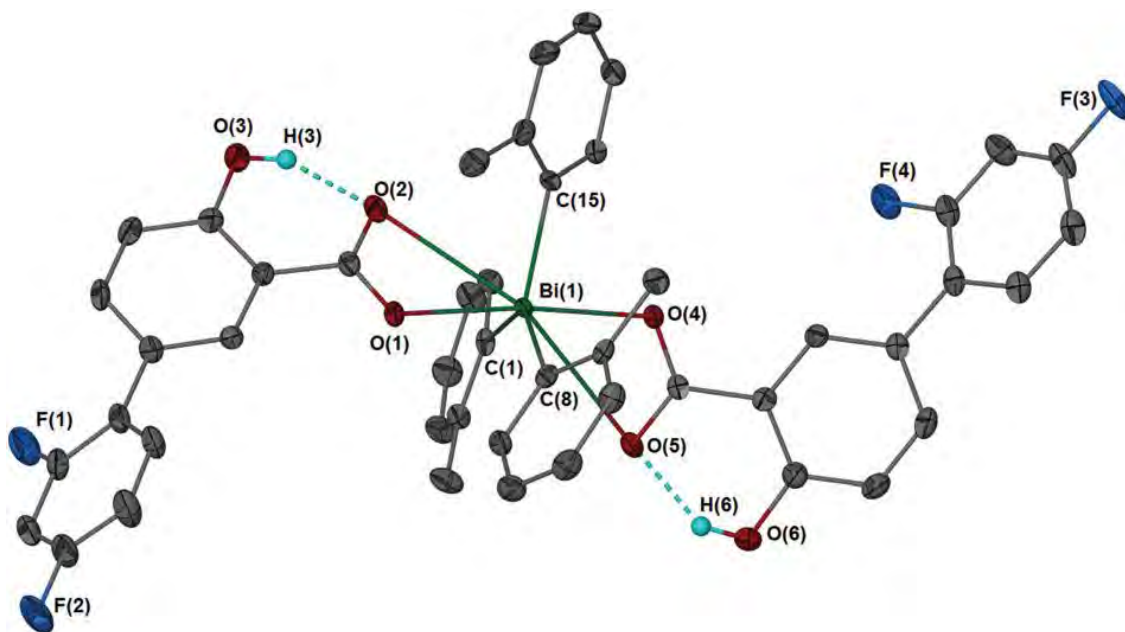


Figure 1.7. Crystal structure for $[\text{Bi}(\text{dif})_2(\text{o-tol})_3]$ [53]

1.5.3.2. Crystal structure for dinuclear Zn/Nd complex

Bi *et al.* formed three complexes with individual neutral molecular unit as $[\text{ZnNdL}(\text{OAc})(\text{NO}_3)_2(\text{DMF})]$ (fig. 1.8), while different solvates resulted in the emergence of pseudo-polymorphism [156]. This representative structure gives an insight into the coordination sites for both 3d and 4f metal as N_2O_2 , where Zn(II) was pentacoordinated having slightly distorted square pyramidal geometry. The acetate (OAc) group and two phenolic O donor groups bridge to Nd(III) and Zn(II) with bond length 3.412(3), 3.422(2) or 3.412(3) Å, respectively, whereas Nd(III) metal occupies O_2O_2 cavity with the coordination number of ten in all target complexes. In all the three complexes, four O come from Schiff base, four from two nitrate groups, one from DMF solvent and one from OAc group [65].

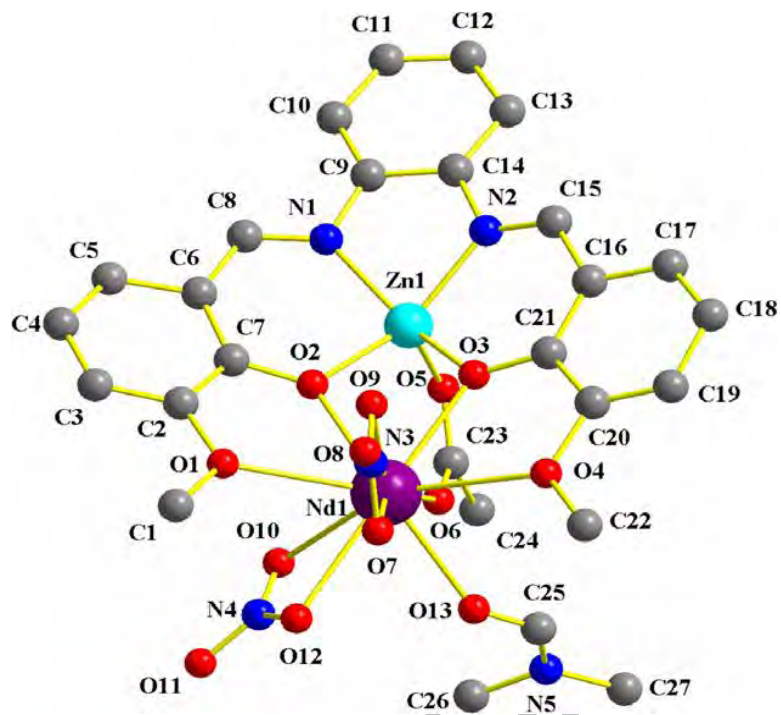


Figure 1.8. Crystal structure for $[\text{ZnNdL}(\text{OAc})(\text{NO}_3)_2(\text{DMF})]$ [65]

1.5.3.3. Crystal structure for trinuclear Zn/Nd/Zn complex

Zhang *et al.* made trinuclear complexes, where asymmetrical unit contained one anion OAc and one cation $[\text{Zn}_2\text{L}_2(\text{OAc})_2\text{Nd}]$, two solvate water and methanol each as depicted in Fig. 1.8. In cationic part, the outer O_2O_2 cavity of mononuclear ZnL components is coordinated with Nd(III) metal, showing coordination number ten. On the other hand, Zn(II) metal in each portion displays coordination number five with distorted square pyramidal geometry. The separation of Zn1 and Zn2 from Nd metal was almost equal as it was bridged with acetate ion on both compartments of the structure. The Zn-O bond lengths (2.042-2.012 Å) were shorter than Zn-N bond lengths (2.056-2.033 Å). The ten Nd-O bond lengths ranged from 2.895-2.404 Å which completely depended on the nature of O moiety [138].

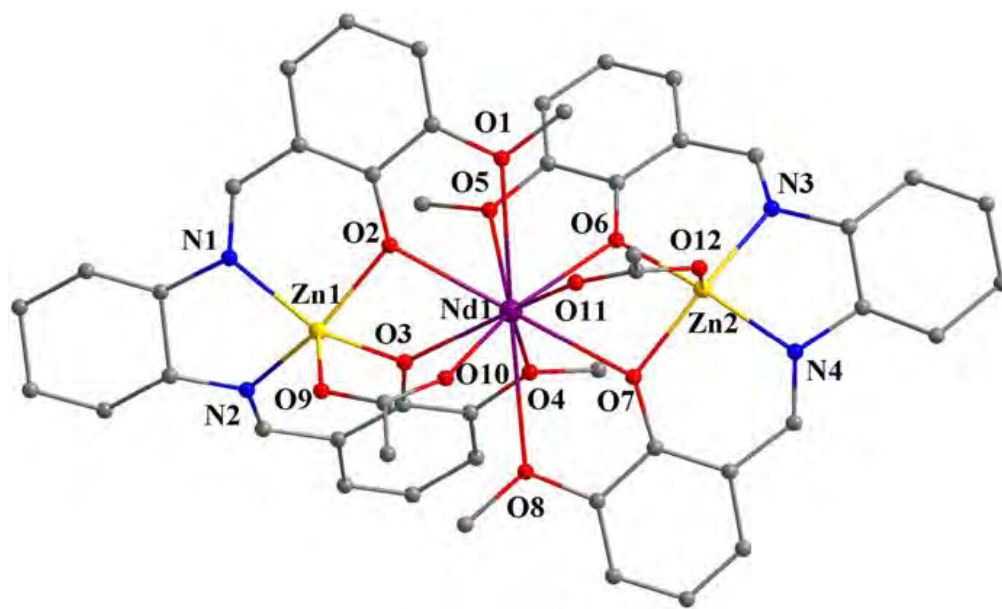


Figure 1.9. Crystal structure for $[\text{Zn}_2\text{L}_2(\text{OAc})_2\text{Nd}]^+$ [138]

1.6. Applications

1.6.1. Biological applications of bismuth complexes

Bismuth is considered to be the least toxic heavy metal which is stable and has possessed medicinal importance since 1900, especially when a mixture of bismuth nitrate/chloride with common hydroxyl carboxylic acid began to be used widely in medicinal capacities [27, 157]. Being a green element and having low toxicity level, most of the bismuth compounds are employed in some commercially available medicines [27, 158].

1.6.1.1. Gastrointestinal activity

The important derivatives of bismuth, being currently utilized as medicinal products, include colloidal bismuth subcitrate (CBS) with the trade name of De-Nol[®] and bismuth subsalicylate (BSS), trade named as Pepto-Bismol[®] [159-163]. These medicines are taken worldwide to control dyspepsia, diarrhea, duodenal and peptic ulcers caused by bacterial strain, *Helicobacter pylori*. The organometallic complexes of bismuth are of extraordinary interest due to their chemically well-defined structure and possibility of tuning their activity and toxicity [25, 164]. Over the past few years, bismuth derivatives of

carboxylates, thiocarboxylates, amides, sulfamates and sulfonates have also been explored for their possible *in vitro* activity against *H. pylori* with promising results [49, 165-168].

Urea amino-hydrolase, commonly known as urease, is a nickel containing enzyme which is responsible for the splitting of urea into carbamic acid and ammonia. The carbamic acid further hydrolyses under the action of urease to form carbonic acid and a molecule of ammonia. Ammonia, being strong base, causes elevation of pH and, consequently, it creates favorable scenario for the survival of *H. pylori* in stomach's harsh acidic conditions as depicted in Fig. 1.10. Moreover, additional production of ammonia also leads to the formation of certain cytotoxins like monochloramine which is liable to foster peptic ulcer and gastric carcinoma [30, 169]. The exact mechanism for the efficient activity of bismuth derivatives against *H. pylori* is still not understood, however, the potential biological efficacy of bismuth complexes clearly effects suppression of urease enzyme which is considered to be an ultimate therapeutic target for *H. pylori* bacterial strain [170-172].

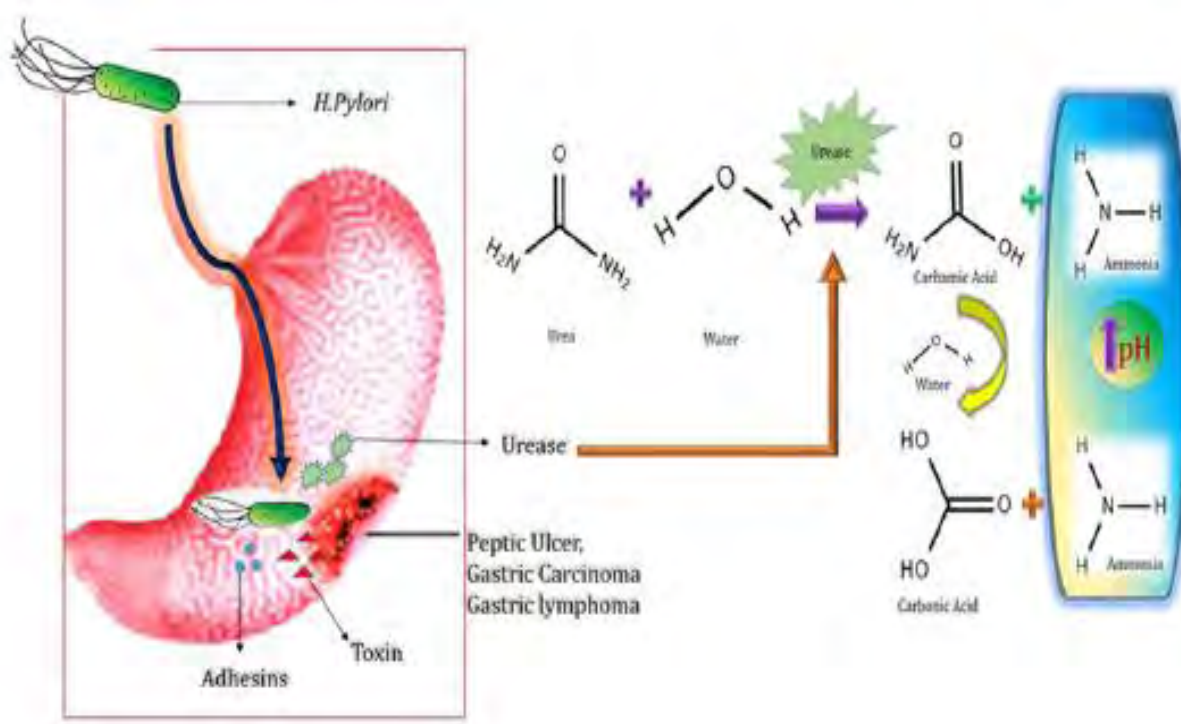


Figure 1.10: Urease-The ultimate therapeutic target for H.pylori

1.6.1.2. Antileishmanial activity

Leishmania is a parasite which belongs to class protozoa, and is transmitted by vector sand fly capable of multiplying as motile promastigotes [173]. Over past 70 years, major clinical trials were conducted using pentavalent antimonials which were considered as prodrugs against leishmania. The present day chemotherapy involves meglumine antimonate and sodium stibogluconate. The mechanism of Sb(V) drugs involves reduction to Sb(III), which coordinates with trypanothione and cysteine [174]. The major obstacle in employing such antimonial drugs is related to toxicity, that's why bismuth compounds serve as viable alternatives owing to the fact that the heavy metal is not only a least toxic but also green. Despite its close relation with antimony, a small-scale research was carried out to evaluate its efficacy as antileishmanial drug on account of insolubility, instability, and synthetic reproducibility of metalorganic bismuth derivatives [175-178].

The two emerging groups, Andrews and Demicheli had exploited potential applications of bismuth complexes towards Leishmania for the last few years. Their studies were mainly based on Bi(III)/(V) oxidation state with number of ligands attached to the metal center. These complexes involved O-binding ligands such as carboxylic acids [179], quinones [26] and α -hydroxycarboxylic acid [180], N-binding ligands like phenazines [181] and porphyrins [182], S-binding ligands; viz. thiols [183] and thiocarboxylic acid [184] and O, S-binding ligands namely β -thioketones [177].

1.6.2. Biological studies of heteronuclear complexes

Over the past few decades, heteronuclear complexes assumed a status of noticeable field for their potential utility in coordination chemistry, applied sciences, synthetic and industrial processes such as photochemistry, catalysis, and biological systems [185]. Furthermore, few researches were conducted regarding biological efficacy of these complexes for antimicrobial, antidiabetic and anticancer activities [186]. Chaudry *et al.* describe the synthesis of monometallic and heterobimetallic complexes of Cu(II) and evaluated their antimicrobial and antifertility applications. The obtained results revealed appreciable antimicrobial activity against *Escherichia coli* and *Fusarium oxysporum*. The

values for antifertility activity suggested that heterobimetallic complexes were more efficient in reducing fertility as compared to mononuclear copper complexes [185].

Now the main focus is being tuned on the synthesis of lanthanide metal complexes with range of organic ligands having outstanding pharmacological importance. In this way, complexes of Nd, Ce and Gd show effective antifungal applications and Gd complexes with hexafluoroacetylacetonate ligand serve as a potent antibacterial agent, While, the complexes of Nd, Eu and Yb manifest anticancer activities as well [187].

1.6.3. Non-biological applications of bismuth complexes

Owing to the nontoxicity and unique properties of bismuth, it has been used in nontoxic pigments, ferroelectric and thermoelectric materials, alloys, catalyst (in SOHIO process where bismuth molybdate is employed for the synthesis of acrylonitrile to catalyze oxidation reaction) [188-191], material applications on industrial scale (superconductors [192-194], sol-gel process [195-197], photorefractive systems [198, 199] and CVD techniques [200-202]) and in synthesis (heterometallic clusters [203-205], cyclobismuthines [206], dibismuthanes [207, 208], dibismuthenes [209, 210] and organobismuth(V) derivatives [25, 55, 211]). Previously, lead-based perovskite solar cells (PvSCs) were considered excellent photovoltaic materials due to exceptional narrow band gap, unique optoelectronic properties, high absorption coefficient and high defect tolerance. Lead-free halide perovskite-based light absorbers mainly include post-transition metal or metalloid elements like Sb and Bi [191].

1.6.4. Non-biological studies of heteronuclear complexes

In non-biological domain, particular emphasis has been laid to synthesize those heteronuclear 3d/4f complexes which exhibit magnetic properties in addition to photoluminescent behavior. Thus, recent advancements have been made to combine optical and magnetic properties [212, 213], conductivity [214], ferroelectricity [215] and luminescence [216].

1.6.4.1. Magnetic properties

In order to design luminescent single molecular magnets (SMM's), it is critical to choose Ln(III) ion because, on one hand, the metal ion must exhibit well-resolved emission spectra having long lifetime, and on the other, it must have large magnetic anisotropy and large magnetic moment to ensure high energy barrier for checking reversal of magnetization as illustrated in Fig. 1.11. These aforementioned properties are generally present in Ln(III) ions, mainly in Yb(III), Dy(III) and Er(III) and to some extent in Ho(III) and Nd(III) [217]. In heteronuclear 3d/4f complexes, different organic and inorganic ligands are also responsible for appreciable stabilization of 4f electronic density. In general Ln(III) ions display forbidden f-f transition due to weak absorption coefficient. However, among these metal ions, Er(III), Nd(III) and Yb(III) reveal luminescence in NIR region, whereas Dy(III) and Tb(III) demonstrate emission in visible region.

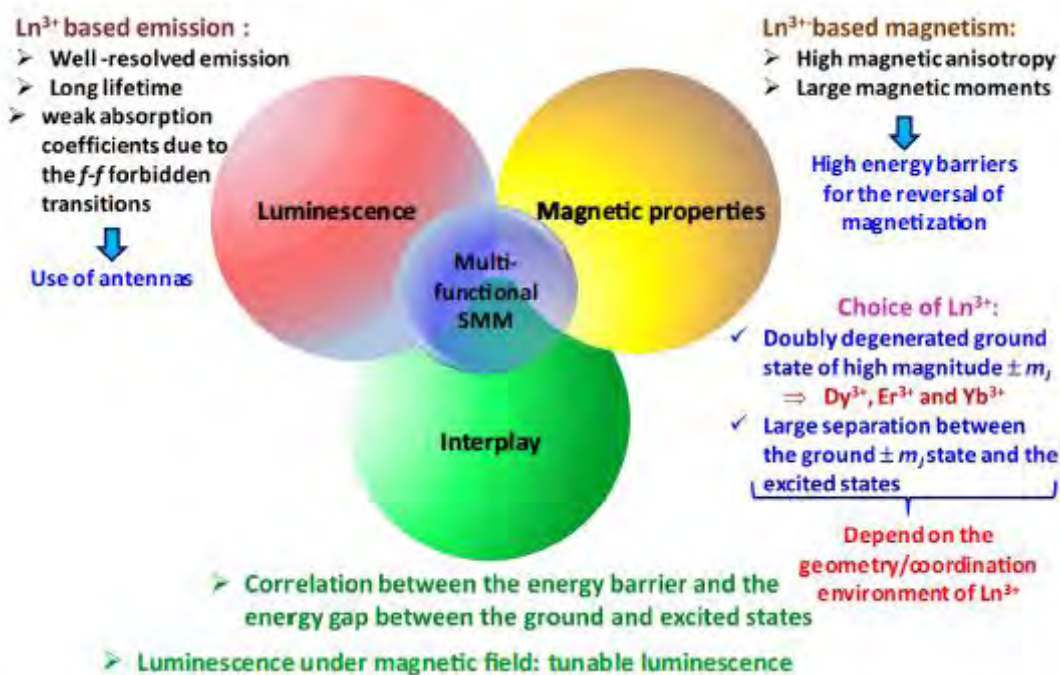


Figure 1.11. Design of luminescent Ln(III)-based single molecular magnets

Among lanthanide metal ions, Dy(III) is commonly employed to design single molecular magnets having luminescent properties due to its high J value ($J = 15/2$) and its emission in the visible region [218]. Apart from these properties Dy(III) usually manifest

strong crystal field splitting energy (CFSE) which is required to design high temperature blocking SMMs. The first example of lanthanide based complexes as luminescent SMM was reported in 2009 by Bi *et al.* using tetranuclear Dy(III) complexes [219]. Later on, Liu *et al.* reported heterotrinnuclear 3d/4f complexes of Dy(III) metal ion with organic ligands such as salicylic acid and phenanthroline for elaborating SMM behavior [220]. Literature is repeated with examples of dysprosium-based heteronuclear complexes in association with organic ligands, such as carboxylic acid [221], Schiff base [81, 222, 223], aromatic amines [224] and amino acids [225]. A comparative study of magnetic susceptibility at various temperatures with respect to nuclearity is set forth in Table 1.1.

Table 1.1. Comparative study of magnetic susceptibility at various temperatures with respect to nuclearity

Compounds	Nuclearity	χ_g (emu g ⁻¹)	$\chi_{m \cdot T}$ (emu mol ⁻¹ K)	μ_{eff} (μ_B)	References
[ZnSm(valpn)(ONO ₂)(O ₂ NO) ₂ (H ₂ O)].2H ₂ O	ZnSm (2)	1.84×10 ⁻⁶	0.42	1.83	[82]
[ZnNd(valpn)(ONO ₂)(O ₂ NO) ₂ (H ₂ O)].2H ₂ O	ZnNd (2)	7.29×10 ⁻⁶	1.65	3.65	[82]
[ZnGd(valpn)(ONO ₂)(O ₂ NO) ₂ (H ₂ O)].2H ₂ O	ZnGd (2)	35.5×10 ⁻⁶	8.16	8.07	[82]
[ZnDy(valpn)(ONO ₂)(O ₂ NO) ₂ (H ₂ O)].2H ₂ O	ZnDy (2)	62.7×10 ⁻⁶	14.54	10.78	[82]
[Zn ₂ Nd(bcn) ₂]ClO ₄ .nH ₂ O	Zn ₂ Nd (3)	-	1.67	3.65	[226]
[Zn ₂ Gd(bcn) ₂]ClO ₄ .nH ₂ O	Zn ₂ Gd (3)	-	7.56	7.77	[226]
[Zn ₂ Dy(bcn) ₂]ClO ₄ .nH ₂ O	Zn ₂ Dy (3)	-	14.16	10.64	[226]
(μ_3 -CO ₃) ₂ [ZnGd(NO ₃)(μ -L)] ₂ .4CH ₃ OH	Zn ₂ Gd ₂ (4)	-	15.75	11.22	[227]
[Zn ₂ Dy ₃ (m-salen) ₃ (OH) ₂ (N ₃) ₅]	Zn ₂ Dy ₃ (5)	-	39.1	17.68	[228]
[Zn ₄ Dy ₂ (L ₂) ₄ (OAc) ₂ (OH) ₂ (DMF) ₄ (NO ₃) ₂]	Zn ₄ Dy ₂ (6)	40.5×10 ⁻⁶	27.2	14.74	[229]

$\chi_{m \cdot T}$ = Magnetic susceptibility, μ_{eff} = Effective magnetic moment, χ_g = Gram magnetic susceptibility, - = not reported

1.6.4.2. Photoluminescence properties

The photoluminescence studies (PL) of Ln(III) complexes of Er(III), Pr(III), Nd(III), Yb(III), etc. display efficient photophysical properties on account of long emission/luminescent life-times, ligand-induced large Stokes shift, narrow emission lines, ligand-dependent luminescence sensitization and high luminescence quantum yields [75]. Thus, they are used in various potential applications viz., optical telecommunication [76], organic light-emitting diodes (OLED) [77], fluoro-immunoassay and imaging [78, 79]. However, the absorption coefficient of lanthanides is quite low which renders these complexes weak absorber, due to parity/Laporte forbidden f-f transition. In order to surmount this limitation, properly designed ligands (chromophores) and d-block metal complexes for sensitization of lanthanide ions have been utilized that might provide necessary antenna effect [80]. Keeping this in view, three effective strategies were adopted to improve the photoluminescence of synthesized compounds, i.e., extended conjugation on the flanking phenyl ring, use of rigid spacers and functional bridge like -OH and various anion groups [75]. On the other hand, the synthesis of dinuclear $ZnLn$, trinuclear Zn_2Ln , tetranuclear Zn_2Ln_2 or Zn_4Ln_2 type salen-based Schiff base complexes having bipyridyl [230], chloride [133], thiocyanate [231], or bicarboxylate [232] as secondary ligands was found helpful for the decrease of non-radiative decay and, in turn, enhancement of luminescence.

1.7. Aims and Objectives

After going through the literature on the subject, it becomes evident that main group and transition metal complexes have found enormous interest in both biological and non-biological domains due to their striking features in diverse fields of studies. Owing to these facts, the ultimate aim of the present research work is to synthesize main group and transition metal complexes derived from N-, O- containing ligands to get preliminary screening data for various biological activities for all these new compounds and to search the “lead” compound for future drug-discovery process. Furthermore, bi-compartmental heteronuclear 3d/4f metal complexes are designed to develop magnetically strong materials having luminescence properties.

1.8. Plan of work

The **first part** of this research project entails synthesis of triorganobismuth(V) carboxylates on account of their vast applications in the field of medicine, there is a pressing need to prepare such compounds having significant medicinal value. In this regard, oxygen-containing biologically-active carboxylic acids in combination with triorganobismuth(V) dibromide are chosen. These precursors will then be utilized to synthesize bismuth derivatives that may serve as potent antimicrobial, anticancer, enzyme inhibitors and may assume candidature as pre-drug to target urease, responsible for the proliferation of *H. pylori* bacteria in stomach.

Keeping these aspects in view, we embarked upon a research project that embodied the synthesis of two series of carboxylates, that is, triphenylbismuth(V) carboxylates and tri(p-tolyl)bismuth(V) carboxylates with Bi(V) center and then exploration of their potential applications. The layout of this work as follows;

- 1) Synthesis of triphenylbismuth(V) dibromide and tri(p-tolyl)bismuth(V) dibromide as precursors for the target compounds
- 2) Preparation of bioactive heteroleptic triorganobismuth(V) dicarboxylates
- 3) Characterization of the synthesized compounds applying sophisticated analytical techniques, i.e., FT-IR, NMR spectroscopy and single crystal X-ray diffraction analysis
- 4) Biological screening to check their biocidal properties like anti-microbial, antidiabetic, brine shrimp lethality assay and protein kinase inhibition to develop a limited structure-to-activity relationship (SAR)
- 5) *In silico* molecular docking studies of the representative compounds against the three enzyme systems namely, *H. pylori* urease, human pancreatic alpha amylase and EGFR tyrosine kinase

The **second part** of research work is based on the synthesis of heterodi-/trinuclear 3d/4f metal complexes, due to current growing trend in synthesis of salen-based bi-compartmental azomethine ligands having 3d and 4f nuclei leading to simultaneous

investigation of their magnetic and photophysical properties. Since the formation synthesis of heterometallic complexes with variable nuclearity is quite a challenging task, so in this part of dissertation, main focus will be on the development of a scheme for the efficient preparation of such type of compounds. This part of studies will be undertaken in the following manner;

- 1) Production of bi-compartmental Schiff base ligands
- 2) Formation of heterodi-/trinuclear metal complexes
- 3) Characterization of the synthesized compounds through FT-IR, NMR spectroscopy and single crystal XRD data
- 4) Exploration of magnetic and photoluminescence properties of the synthesized heterometallic complexes

DRSML QAU

CHAPTER-2

EXPERIMENTAL

2.1. Materials

The commercially available chemicals were purchased from Alfa Aesar and Sigma-Aldrich (USA); some of which are: 3,5-dinitrosalicylic acid, indole-2-carboxylic acid, 3,5-diiodosalicylic acid, 3-fluorocarboxylic acid, 2-napthoic acid, 4-chlorobenzoic acid, o-toluic acid, 3-bromobenzoic acid, 3,4-diethoxybenzoic acid, 2-chlorobenzoic acid, 4-bromobenzoic acid, 3-(trifluoromethyl)benzoic acid, thiophene-2-carboxylic acid, magnesium turnings, bromobenzene, 4-bromotoluene, triethylamine, o-phenylenediamine, ethylenediamine, salicylaldehyde, o-vanillin, bismuth(III) chloride, zinc acetate dihydrate, samarium nitrate hexahydrate, lanthanum nitrate hexahydrate, gadolinium nitrate hexahydrate, neodymium nitrate hexahydrate and dysprosium nitrate hexahydrate (these were used as received). Tri-phenylbismuth(V)/tri-p-tolylbismuth(V) dibromide were prepared by a reported methodology [233]. All solvents (toluene, petroleum ether, chloroform, acetone, n-hexane, etc.) utilized here, were of analytical grade and dried before employing the standard procedures [234].

2.2. Instrumentation

The electro-thermal melting point apparatus (model MP-D Mitamura Riken Kogyo Japan) was used in to determine melting points of the synthesized compounds. The IR spectra were recorded on KBr discs, taking advantage of Bio-Rad Excalibur (model FTS 3000 MX) in the range of 4000–400 cm^{-1} . The multinuclear (^1H , ^{13}C) NMR spectra were rolled on Bruker Advance Digital 300 MHz FT-NMR spectrometer for ^1H NMR spectrum and 75MHz for ^{13}C NMR spectrum in deuterated CDCl_3 and $(\text{CD}_3)_2\text{SO}$ as solvent relative to tetramethyl silane (TMS) as internal reference. The single crystal X-ray structures for **7**, **17**, **18**, **19**, **27** and **45** were accomplished at 296(2) K by mounting a crystal of suitable size on thin glass fiber. All the reflections were collected on Kappa APEXII CCD (Bruker) diffractometer equipped by graphite monochromatic radiation MoKa (0.71073Å), whereas

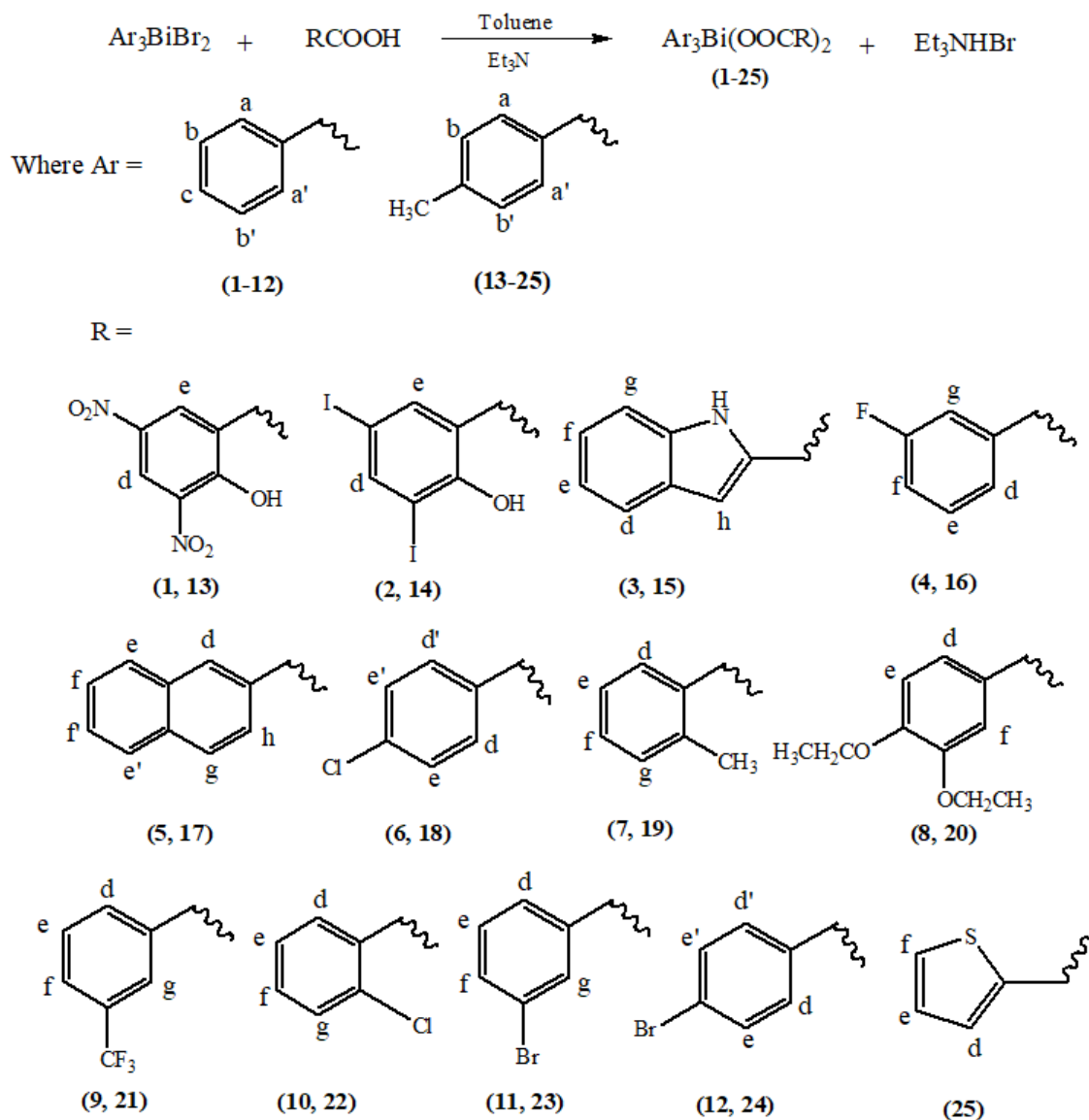
structures were solved using *ShelXT* structure solution program and direct methods structural refinement was conducted with '*SHELXL-2018/3*' (refinement package) employing least squares minimization [235]. The disordered C-atoms were treated as having similar thermal parameters. The H-atoms were positioned geometrically with C-H bond distance and refined as riding [236].

2.3. Synthesis

2.3.1. Preparation of bismuth derivatives

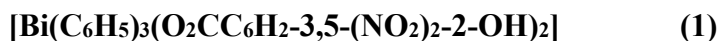
The target compounds (**1-25**) were synthesized by applying the procedure as reported earlier with slight modifications [53, 54, 168]. Triaryl bismuth(III) species, with general formula $\text{Ar}_3\text{Bi(III)}$ (where, Ar = C_6H_5 -, $\text{H}_3\text{C-C}_6\text{H}_4$), were synthesized by reacting the respective Grignard's reagent with BiCl_3 in dry THF under argon at 0°C , stirring the reaction mixture for 8-10 hours followed by extraction in chloroform. The oxidative addition of the respective $\text{Ar}_3\text{Bi(III)}$ species was effected by drop wise introduction of liquid bromine into it to achieve the precursor as $\text{Ar}_3\text{Bi(V) Br}_2$ for subsequent complexation [33].

The target compounds were prepared by utilizing appropriate stoichiometric amounts of the respective ligands (1 mmole), Ar_3BiBr_2 (0.5 mmole) and triethylamine (1 mmole) in 20 mL toluene as a solvent. The reaction mixture was refluxed for 3-4 hours at room temperature under argon gas. The triethylammonium bromide salt, thus formed, was filtered and the clear filtrate was allowed to evaporate at room temperature in to obtain solid compounds, which were recrystallized afterwards in a mixture of chloroform and pet-ether (3:1) to get the pure products (Scheme 2.1).



Scheme 2.1: Synthesis of triorganobismuth(V) carboxylates (1-25)

The spectroscopic and physico-analytical data pertaining to the synthesized compounds are summarized as follows:



Quantities used; 3,5-dinitrosalicylic acid (0.22 g, 1 mmole), triphenylbismuth dibromide (0.3 g, 0.5 mmole), amorphous product, yield: 88%, m.p.: 175-177 °C, Analytical Calculation for $\text{C}_{32}\text{H}_{21}\text{BiN}_4\text{O}_{14}$ (894.51 g/mole), C, 42.97, H, 2.37, N, 6.26%,

Found, C, 42.95, H, 2.39, N, 6.24%; FT-IR data (ν , cm^{-1} , KBr) C-H_{aromatic} (3052), COO_{asym} (1563), COO_{sym} (1356), $\Delta\nu$ (207), Bi-C (520), Bi-O (426); ¹H NMR data (CDCl₃, 300 MHz, ppm) δ 9.03 (2H, s, -OH), 7.79-7.75 (6H, d, Ar- H_a = a', $J=8.1\text{Hz}$), 7.44-7.43 (6H, t, Ar-H_b = b', $J=7.3\text{Hz}$), 7.39 (2H, s, Ar-H_d), 7.37-7.36 (3H, t, Ar-H_c, $J=6.9\text{Hz}$), 7.28 (2H, s, Ar-H_e); ¹³C NMR data (CDCl₃, 75 MHz, ppm) δ 170.1 (COO), 131.3 (C-COO), 130.1 (o-CH_{aromatic}), 129.2 (m-CH_{aromatic}), 134.2 (p-CH_{aromatic}).

[Bi(C₆H₅)₃(O₂CC₆H₂-3,5-I₂-2-OH)₂] (2)

Quantities used; 3,5-diiodosalicylic acid (0.38 g, 1 mmole), triphenylbismuth dibromide (0.3 g, 0.5 mmole), amorphous product, yield: 76%, m.p.: 152-155 °C, Anal. Calcd. for C₃₂H₂₁BiI₄O₆ (1217.73 g/mole), C, 31.55, H, 1.74%, Found, C, 31.53, H, 1.72%; FT-IR data (ν , cm^{-1} , KBr) C-H_{aromatic} (3065), COO_{asym} (1582), COO_{sym} (1350), $\Delta\nu$ (232), Bi-C (515), Bi-O (447); ¹H NMR data (CDCl₃, 300 MHz, ppm) δ 8.93 (2H, s, -OH), 8.32-8.35 (6H, d, Ar- H_a = a', $J=8.1\text{Hz}$), 7.62-7.57 (6H, t, Ar-H_b = b', $J=7.5\text{Hz}$), 7.51 (2H, s, Ar-H_d), 7.53-7.47 (3H, s, Ar-H_c, $J=7.2\text{Hz}$), 7.86 (2H, s, Ar-H_e); ¹³C NMR data (CDCl₃, 75 MHz, ppm) δ 172.2 (COO), 133.2 (C-COO), 131.2 (o-CH_{aromatic}), 130.6 (m-CH_{aromatic}), 133.2 (p-CH_{aromatic}).

[Bi(C₆H₅)₃(O₂CC₈H₅NH)₂] (3)

Quantities used; indole-2-carboxylic acid (0.16 g, 1 mmole), triphenylbismuth dibromide (0.3 g, 0.5 mmole), amorphous product, yield: 72%, m.p.: 169-172 °C, Anal. Calcd. for C₃₆H₂₇BiN₂O₄ (760.59 g/mole), C, 56.85, H, 3.58, N, 3.68%, Found, C, 56.84, H, 3.40, N, 3.69%; FT-IR data (ν , cm^{-1} , KBr) C-H_{aromatic} (3053), COO_{asym} (1571), COO_{sym} (1366), $\Delta\nu$ (205), Bi-C (438), Bi-O (411); ¹H NMR data (CDCl₃, 300 MHz, ppm) δ 9.44 (2H, s, -NH), 8.94 (2H, s, Ar-H_h); 8.34-8.31 (6H, t, Ar- H_b = b', $J=8.1\text{Hz}$), 7.66-7.65 (3H, t, Ar-H_c, $J=5.1\text{Hz}$), 7.62-7.14 (8H, m, Ar-H), 7.52-7.49 (6H, d, Ar- H_a = a', $J=7.2\text{Hz}$); ¹³C NMR data (CDCl₃, 75 MHz, ppm) δ 161.2 (COO), 133.7 (C-COO), 133.3 (o-CH_{aromatic}), 131.7 (m-CH_{aromatic}), 134.2 (p-CH_{aromatic}).

[Bi(C₆H₅)₃(O₂CC₆H₄-3-F)₂] (4)

Quantities used; 3-fluorobenzoic acid (0.14 g, 1 mmole), triphenylbismuth dibromide (0.3 g, 0.5 mmole), crystalline product, yield: 80%, m.p.: 163-165 °C, Anal. Calcd. for C₃₂H₂₃BiF₂O₄ (718.14 g/mole), C, 53.14, H, 3.23%, Found, C, 53.15, H, 3.20%; FT-IR data (ν, cm⁻¹, KBr) C-H_{aromatic} (3062), C-H_{aliphatic} (2961), COO_{asym} (1571), COO_{sym} (1340), Δν (232), Bi-C (506), Bi-O (436); ¹H NMR data (CDCl₃, 300 MHz, ppm) δ 8.32-8.29 (6H, d, Ar-H_a = a', J=7.5Hz), 7.78-7.75 (2H, d, Ar-H_d, J=7.2Hz), 7.66-7.61 (6H, t, Ar-H_b = b', J=7.5Hz), 7.51-7.47 (3H, t, Ar-H_c, J=7.2Hz), 7.35 -7.30 (2H, t, Ar-H_f, J=7.3Hz), 7.28 (2H, s, Ar-H_g), 7.16-7.11 (2H, t, Ar-H_e, J=6.9Hz); ¹³C NMR data (CDCl₃, 75 MHz, ppm) δ 171.2 (COO), 164.0 (Bi-C_{ipso}), 160.7 (C-F), 134.0 (C-COO), 125.6 (o-CH_{aromatic}), 116.9 (m-CH_{aromatic}), 116.6 (p-CH_{aromatic}).

[Bi(C₆H₅)₃(O₂CC₁₀H₇)₂] (5)

Quantities used; 2-naphthoic acid (0.17 g, 1 mmole), triphenylbismuth dibromide (0.3 g, 0.5 mmole), crystalline product, yield: 75%, m.p.: 159 °C, Anal. Calcd. for C₄₀H₂₉BiO₄ (782.64 g/mole), C, 61.39, H, 3.73%, Found, C, 61.36, H, 3.74%; FT-IR data (ν, cm⁻¹, KBr) C-H_{aromatic} (3052), COO_{asym} (1555), COO_{sym} (1323), Δν (232), Bi-C (469), Bi-O (444); ¹H NMR data (CDCl₃, 300 MHz, ppm) δ 8.56 (2H, s, Ar-H_d), 8.42-8.40 (2H, d, Ar-H_h, J=7.2Hz), 8.08-8.05 (2H, d, Ar-H_g, J=7.5Hz), 7.93-7.91 (4H, d, Ar-H_e = e', J=7.5Hz), 7.85-7.79 (4H, t, Ar-H_f = f', J=7.8Hz), 7.66 -7.61 (9H, t, Ar-H_b = b' = c, J=7.5Hz), 7.55-7.53 (6H, d, Ar-H_a = a', J=6.9Hz); ¹³C NMR data (CDCl₃, 75MHz, ppm) δ 160.7 (COO), 134.1 (Bi-C_{ipso}), 131.3 (o-CH_{aromatic}), 130.8 (m-CH_{aromatic}), 129.1 (C-COO), 127.6 (p-CH_{aromatic}).

[Bi(C₆H₅)₃(O₂CC₆H₄-4-Cl)₂] (6)

Quantities used; 4-chlorobenzoic acid (0.16 g, 1 mmole), triphenylbismuth dibromide (0.3 g, 0.5 mmole), crystalline product, yield: 75%, m.p.: 165-168 °C, Anal. Calcd. for C₃₂H₂₃BiCl₂O₄ (750.08 g/mole), C, 51.15, H, 3.09%, Found, C, 51.17, H, 3.06%; FT-IR data (ν, cm⁻¹, KBr) C-H_{aromatic} (3043), C-H_{aliphatic} (2930), COO_{asym} (1590), COO_{sym} (1335), Δν (255), Bi-C (520), Bi-O (444); ¹H NMR data (CDCl₃, 300 MHz, ppm) δ 8.30-

8.28 (6H, d, Ar- H_a = a', *J*=7.5Hz), 7.92-7.90 (4H, d, Ar- H_d = d', *J*=7.8Hz), 7.64-7.59 (6H, t, Ar-H_b = b', *J*=7.5Hz), 7.51-7.46 (3H, t, Ar-H_c, *J*=7.2Hz), 7.32 -7.30 (4H, d, Ar- H_e = e', *J*=7.5Hz); ¹³C NMR data (CDCl₃, 75 MHz, ppm) δ 160.1 (COO), 134.0 (C-Cl), 131.3 (Bi-C_{ipso}), 130.9 (C-COO), 128.5 (o-CH_{aromatic}), 127.7 (m-CH_{aromatic}), 126.9 (p-CH_{aromatic}).

[Bi(C₆H₅)₃(O₂CC₆H₄-2-CH₃)₂] (7)

Quantities used; 2-methylbenzoic acid (0.14 g, 1 mmole), triphenylbismuth dibromide (0.3 g, 0.5 mmole), crystalline product, yield: 81%, m.p.: 128 °C, Anal. Calcd. for C₃₄H₂₉BiO₄ (710.57 g/mole), C, 57.47, H, 4.11%, Found, C, 57.48, H, 4.12%; FT-IR data (ν, cm⁻¹, KBr) C-H_{aromatic} (3052), C-H_{aliphatic} (2962), COO_{asym} (1547), COO_{sym} (1336), Δν (211), Bi-C (488), Bi-O (444); ¹H NMR data (CDCl₃, 300 MHz, ppm) δ 8.37-8.35 (6H, d, Ar- H_a = a', *J*=7.2Hz), 7.74-7.72 (2H, d, Ar-H_d, *J*=7.5Hz), 7.64-7.59 (6H, t, Ar-H_b = b', *J*=7.5Hz), 7.51-7.46 (3H, t, Ar-H_c, *J*=7.2Hz), 7.28-7.24 (2H, t, Ar- H_e, *J*=7.5Hz), 7.17-7.11 (4H, t, Ar- H_{f, g}, *J*=7.5Hz), 2.41 (6H, s, -CH₃); ¹³C NMR data (CDCl₃, 75 MHz, ppm) δ 174.8 (COO), 161.5 (Bi-C_{ipso}), 138.6 (C-CH₃), 133.3 (C-COO), 134.1 (o-CH_{aromatic}), 131.0 (m, p-CH_{aromatic}), 21.4 (-CH₃).

[Bi(C₆H₅)₃(O₂CC₆H₃-3,4-(OCH₂CH₃)₂)₂] (8)

Quantities used; 3,4-diethoxybenzoic acid (0.21 g, 1 mmole), triphenylbismuth dibromide (0.3 g, 0.5 mmole), crystalline product, yield: 82%, m.p.: 170 °C, Anal. Calcd. for C₄₀H₄₁BiO₈ (858.73 g/mole), C, 55.95, H, 4.81%, Found, C, 55.93, H, 4.80%; FT-IR data (ν, cm⁻¹, KBr) C-H_{aromatic} (3051), C-H_{aliphatic} (2982), COO_{asym} (1558), COO_{sym} (1327), Δν (231), Bi-C (510), Bi-O (443); ¹H NMR data (CDCl₃, 300 MHz, ppm) δ 8.32-8.30 (6H, d, Ar-H_a = a', *J*=7.5Hz), 7.63-7.61 (6H, t, Ar-H_b = b', *J*=4.8Hz), 7.59 (2H, s, Ar-H_f), 7.57-7.48 (3H, t, Ar- H_c, *J*=13.2Hz), 7.45-7.43 (2H, d, Ar- H_d, *J*=7.2Hz), 6.83 -6.81 (2H, d, Ar- H_e, *J*=8.4Hz), 4.15-4.08 (8H, q, -CH₂, *J*=6.6Hz), 1.47-1.43 (12H, t, -CH₃, *J*=6.6 Hz); ¹³C NMR data (CDCl₃, 75 MHz, ppm) δ 172.4 (COO), 161.1 (Bi-C_{ipso}), 151.7 (C₃-OEt), 147.7 (C₄-OEt), 133.9 (o-CH_{aromatic}), 131.2 (m-CH_{aromatic}), 130.6 (p-CH_{aromatic}), 64.5 (-CH₂), 14.8 (-CH₃).

[Bi(C₆H₅)₃(O₂CC₆H₄-2-CF₃)₂] (9)

Quantities used; 3-(trifluoromethyl)benzoic acid (0.19 g, 1 mmole), triphenylbismuth dibromide (0.3 g, 0.5 mmole), amorphous product, yield: 88%, m.p.: 165-167 °C, Anal. Calcd. for C₃₄H₂₃BiF₆O₄ (818.13 g/mole), C, 49.89, H, 2.83%, Found, C, 49.91, H, 2.82%; FT-IR data (ν, cm⁻¹, KBr) C-H_{aromatic} (3053), COO_{asym} (1561), COO_{sym} (1358), Δν (203), Bi-C (443), Bi-O (424); ¹H NMR data (CDCl₃, 300 MHz, ppm) δ 8.33-8.31 (6H, d, Ar- H_a=_{a'}, J=7.2Hz), 7.30 (2H, s, Ar- H_g), 8.12-8.15 (2H, d, Ar- H_d, J=7.2Hz), 7.68-7.63 (2H, t, Ar-H_c, J=7.5Hz), 7.54-7.48 (6H, d, Ar-H_b=_{b'}, J=7.5Hz); ¹³C NMR data (CDCl₃, 75 MHz, ppm) δ 171.1 (COO), 133.7 (C-COO), 131.5 (o-CH_{aromatic}), 128.2 (m-CH_{aromatic}), 134.0 (p-CH_{aromatic}).

[Bi(C₆H₅)₃(O₂CC₆H₄-2-Cl)₂] (10)

Quantities used; 2-chlorobenzoic acid (0.16 g, 1 mmole), triphenylbismuth dibromide (0.3 g, 0.5 mmole), crystalline product, yield: 75%, m.p.: 138 °C, Anal. Calcd. for C₃₂H₂₃BiCl₂O₄ (750.41 g/mole), C, 51.15, H, 3.09%, Found, C, 51.17, H, 3.06%; FT-IR data (ν, cm⁻¹, KBr) C-H_{aromatic} (3062), COO_{asym} (1587), COO_{sym} (1347), Δν (240), Bi-C (464), Bi-O (405); ¹H NMR data (CDCl₃, 300 MHz, ppm) δ 8.40-8.37 (6H, d, Ar- H_a=_{a'}, J=7.2 Hz), 7.69-6.70 (6H, d, Ar-H_b=_{b'}, J=6.9Hz), 7.65-7.62 (2H, d, Ar- H_d, J=6.9Hz), 7.53-7.50 (6H, m, Ar-H_{e, f, g}), 7.31-7.26 (3H, t, Ar-H_c, J=8.7Hz); ¹³C NMR data (CDCl₃, 75 MHz, ppm) δ 172.2 (COO), 159.7 (Bi-C_{ipso}), 134.3 (o-CH_{aromatic}), 133.9 (C-Cl), 131.7 (C-COO), 131.4 (m, p-CH_{aromatic}).

[Bi(C₆H₅)₃(O₂CC₆H₄-3-Br)₂] (11)

Quantities used; 3-bromobenzoic acid (0.20 g, 1 mmole), triphenylbismuth dibromide (0.3 g, 0.5 mmole), crystalline product, yield: 88%, m.p.: 133-136 °C, Anal. Calcd. for C₃₂H₂₃BiBr₂O₄ (840.31 g/mole), C, 45.74, H, 2.76%, Found, C, 45.72, H, 2.75%; FT-IR data (ν, cm⁻¹, KBr) C-H_{aromatic} (3053), COO_{asym} (1594), COO_{sym} (1369), Δν (232), Bi-C (528), Bi-O (417); ¹H NMR data (CDCl₃, 300 MHz, ppm) δ 8.35-8.33 (6H, d, Ar- H_a=_{a'}, J=7.2Hz), 8.02-8.00 (2H, d, Ar-H_d, J=7.5 Hz), 7.64-7.58 (6H, t, Ar-H_b=_{b'}, J=7.8Hz), 7.49-7.43 (3H, t, Ar- H_c, J=7.5Hz), 7.38-7.33 (2H, t, Ar- H_e, J=7.2Hz), 7.28 (2H, s, Ar-

H_g); ¹³C NMR data (CDCl₃, 75 MHz, ppm) δ 172.4 (COO), 164.0, 133.2 (C-COO), 131.2 (o-CH_{aromatic}), 127.9 (m-CH_{aromatic}), 134.0 (p-CH_{aromatic}).

[Bi(C₆H₅)₃(O₂CC₆H₄-4-Br)₂] (12)

Quantities used; 4-bromobenzoic acid (0.20 g, 1 mmole), triphenylbismuth dibromide (0.3 g, 0.5 mmole), crystalline product, yield: 88%, m.p.: 122-125 °C, Anal. Calcd. for C₃₂H₂₃BiBr₂O₄ (840.31 g/mole), C, 45.74, H, 2.76%, Found, C, 45.75, H, 2.77%; FT-IR data (ν, cm⁻¹, KBr) C-H_{aromatic} (3053), COO_{asym} (1596), COO_{sym} (1358), Δν (238), Bi-C (528), Bi-O (415); ¹H NMR data (CDCl₃, 300 MHz, ppm) δ 8.36-8.33 (6H, d, Ar-H_a = a', J=7.5Hz), 8.03-8.00 (4H, d, Ar-H_d=d', J=7.5 Hz), 7.64-7.59 (6H, t, Ar-H_b=b', J=7.8Hz), 7.49-7.47 (4H, d, Ar-H_e=e', J=7.2 Hz), 7.39-7.34 (3H, t, Ar-H_c, J=7.5Hz); ¹³C NMR data (CDCl₃, 75 MHz, ppm) δ 172.4 (COO), 133.2 (C-COO), 131.2 (o-CH_{aromatic}), 127.9 (m-CH_{aromatic}), 134.0 (p-CH_{aromatic}).

[Bi(p-toly)₃(O₂CC₆H₂-3,5-(NO₂)₂-2-OH)₂] (13)

Quantities used; 3,5-dinitrosalicylic acid (0.22 g, 1 mmole), p-tritolylbismuth dibromide (0.31 g, 0.5 mmole), crystalline product, yield: 72%, m.p.: 155-157 °C, Anal. Calcd. for C₃₅H₂₇BiN₄O₁₄ (936.59 g/mole), C, 44.88, H, 2.91, N, 5.98%, Found, C, 44.89, H, 2.94, N, 5.96%; FT-IR data (ν, cm⁻¹, KBr) C-H_{aromatic} (3059), C-H_{aliphatic} (2924), COO_{asym} (1574), COO_{sym} (1349), Δν (225), Bi-C (478), Bi-O (420); ¹H NMR data (CDCl₃, 300 MHz, ppm) δ 9.12 (2H, s, -OH), 8.38-8.40 (6H, d, Ar-H_a = a', J=7.5Hz), 7.74-7.76 (6H, t, Ar-H_b=b', J=7.3Hz), 7.79 (s, 2H, Ar-H_d), 7.79 (s, 2H, Ar-H_e), 2.42 (s, 9H, -CH₃); ¹³C NMR data (75 MHz, CDCl₃, ppm) δ 172.8 (COO), 141.8 (C-COO), 134.8 (o-CH_{aromatic}), 130.2 (m-CH_{aromatic}), 141.8 (p-CH_{aromatic}), 21.4 (CH₃-CH_{aromatic}).

[Bi(p-toly)₃(O₂CC₆H₂-3,5-I₂-2-OH)₂] (14)

Quantities used; 3,5-diiodosalicylic acid (0.38 g, 1 mmole), p-tritolylbismuth dibromide (0.31 g, 0.5 mmole), amorphous product, yield: 75%, m.p.: 143-145 °C, Anal. Calcd. for C₃₅H₂₇BiI₄O₆ (1260.18 g/mole), C, 33.36, H, 2.16%, Found, C, 33.37, H, 2.14%; FT-IR data (ν, cm⁻¹, KBr) C-H_{aromatic} (3063), C-H_{aliphatic} (2965), COO_{asym} (1564), COO_{sym}

(1353), $\Delta\nu$ (211), Bi-C (482), Bi-O (437); ^1H NMR data (CDCl_3 , 300 MHz, ppm) δ 8.85 (2H, s, -OH), 8.38-8.35 (6H, d, Ar- $\text{H}_{a=a'}$, $J=8.4\text{Hz}$), 7.65-7.63 (6H, t, Ar- $\text{H}_{b=b'}$, $J=7.8\text{Hz}$), 7.46 (2H, s, Ar- H_d), 7.10 (2H, s, Ar- H_e), 2.41 (9H, s, $-\text{CH}_3$); ^{13}C NMR data (CDCl_3 , 75 MHz, ppm) δ 171.9 (COO), 133.7 (C-COO), 133.1 (o- $\text{CH}_{\text{aromatic}}$), 129.1 (m- $\text{CH}_{\text{aromatic}}$), 141.1 (p- $\text{CH}_{\text{aromatic}}$), 21.4 ($\text{CH}_3\text{-CH}_{\text{aromatic}}$).

[Bi(p-toly) $_3$ (O $_2$ CC $_8$ H $_5$ NH) $_2$] (15)

Quantities used; indole-2-carboxylic acid (0.16 g, 1 mmole), p-tritolylbismuth dibromide (0.31 g, 0.5 mmole), amorphous product, yield: 70%, m.p.: 181-183 °C, Anal. Calcd. for $\text{C}_{39}\text{H}_{33}\text{BiN}_2\text{O}_4$ (802.67 g/mole), C, 58.36, H, 4.14, N, 3.49%, Found, C, 58.37, H, 4.15, N, 3.51%; FT-IR data (ν , cm^{-1} , KBr) C- $\text{H}_{\text{aromatic}}$ (3053), C- $\text{H}_{\text{aliphatic}}$ (2963), COO_{asym} (1557), COO_{sym} (1352), $\Delta\nu$ (205), Bi-C (533), Bi-O (442); ^1H NMR data (CDCl_3 , 300 MHz, ppm) δ 9.46 (2H, s, -NH), 8.34-8.31 (6H, d, Ar- $\text{H}_{a=a'}$, $J=8.1\text{Hz}$), 8.15-8.12 (6H, d, Ar- $\text{H}_{b=b'}$, $J=7.5\text{Hz}$), 7.52-7.37 (8H, m, Ar-H), 7.73 (2H, s, Ar- H_d), 7.10 (2H, s, Ar- H_e), 2.41 (9H, s, $-\text{CH}_3$); ^{13}C NMR data (CDCl_3 , 75 MHz, ppm) δ 168.5 (COO), 138.2 (C-COO), 130.9 (o- $\text{CH}_{\text{aromatic}}$), 129.7 (m- $\text{CH}_{\text{aromatic}}$), 140.1 (p- $\text{CH}_{\text{aromatic}}$), 21.4 ($\text{CH}_3\text{-CH}_{\text{aromatic}}$).

[Bi(p-toly) $_3$ (O $_2$ CC $_6$ H $_4$ -3-F) $_2$] (16)

Quantities used; 3-fluorobenzoic acid (0.14 g, 1 mmole), p-tritolylbismuth dibromide (0.31 g, 0.5 mmole), crystalline product, yield: 73%, m.p.: 156-160 °C, Anal. Calcd. for $\text{C}_{35}\text{H}_{29}\text{BiFO}_4$ (760.18 g/mole), C, 55.27, H, 3.84%, Found, C, 55.29, H, 3.81%; FT-IR data (ν , cm^{-1} , KBr) C- $\text{H}_{\text{aromatic}}$ (3061), C- $\text{H}_{\text{aliphatic}}$ (2919), COO_{asym} (1579), COO_{sym} (1342), $\Delta\nu$ (236), Bi-C (473), Bi-O (438); ^1H NMR data (CDCl_3 , 300 MHz, ppm) δ 8.19-8.18 (6H, d, Ar- $\text{H}_{a=a'}$, $J=7.4\text{Hz}$), 7.89-7.69 (6H, t, Ar- $\text{H}_{b=b'}$, $J=6.7\text{Hz}$), 7.46-7.44 (2H, d, Ar- H_d , $J=6.6\text{Hz}$), 7.41-7.38 (2H, d, Ar- H_f , $J=8.7\text{Hz}$), 7.31 (2H, s, Ar- H_g), 7.26-7.15 (2H, t, Ar- H_e , $J=7.4\text{Hz}$), 2.39 (9H, s, $-\text{CH}_3$); ^{13}C NMR data (CDCl_3 , 75 MHz, ppm) δ 170.9 (COO), 164.1 (Bi- C_{ipso}), 160.8 (C-F), 158.0, 154.0 (C-COO), 125.7 (o- $\text{CH}_{\text{aromatic}}$), 118.3 (m- $\text{CH}_{\text{aromatic}}$), 21.4 ($\text{CH}_3\text{-CH}_{\text{aromatic}}$).

[Bi(p-toly)₃(O₂CC₁₀H₇)₂] (17)

Quantities used; 2-naphthoic acid (0.17 g, 1 mmole), p-tritolylbismuth dibromide (0.31 g, 0.5 mmole), crystalline product, yield: 78%, m.p.: 232 °C, Anal. Calcd. for C₄₃H₃₅BiO₄ (824.72 g/mole), C, 62.62, H, 4.28%, Found, C, 62.62, H, 4.27%; FT-IR data (ν, cm⁻¹, KBr) C-H_{aromatic} (3055), C-H_{aliphatic} (2961), COO_{asym} (1562), COO_{sym} (1326), Δν (236), Bi-C (470), Bi-O (415); ¹H NMR data (CDCl₃, 300 MHz, ppm) δ 8.56 (2H, s, Ar-H_d), 8.29-8.27 (2H, d, Ar-H_h, J=8.1Hz), 8.08-8.06 (2H, d, Ar-H_g, J=7.8Hz), 7.93-7.91 (4H, d, Ar-H_{e=e'}, J=6.3Hz), 7.85-7.79 (4H, t, Ar-H_{f=f'}, J=7.8Hz), 7.52-7.49 (6H, d, Ar-H_{a=a'}, J=8.1Hz), 7.44-7.41 (6H, d, Ar-H_{b=b'}, J=8.1Hz), 2.41 (9H, s, -CH₃); ¹³C NMR data (CDCl₃, 75 MHz, ppm) δ 157.1 (COO), 1401.0 (Bi-C_{ipso}), 133.9 (o-CH_{aromatic}), 131.8 (m-CH_{aromatic}), 130.8 (CCOO), 127.4 (p-CH_{aromatic}), 21.4 (-CH₃).

[Bi(p-toly)₃(O₂CC₆H₄-4-Cl)₂] (18)

Quantities used; 4-chlorobenzoic acid (0.16 g, 1 mmole), p-tritolylbismuth dibromide (0.31 g, 0.5 mmole), crystalline product, yield: 80%, m.p.: 150-155 °C, Anal. Calcd. for C₃₅H₂₉BiCl₂O₄ (792.12 g/mole), C, 52.98, H, 3.68%, Found, C, 52.96, H, 3.70%; FT-IR data (ν, cm⁻¹, KBr) C-H_{aromatic} (3054), C-H_{aliphatic} (2920), COO_{asym} (1587), COO_{sym} (1339), Δν (248), Bi-C (473), Bi-O (445); ¹H NMR data (CDCl₃, 300 MHz, ppm) δ 8.17-8.15 (6H, d, Ar-H_{a=a'}, J=8.4Hz), 7.92-7.90 (4H, d, Ar-H_{d=d'}, J=8.4Hz), 7.43-7.40 (6H, d, Ar-H_{b=b'}, J=9Hz), 7.32-7.29 (4H, d, Ar-H_{e=e'}, J=8.1Hz), 7.31 (2H, s, Ar-H_g), 2.38 (9H, s, -CH₃); ¹³C NMR data (CDCl₃, 75 MHz, ppm) δ 171.2 (COO), 156.6 (C-F), 141.2 (Bi-C_{ipso}), 158.0, 133.6 (C-COO), 133.8 (o-CH_{aromatic}), 131.9 (m-CH_{aromatic}), 21.4 (CH₃-CH_{aromatic}).

[Bi(p-toly)₃(O₂CC₆H₄-2-CH₃)₂] (19)

Quantities used; 2-methylbenzoic acid (0.14 g, 1 mmole), p-tritolylbismuth dibromide (0.31 g, 0.5 mmole), crystalline product, yield: 75%, m.p.: 151 °C, Anal. Calcd. for C₃₇H₃₅BiO₄ (752.65 g/mole), C, 59.04, H, 4.69%, Found, C, 59.02, H, 4.71%; FT-IR data (ν, cm⁻¹, KBr) C-H_{aromatic} (3053), C-H_{aliphatic} (2964), COO_{asym} (1588), COO_{sym} (1338), Δν (250), Bi-C (474), Bi-O (434); ¹H NMR data (CDCl₃, 300 MHz, ppm) δ 8.24-8.22 (6H, d, Ar-H_{a=a'}, J=8.4Hz), 7.75-7.31 (2H, d, Ar-H_d, J=6Hz), 7.46-7.39 (6H, t, Ar-H_{b=b'},

$J=8.1\text{Hz}$), 7.42-7.39 (2H, d, Ar-H_g, $J=8.1\text{Hz}$), 7.28-7.12 (4H, t, Ar-H_{e, f}, $J=9\text{Hz}$), 2.41 (15H, s, -CH₃); ¹³C NMR data (CDCl₃, 75 MHz, ppm) δ 174.5 (COO), 170.4 (Bi-C_{ipso}), 158.0 (C-CH₃), 141.5 (p-CH₃), 140.8 (C-COO), 133.9 (o-CH_{aromatic}), 131.0 (m-CH_{aromatic}), 22.0 (CH₃-CH_{aromatic}), 21.4 (CH₃-p-CH_{aromatic}).

[Bi(p-toly)₃(O₂CC₆H₃-3,4-(OCH₂CH₃)₂)] (20)

Quantities used; 3,4-diethoxybenzoic acid (0.21 g, 1 mmole), p-tritolylbismuth dibromide (0.31 g, 0.5 mmole), crystalline product, yield: 75%, m.p.: 201 °C, Anal. Calcd. for C₄₃H₄₇BiO₈ (900.81 g/mole), C, 57.33, H, 5.26%, Found, C, 57.34, H, 45.26%; FT-IR data (ν , cm⁻¹, KBr) C-H_{aromatic} (2984), C-H_{aliphatic} (2922), COO_{asym} (1549), COO_{sym} (1351), $\Delta\nu$ (198), Bi-C (474), Bi-O (434); ¹H NMR data (CDCl₃, 300 MHz, ppm) δ 8.19-8.16 (6H, d, Ar-H_{a = a'}, $J=8.1\text{Hz}$), 7.62-7.59 (2H, t, Ar-H_d, $J=4.8\text{Hz}$), 7.52 (2H, s, Ar-H_f), 7.40-7.37 (6H, d, Ar-H_{b = b'}, $J=8.1\text{Hz}$), 6.82-6.80 (2H, d, Ar-H_e, $J=8.1\text{Hz}$), 4.15-4.08 (8H, q, -CH₂, $J=6.6\text{Hz}$), 2.37 (9H, s, p-CH₃), 1.47-1.43 (12H, t, -CH₃, $J=6.9\text{Hz}$); ¹³C NMR data (CDCl₃, 75 MHz, ppm) δ 172.1 (COO), 154.4 (C₃-OEt), 151.5 (C₄-OEt), 140.8 (p-CH_{aromatic}), 133.8 (o-CH_{aromatic}), 132.1 (m-CH_{aromatic}), 64.5 (-CH₂), 21.4 (p-CH_{3aromatic}), 14.6 (-CH₃).

[Bi(p-toly)₃(O₂CC₆H₄-3-CF₃)₂] (21)

Quantities used; 3-(trifluoromethyl)benzoic acid (0.19 g, 1 mmole), p-tritolylbismuth dibromide (0.31 g, 0.5 mmole), crystalline product, yield: 88%, m.p.: 155-157 °C, Anal. Calcd. for C₃₇H₂₉BiF₆O₄ (860.59 g/mole), C, 51.64, H, 3.40%, Found, C, 51.65, H, 3.38%; FT-IR data (ν , cm⁻¹, KBr) C-H_{aromatic} (3044), C-H_{aliphatic} (2953), COO_{asym} (1589), COO_{sym} (1352), $\Delta\nu$ (237), Bi-C (475), Bi-O (444); ¹H NMR data (CDCl₃, 300 MHz, ppm) δ 8.24 (2H, s, Ar-H_g), 8.20-8.17 (6H, d, Ar-H_{a = a'}, $J=8.1\text{Hz}$), 7.69-7.67 (2H, d, Ar-H_d, $J=7.2\text{Hz}$), 7.46-7.43 (6H, d, Ar-H_{b = b'}, $J=8.1\text{Hz}$), 2.38 (9H, s, p-CH₃); ¹³C NMR data (CDCl₃, 75 MHz, ppm) δ 170.7 (COO), 134.3 (C-COO), 133.6 (o-CH_{aromatic}), 128.4 (m-CH_{aromatic}), 140.8 (p-CH_{aromatic}), 21.4 (CH₃-CH_{aromatic}).

[Bi(p-toly)₃(O₂CC₆H₄-2-Cl)₂] (22)

Quantities used; 2-chlorobenzoic acid (0.16 g, 1 mmole), p-tritolylbismuth dibromide (0.31 g, 0.5 mmole), crystalline product, yield: 75%, m.p.: 110 °C, Anal. Calcd. for C₃₅H₂₉BiCl₂O₄ (793.49 g/mole), C, 52.98, H, 3.68%, Found, C, 52.95, H, 3.70%; FT-IR data (ν, cm⁻¹, KBr) C-H_{aromatic} (3068), C-H_{aliphatic} (2917), COO_{asym} (1585), COO_{sym} (1353), Δν (232), Bi-C (472), Bi-O (426); ¹H NMR data (CDCl₃, 300 MHz, ppm) δ 8.26-8.24 (6H, d, Ar-H_a = a', J=8.1Hz), 7.52-7.42 (8H, m, Ar-H_{d, e, f, g}), 7.27-7.24 (6H, d, Ar-H_{b=b'}, J=8.1Hz), 2.41 (9H, s, -CH₃); ¹³C NMR data (CDCl₃, 75 MHz, ppm) δ 156.2 (COO), 154.1 (Bi-C_{ipso}), 141.7 (C-Cl), 141.2 (p-CH_{aromatic}), 138.2 (CCOO), 134.1 (o-CH_{aromatic}), 132.1 (m-CH_{aromatic}), 21.4 (-CH₃).

[Bi(p-toly)₃(O₂CC₆H₄-3-Br)₂] (23)

Quantities used; 3-bromobenzoic acid (0.20 g, 1 mmole), p-tritolylbismuth dibromide (0.31 g, 0.5 mmole), crystalline product, yield: 91%, m.p.: 220-223 °C, Anal. Calcd. for C₃₅H₂₉BiBr₂O₄ (882.39 g/mole), C, 47.64, H, 3.31%, Found, C, 47.62, H, 3.30%; FT-IR data (ν, cm⁻¹, KBr) C-H_{aromatic} (3065), C-H_{aliphatic} (2983), COO_{asym} (1558), COO_{sym} (1337), Δν (221), Bi-C (474), Bi-O (417); ¹H NMR data (CDCl₃, 300 MHz, ppm) δ 8.23-8.22 (6H, d, Ar-H_a = a', J=7.1Hz), 8.01-7.99 (2H, d, Ar-H_d, J=6.6Hz), 7.41-7.38 (6H, d, Ar-H_{b=b'}, J=8.1Hz), 7.28 (2H, s, Ar-H_g) 2.37 (9H, s, -CH₃); ¹³C NMR data (CDCl₃, 75 MHz, ppm) δ 172.2 (COO), 139.9 (C-COO), 132.1 (o-CH_{aromatic}), 129.4 (m-CH_{aromatic}), 141.0 (p-CH_{aromatic}), 21.4 (CH₃-CH_{aromatic}).

[Bi(p-toly)₃(O₂CC₆H₄-4-Br)₂] (24)

Quantities used; 4-bromobenzoic acid (0.20 g, 1 mmole), p-tritolylbismuth dibromide (0.31 g, 0.5 mmole), crystalline product, yield: 74%, m.p.: 186-187 °C, Anal. Calcd. for C₃₅H₂₉BiBr₂O₄ (882.39 g/mole), C, 47.64, H, 3.31%, Found, C, 47.63, H, 3.30%; FT-IR data (ν, cm⁻¹, KBr) C-H_{aromatic} (3051), C-H_{aliphatic} (2921), COO_{asym} (1587), COO_{sym} (1336), Δν (231), Bi-C (474), Bi-O (420); ¹H NMR data (CDCl₃, 300 MHz, ppm) δ 8.22-8.19 (6H, d, Ar-H_a = a', J=8.4Hz), 8.01-7.99 (4H, d, Ar-H_{d=d'}, J=8.4Hz), 7.41-7.39 (6H, d, Ar-H_{b=b'}, J=8.1Hz), 2.37 (9H, s, -CH₃); ¹³C NMR data (CDCl₃, 75 MHz, ppm) δ 172.1

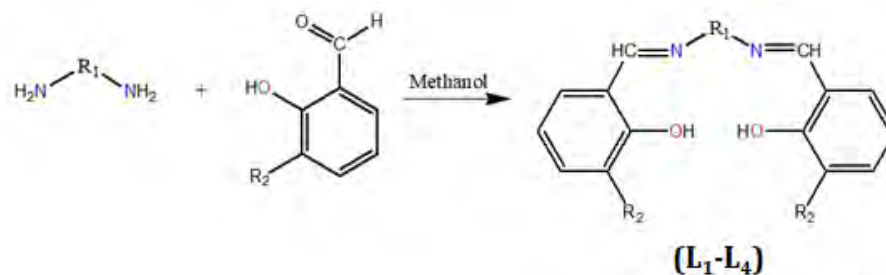
(COO), 133.9 (C-COO), 131.4 (o-CH_{aromatic}), 127.8 (m-CH_{aromatic}), 140.9 (p-CH_{aromatic}), 21.4 (CH₃-CH_{aromatic}).

[Bi(p-toly)₃(O₂CC₄H₃S)₂] (25)

Quantities used; 2-thiophene carboxylic acid (0.13 g, 1 mmole), p-tritolylbismuth dibromide (0.31 g, 0.5 mmole), crystalline product, yield: 72%, m.p.: 172-175 °C, Anal. Calcd. for C₃₁H₂₇BiS₂O₄ (736.65 g/mole), C, 50.54, H, 3.69%, Found, C, 50.55, H, 3.70%; FT-IR data (ν, cm⁻¹, KBr) C-H_{aromatic} (3077), C-H_{aliphatic} (2917), COO_{asym} (1574), COO_{sym} (1363), Δν (211), Bi-C (472), Bi-O (406); ¹H NMR data (CDCl₃, 300 MHz, ppm) δ 8.24-8.21 (6H, d, Ar-H_a=_{a'}, J=8.4Hz), 8.20-8.17 (2H, d, Ar-H_d, J=8.1Hz), 7.43-7.40 (6H, d, Ar-H_b=_{b'}, J=8.1Hz), 2.37 (9H, s, -CH₃); ¹³C NMR data (CDCl₃, 75 MHz, ppm) δ 167.3 (COO), 138.2 (C-COO), 134.3 (o-CH_{aromatic}), 133.7 (m-CH_{aromatic}), 141.6 (p-CH_{aromatic}), 21.4 (CH₃-CH_{aromatic}).

2.3.2. Bi-compartmental Schiff base ligands

The bi-compartmental Schiff base ligands (**L₁-L₄**) were synthesized in excellent yield using already reported procedure via condensation reaction between substituted-diamine (1 mole) and substituted-aldehyde (2 mole) in methanol, refluxing for 2-3 h [237, 238]. The resulting precipitates were filtered, recrystallized in suitable solvent and employing for complexation as detailed in Scheme 2.2.

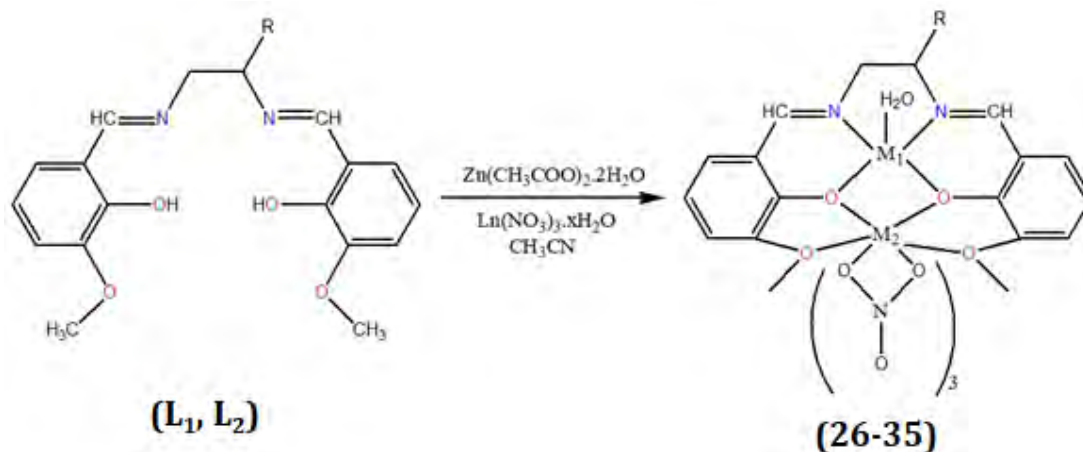


Ligands	R ₁	R ₂
L ₁		-OCH ₃
L ₂		-OCH ₃
L ₃		-H
L ₄		-H

Scheme 2.2 Synthetic route for Schiff base ligands (L₁-L₄)

2.3.3. Heterodi-/trinuclear 3d/4f complexes

Synthesis of target complexes (**26-45**) was done by refluxing stoichiometric amounts (1:1) of clear methanolic solution of $\text{Zn}(\text{CH}_3\text{COO})_2 \cdot 2\text{H}_2\text{O}$ and the appropriate ligand (**L₁-L₂**) in a round bottom flask for 3h to obtain yellow precipitates of $[\text{Zn}(\text{H}_2\text{L})\text{H}_2\text{O}]$ (**1**), which were then filtered and recrystallized in chloroform and pet-ether (3:1) to get the pure product. In order to yield di-/trinuclear 3d/4f complexes (**26-45**), already prepared monometallic Zn-complex was dissolved in 15mL of acetonitrile to get turbid solution, followed by the addition of the respective rare earth metal salts [as $\text{Ln}(\text{NO}_3)_3 \cdot x\text{H}_2\text{O}$]. The resulting solution was stirred for 4-5h to become clear solution, which was allowed to evaporate at room temperature to secure crude solid product as shown in Schemes 2.3 and 2.4. The recrystallization was carried out in appropriate mixture of solvents, such as acetone and n-hexane (3:1) [237, 238].



Where,

R = -H (L₁), -CH₃ (L₂)

M₁ = Zn (26-35)

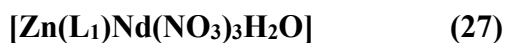
M₂ = La (26,31), Nd (27, 32), Sm (28, 33), Gd (29, 34), Dy (30,35)

Scheme 2.3. Synthesis of heterodinuclear 3d/4f complexes

The spectroscopic and physico-analytical data for the compounds **(26-35)** are summarized as follows:



Quantities used: [Zn(L₁)H₂O] (1mmole, 0.32g), La(NO₃)₃.6H₂O (1mmole, 0.33g), amorphous product, yield : 72%, m.p.: 325-327°C, Anal. Calcd. for C₁₈H₂₀N₅LaO₁₄Zn (735g/mole), C, 29.40, H, 2.73, N, 9.54%, Found: C, 29.38, H, 2.72, N, 9.52%, FT-IR (ν, cm⁻¹, KBr): O-H (3331), C=N (1461), C-O (1278), Zn-N (532), Zn-O (490), La-O (435).



Quantities used: [Zn(L₁)H₂O] (1mmole, 0.32g), Nd(NO₃)₃.6H₂O (1mmole, 0.43g), amorphous product, yield : 85%, m.p.: 332-335°C, Anal. Calcd. for C₁₈H₂₀N₅NdO₁₄Zn

(740g/mole), C, 29.16, H, 2.74, N, 9.43%, Found: C, 29.18, H, 2.70, N, 9.45%, FT-IR (ν , cm^{-1} , KBr): O-H (3345), C=N (1453), C-O (1274), Zn-N (530), Zn-O (507), Nd-O (448).

[Zn(L₁)Sm(NO₃)₃H₂O] (28)

Quantities used: [Zn(L₁)H₂O] (1mmole, 0.32g), Sm(NO₃)₃.6H₂O (1mmole, 0.44g), amorphous product, yield : 80%, m.p.: 320-322°C, Anal. Calcd. for C₁₈H₂₀N₅SmO₁₄Zn (746g/mole), C, 29.98, H, 2.66, N, 9.41%, Found: C, 29.95, H, 2.68, N, 9.38%, FT-IR (ν , cm^{-1} , KBr): O-H (3355), C=N (1453), C-O (1275), Zn-N (597), Zn-O (507), Sm-O (449).

[Zn(L₁)Gd(NO₃)₃H₂O] (29)

Quantities used: [Zn(L₁)H₂O] (1mmole, 0.32g), Gd(NO₃)₃.6H₂O (1mmole, 0.46g), amorphous product, yield : 82%, m.p.: 362-364°C, Anal. Calcd. for C₁₈H₂₀N₅GdO₁₄Zn (753g/mole), C, 28.69, H, 2.66, N, 9.32%, Found: C, 28.68, H, 2.65, N, 9.29%, FT-IR (ν , cm^{-1} , KBr): O-H (3355), C=N (1454), C-O (1277), Zn-N (599), Zn-O (509), Gd-O (452).

[Zn(L₁)Dy(NO₃)₃H₂O] (30)

Quantities used: [Zn(L₁)H₂O] (1mmole, 0.32g), Dy(NO₃)₃.6H₂O (1mmole, 0.35g), amorphous product, yield : 77%, m.p.: 333-335°C, Anal. Calcd. for C₁₈H₂₀N₅DyO₁₄Zn (758.5g/mole), C, 28.49, H, 2.61, N, 9.23%, Found: C, 28.47, H, 2.63, N, 9.22%, FT-IR (ν , cm^{-1} , KBr): O-H (3226), C=N (1461), C-O (1279), Zn-N (567), Zn-O (517), Dy-O (448).

[Zn(L₂)La(NO₃)₃H₂O] (31)

Quantities used: [Zn(L₂)H₂O] (1mmole, 0.34g), La(NO₃)₃.6H₂O (1mmole, 0.33g), amorphous product, yield : 72%, m.p.: 335-337°C, Anal. Calcd. for C₁₉H₂₂N₅LaO₁₄Zn (749g/mole), C, 30.43, H, 2.92, N, 9.30%, Found: C, 30.44, H, 2.93, N, 9.34%, FT-IR (ν , cm^{-1} , KBr): O-H (3358), C=N (1460), C-O (1272), Zn-N (538), Zn-O (506), La-O (441).

[Zn(L₂)Nd(NO₃)₃H₂O] (32)

Quantities used: [Zn(L₂)H₂O] (1mmole, 0.34g), Nd(NO₃)₃.6H₂O (1mmole, 0.43g), amorphous product, yield : 85%, m.p.: 321-323°C, Anal. Calcd. for C₁₉H₂₂N₅NdO₁₄Zn (754g/mole), C, 30.24, H, 2.92, N, 9.31%, Found: C, 30.23, H, 2.91, N, 9.28%, FT-IR (ν, cm⁻¹, KBr): O-H (3343), C=N (1471), C-O (1292), Zn-N (585), Zn-O (513), Nd-O (432).

[Zn(L₂)Sm(NO₃)₃H₂O] (33)

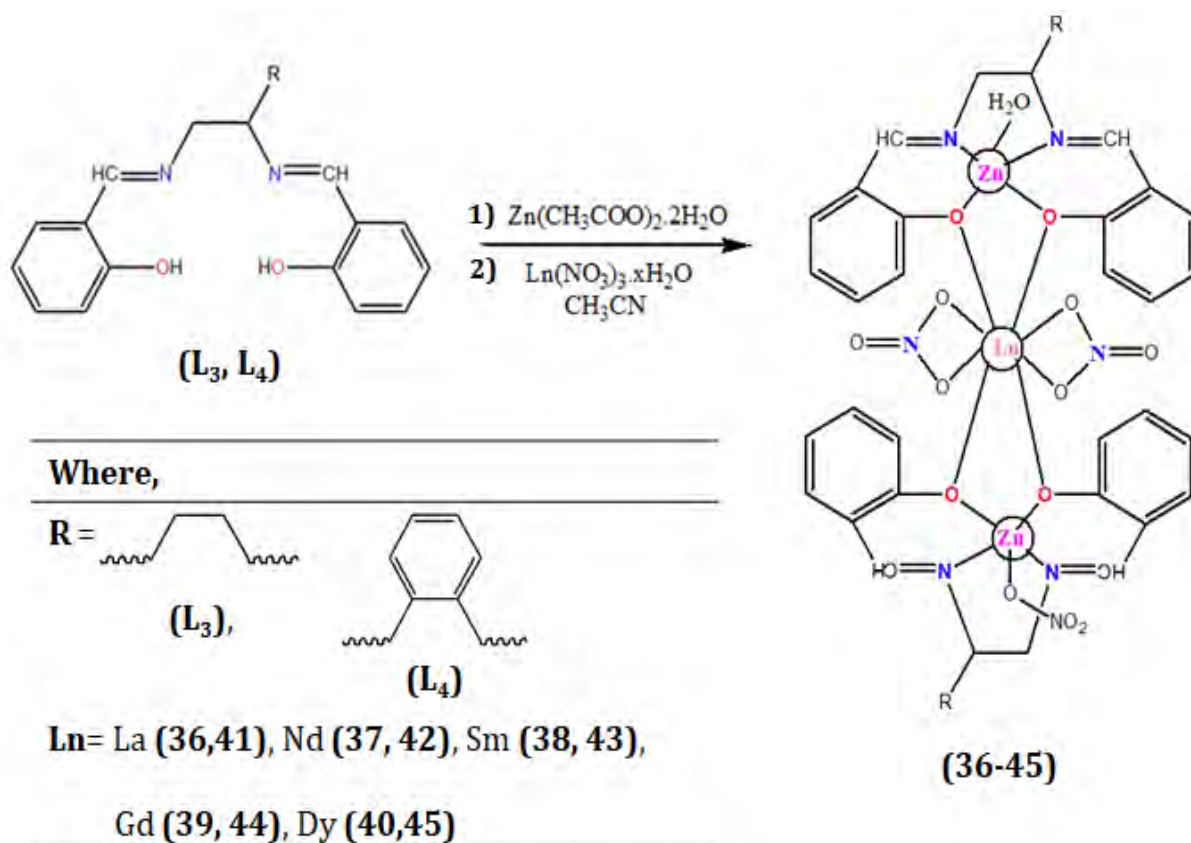
Quantities used: [Zn(L₂)H₂O] (1mmole, 0.34g), Sm(NO₃)₃.6H₂O (1mmole, 0.44g), amorphous product, yield : 85%, m.p.: 372-374°C, Anal. Calcd. for C₁₉H₂₂N₅SmO₁₄Zn (760g/mole), C, 30.02, H, 2.91, N, 9.20%, Found: C, 30.00, H, 2.89, N, 9.21%, FT-IR (ν, cm⁻¹, KBr): O-H (3387), C=N (1444), C-O (1295), Zn-N (593), Zn-O (501), Sm-O (438).

[Zn(L₂)Gd(NO₃)₃H₂O] (34)

Quantities used: [Zn(L₂)H₂O] (1mmole, 0.34g), Gd(NO₃)₃.6H₂O (1mmole, 0.46g), amorphous product, yield : 80%, m.p.: 362-364°C, Anal. Calcd. for C₁₉H₂₂N₅GdO₁₄Zn (767g/mole), C, 29.75, H, 2.90, N, 9.10%, Found: C, 29.72, H, 2.86, N, 9.12%, FT-IR (ν, cm⁻¹, KBr): O-H (3331), C=N (1462), C-O (1285), Zn-N (530), Zn-O (497), Gd-O (444).

[Zn(L₂)Dy(NO₃)₃H₂O] (35)

Quantities used: [Zn(L₂)H₂O] (1mmole, 0.34g), Dy(NO₃)₃.6H₂O (1mmole, 0.35g), amorphous product, yield : 80%, m.p.: 327-329°C, Anal. Calcd. for C₁₉H₂₂N₅DyO₁₄Zn (772.5g/mole), C, 29.53, H, 2.83, N, 9.09%, Found: C, 29.51, H, 2.84, N, 9.06%, FT-IR (ν, cm⁻¹, KBr): O-H (3355), C=N (1462), C-O (1305), Zn-N (531), Zn-O (520), Dy-O (441).



Scheme 2.4. Synthesis of Heterotrinnuclear 3d/4f Complexes

The spectroscopic and physico-analytical data for the prepared compounds (35-45) are given below:



Quantities used: $[\text{Zn}(\text{L}_3)\text{H}_2\text{O}]$ (1mmole, 0.35g), $\text{La}(\text{NO}_3)_3 \cdot 6\text{H}_2\text{O}$ (1mmole, 0.33g), amorphous product, yield : 70%, m.p.: 322-324°C, Anal. Calcd. for $\text{C}_{34}\text{H}_{30}\text{LaN}_8\text{O}_{15}\text{Zn}_2$ (1059 g/mole), C, 38.50, H, 2.80, N, 10.56%, Found: C, 38.52, H, 2.83, N, 10.59%, FT-IR (ν , cm^{-1} , KBr): O-H (3389), C=N (1441), C-O (1272), Zn-N (569), Zn-O (501), La-O (426).



Quantities used: $[\text{Zn}(\text{L}_3)\text{H}_2\text{O}]$ (1mmole, 0.35g), $\text{Nd}(\text{NO}_3)_3 \cdot 6\text{H}_2\text{O}$ (1mmole, 0.43g), amorphous product, yield : 75%, m.p.: 345-346°C, Anal. Calcd. for $\text{C}_{34}\text{H}_{30}\text{NdN}_8\text{O}_{15}\text{Zn}_2$

(1064 g/mole), C, 38.37, H, 2.79, N, 10.47%, Found: C, 38.34, H, 2.82, N, 10.52%, FT-IR (ν , cm^{-1} , KBr): O-H (3189), C=N (1458), C-O (1243), Zn-N (530), Zn-O (508), Nd-O (436).

[Zn₂(L₃)₂Sm(NO₃)₃H₂O].CH₃CN.H₂O (38)

Quantities used: [Zn(L₃)H₂O] (1mmole, 0.35g), Sm(NO₃)₃.6H₂O (1mmole, 0.44g), amorphous product, yield : 71%, m.p.: 352-354°C, Anal. Calcd. for C₃₄H₃₀SmN₈O₁₅Zn₂ (1070 g/mole), C, 38.10, H, 2.77, N, 10.47%, Found: C, 38.13, H, 2.80, N, 10.46%, FT-IR (ν , cm^{-1} , KBr): O-H (3313), C=N (1441), C-O (1290), Zn-N (532), Zn-O (491), Sm-O (436).

[Zn₂(L₃)₂Gd(NO₃)₃H₂O].CH₃CN.H₂O (39)

Quantities used: [Zn(L₃)H₂O] (1mmole, 0.35g), Gd(NO₃)₃.6H₂O (1mmole, 0.46g), amorphous product, yield : 78%, m.p.: 354-356°C, Anal. Calcd. for C₃₄H₃₀GdN₈O₁₅Zn₂ (1077 g/mole), C, 37.91, H, 2.75, N, 10.39%, Found: C, 37.88, H, 2.78, N, 10.39%, FT-IR (ν , cm^{-1} , KBr): O-H (3207), C=N (1442), C-O (1293), Zn-N (541), Zn-O (494), Gd-O (439).

[Zn₂(L₄)₂Dy(NO₃)₃H₂O].CH₃CN.H₂O (40)

Quantities used: [Zn(L₃)H₂O] (1mmole, 0.35g), Dy(NO₃)₃.6H₂O (1mmole, 0.35g), amorphous product, yield : 80%, m.p.: 368-370°C, Anal. Calcd. for C₃₄H₃₀DyN₈O₁₅Zn₂ (1082.5g/mole), C, 37.73, H, 2.78, N, 10.33%, Found: C, 37.69, H, 2.77, N, 10.34%, FT-IR (ν , cm^{-1} , KBr): O-H (3355), C=N (1440), C-O (1303), Zn-N (597), Zn-O (530), Dy-O (437).

[Zn₂(L₄)₂La(NO₃)₃H₂O].CH₃CN.H₂O (41)

Quantities used: [Zn(L₄)H₂O] (1mmole, 0.39g), La(NO₃)₃.6H₂O (1mmole, 0.33g), amorphous product, yield : 72%, m.p.: 321-323°C, Anal. Calcd. for C₄₂H₃₅LaN₈O₁₅Zn₂ (1182 g/mole), C, 43.35, H, 3.03, N, 9.63%, Found: C, 43.37, H, 3.05, N, 9.60%, FT-IR (ν , cm^{-1} , KBr): O-H (3355), C=N (1610), C-O (1303), Zn-N (530), Zn-O (488), La-O (437).

[Zn₂(L₄)₂Nd(NO₃)₃H₂O].CH₃CN.H₂O (42)

Quantities used: [Zn(L₄)H₂O] (1mmole, 0.39g), Nd(NO₃)₃.6H₂O (1mmole, 0.43g), amorphous product, yield : 78%, m.p.: 343-345°C, Anal. Calcd. for C₄₂H₃₅NdN₈O₁₅Zn₂ (1186 g/mole), C, 43.20, H, 3.02, N, 9.60%, Found: C, 43.24, H, 3.01, N, 9.62%, FT-IR (ν, cm⁻¹, KBr): O-H (3182), C=N (1611), C-O (1321), Zn-N (508), Zn-O (488), Nd-O (436).

[Zn₂(L₄)₂Sm(NO₃)₃H₂O].CH₃CN.H₂O (43)

Quantities used: [Zn(L₄)H₂O] (1mmole, 0.39g), Sm(NO₃)₃.6H₂O (1mmole, 0.44g), crystalline product, yield : 71%, m.p.: 331-333°C, Anal. Calcd. for C₄₂H₃₅SmN₈O₁₅Zn₂ (1192 g/mole), C, 42.98, H, 3.00, N, 9.55%, Found: C, 42.95, H, 3.02, N, 9.53%, FT-IR (ν, cm⁻¹, KBr): O-H (3331), C=N (1609), C-O (1278), Zn-N (532), Zn-O (487), Sm-O (436).

[Zn₂(L₄)₂Gd(NO₃)₃H₂O].CH₃CN.H₂O (44)

Quantities used: [Zn(L₄)H₂O] (1mmole, 0.39g), Gd(NO₃)₃.6H₂O (1mmole, 0.46g), crystalline product, yield : 75%, m.p.: 353-355°C, Anal. Calcd. for C₄₂H₃₅GdN₈O₁₅Zn₂ (1199 g/mole), C, 43.72, H, 2.99, N, 9.49%, Found: C, 43.69, H, 3.01, N, 9.51%, FT-IR (ν, cm⁻¹, KBr): O-H (3189), C=N (1611), C-O (1330), Zn-N (508), Zn-O (491), Gd-O (436).

[Zn₂(L₄)₂Dy(NO₃)₃H₂O].CH₃CN.H₂O (45)

Quantities used : [Zn(L₄)H₂O] (1mmole, 0.39g), Dy(NO₃)₃.6H₂O (1mmole, 0.35g), crystalline product, yield : 75%, m.p.: 371-373°C, Anal. Calcd. for C₄₂H₃₅DyN₈O₁₅Zn₂ (1204.5 g/mole), C, 42.53, H, 2.97, N, 9.45%, Found: C, 42.52, H, 2.99, N, 9.42%, FT-IR (ν, cm⁻¹, KBr): O-H (3313), C=N (1609), C-O (1290), Zn-N (532), Zn-O (491), Dy-O (436).

2.4. Applications

2.4.1. Antibacterial activity

To evaluate the antibacterial activity for (1-25), broth dilution technique was used [239], where bacterial cultures of *Klebsiella pneumoniae*, *Staphylococcus aureus*, *Bacillus subtilis* and *Escherichia coli* were used in inoculum of nutrient broth to ascertain their minimum inhibitory concentration (MIC). Inoculum was prepared by suspending 8 grams of nutrient broth in one-liter distilled water, which was heated with constant agitation and boiled until complete dissolution and sterilized in autoclave at 121 °C. Dilute the above cultures with nutrient broth using 10-fold dilution (1:10 mL), i.e., 1 mL test culture in 9 ml nutrient broth. The bacterial cultures were adjusted for their turbidity to estimate the concentration in the media. Each tested compound (5µL from 10 mg/mL DMSO), standard drug (cefixime monohydrate and roxithromycin, 5µL from 4mg/mL in DMSO) and negative control (5 µL DMSO) were loaded in well plate along with the addition of 195 µL of fresh bacterial inoculum in each well to have final test concentration of 50 µg/mL). All the well plates were incubated for two hours at 37 °C and start readings were taken exponentially with the help of micro-plate reader at 630 nm. After the incubation of 24 hours, growth was monitored spectrophotometrically and compounds with clear wells were further taken into an account for determining MICs at two-fold dilutions, i.e., 50, 25, 12.5, 6.25 µg/mL. The MIC of the synthesized complexes were determined both visually as well as spectrophotometrically at 630 nm, the absorbance was measured at 0 hours and after incubation of 24 hours. The obtained results were subtracted and compared with the positive and negative control.

2.4.2. Antifungal activity

Antifungal activity was explored utilizing agar well disc diffusion method [240]. The fungal spores of various strains, namely *Mucor* species, *Aspergillus flavus*, *Aspergillus fumigatus*, and *Aspergillus niger* were suspended in 0.02% Tween 20. Then 100 µL of each strain was swabbed on each agar plate which was prepared by pouring Sabouraud dextrose agar on pre-sterilized glass plates. The filter paper discs soaked with 5 µL of tested compound (10 mg/mL in DMSO), DMSO (as negative control) and clotrimazole (as

positive standard, 4 mg/mL DMSO) were also placed on the dextrose agar plates. The zone of inhibition were documented after an incubation period of 24-48 hours at 28 °C. The active samples were tested for MIC at low concentration by two folds i.e., 50, 25, 12.5, 6.25, 3.125 µg/mL.

2.4.3. *Alpha amylase inhibition assay*

Antidiabetic potential of the synthesized heteroleptic triorganobismuth(V) carboxylates (**1-25**) was quantified using alpha amylase inhibition activity and adopting standard protocol with trivial changes [241]. The mixture having 15µL phosphate buffer with preadjusted pH 6.8, 25µL of amylase enzyme, 10µL of the prepared compound and 40µL starch solution was incubated at 50 °C for 30 min in well plate, followed by the addition of HCl (1M). About 90µL of iodine solution was inserted in each well, employing DMSO as a negative control. Acarbose was taken as positive control in this assay. The absorbance of the reaction mixture was evaluated at 540 nm. The inherent activity of the synthesized compounds was quantified as % age α -amylase inhibition.

2.4.4. *Protein kinase inhibition assay*

Protein kinase inhibition assay for (**1-25**) was performed by utilizing purified Streptomyces 85E bacterial strain. The culture was refreshed in tryptone soy broth for 24 hrs at 30 °C. The bacterial culture was swabbed on petri plates containing ISP4 media under sterilized conditions. The sterile filter paper discs were loaded with 100 µg/mL of the synthesized compounds (in DMSO) and placed on the media seeded with Streptomyces 85E. The surfactin (5 µL of 4 mg/mL) and DMSO impregnated discs were used as positive and negative controls, respectively. These plates were incubated at 30 °C for 72 h and results were visually interpreted as clear and bald zones of inhibition (mm) [242].

2.4.5. *Brine shrimp lethality assay (Cytotoxicity)*

Cytotoxicity assay of the synthesized complexes was done according to the standard protocol with slight changes [240]. Firstly, the eggs of *Artemia salina* (Ocean 90, USA) were incubated in simulated sea water that was presaturated with oxygen for 24

hours at 30 °C. A specifically-designed tank with two separate compartments was engaged having perforated partition. In one compartment, eggs were placed in sea water solution while other compartment was covered with foil and kept under constant illumination (the hatched nauplii travelled prototropically to the other compartment through the pores). About 10 shrimp larvae were transferred to the 96 well plates from beaker having the test samples (**1-25**) in serial dilutions. The compounds were tested for brine shrimp lethality assay at two-fold concentrations that range from 200 to 25 µg/mL, where doxorubicin served as positive. After 24 hours, the degree of lethality for each compound was worked out as LD₅₀ value.

2.4.6. Computational studies

Molecular docking studies were performed using GOLD program to explore the antibacterial, anticancer and antidiabetic potential of the synthesized compounds [243, 244]. The structure of Helicobacter pylori urease (PDB ID: 1E9Y), human pancreatic alpha amylase (PDB ID: 5U3A), and epidermal growth factor receptor tyrosine kinase (PDB ID: 1M17) were retrieved from RCSB Protein Data Bank (PDB) for molecular docking probe. It is crucial to identify the active pocket of the protein for targeted inhibition. The binding site of the selected target proteins was taken from the literature [245-247] and for more details consult [248]. Compounds exhibiting greater GOLD fitness score are considered as having better binding affinity with the receptor [249].

2.5. Photoluminescence studies

All the solutions were analyzed applying quartz cuvetts in absolute methanol at concentration of 2×10^{-5} M. The steady-state photoluminescence (SSPL) and time-resolved photoluminescence (TRPL) investigations were performed employing a PicoQuant Fluo Time-300 (FT-300) spectrophotometer that worked on the principle of a time-correlated single-photon counting technique (TCSPT), which was coupled with a pulsed PLS laser excitation source, where the pulses of the PLS laser were centered at 306 nm [250, 251].

2.6. Magnetic studies

The magnetic susceptibility measurements for the homoleptic heterodi-/trinuclear 3d/4f metal complexes were conducted by engaging Evans balance at 291K in an applied magnetic field. Evans balance works with the assistance of two magnets and is equipped with suspension strip. One of the magnets is attached with the strip that generates counteracted current which is proportional to the force exerted by the sample and, therefore, allows the recording of readings [252]. The gram susceptibility value must be positive for paramagnetic materials and calculations are made by the following relationship:

$$\chi_g = \frac{C_{Bal} \times l \times (R - R^0)}{10^9 \times m} \dots \dots \dots (1)$$

Where, l = length of the sample (cm), m = mass of the sample (g), R^0 = measurement of the empty tube, R = measurement of the tube with added sample and C_{Bal} = balance calibration constant. The molar susceptibility (χ_m .T) and magnetic moment (μ_{eff}) values can be determined from gram susceptibility (χ_g) data by solving following relations [253].

$$\chi_m = \chi_g \times \text{molecular mass of the sample} \dots \dots \dots (2)$$

$$\mu_{eff} = 2.828 \sqrt{\chi_m \times T} \dots \dots \dots (3)$$

Where, χ_m = molar susceptibility, T = temperature (K). Diamagnetic correction was made by using the Pascal's constant [254].

CHAPTER-3

RESULTS AND DISCUSSION

3.1. Chemistry

The **first part** of the dissertation deals with the synthesis of a series of heteroleptic triorganobismuth(V) complexes and for which salt metathesis method was adopted to achieve pure product(s). The heteroleptic triorganobismuth(V) derivatives (**1-25**) were synthesized by stirring the appropriate substituted benzoic acids in dry toluene, followed by the addition of triethylamine and the respective triarylbismuth(V) dibromide and separation of triethylammonium bromide salt as byproduct. The target products were obtained in good yield as $\text{Ar}_3\text{Bi}(\text{OOCR})_2$.

The **second part** of the presented research work pertains to the synthesis of bi-compartmental heterotrinary 3d/4f metal complexes. The condensation method was employed here to secure the pure product. The ligand (**L1-L4**) were produced by refluxing salicylaldehyde and substituted-diamine in molar ratio 2:1 and then complexing with $\text{Zn}(\text{CH}_3\text{COO})_2 \cdot 2\text{H}_2\text{O}$ stoichiometrically to yield precipitates of the monometallic zinc complex. Finally, stoichiometric amount of monometallic Zn complex was made to react with the respective 4f metals to afford the target product (**26-45**) as enunciated in Schemes 2.2 and 2.3 [151, 255].

3.2. FT-IR spectroscopic data

The IR absorption band for hydroxyl stretching frequency, ν_{OH} , appeared around 3400 cm^{-1} in the free carboxylic acid, whereas it disappeared in the complexes (**1-25**) which clearly indicated deprotonation of acid and successful coordination to the organobismuth moiety through its oxygen(s). The stretching frequencies for carboxyl group appeared in the range of $1547\text{-}1596$ and $1323\text{-}1369 \text{ cm}^{-1}$ for $\nu_{\text{asym}}(\text{COO})$ and $\nu_{\text{sym}}(\text{COO})$, respectively. The $\Delta\nu$ value [$= \nu_{\text{asym}}(\text{COO}) - \nu_{\text{sym}}(\text{COO})$] for carboxyl group(s) was determined and found to be greater or less than 200 cm^{-1} for all the synthesized complexes [148, 256],

which referred to its monodentate, bidentate and/or anisobidentate mode of coordination with the metal center and got further confirmed by single crystal XRD data for (**7**, **17**, **18** and **19**). Another indication for the deprotonation of the carboxylic acid(s) was inferred from lowering values of symmetric and asymmetric stretch by 30-40 cm^{-1} in the complexes with respect to the free ligands. The presence of two new stretching bands in the ranges of 438-533 and 405-447 cm^{-1} pointed to the bismuth linkages to carbon (Bi-C) and oxygen (Bi-O), respectively, in the compounds when compared with the spectra of the free ligands [233]. The other characteristic vibrational bands, attributed to certain organic groups present in the compounds, were found in the ranges of 2984-3068 cm^{-1} for ν (C-H_{aromatic}) and 2917-2983 cm^{-1} for ν (C-H_{aliphatic}).

The IR absorption bands arose for (**19**) were, ν C-H_{aromatic} (3053), ν C-H_{aliphatic} (2964), ν_{asym} COO (1588), ν_{sym} COO (1338), ν Bi-C (474), ν Bi-O (434). The characteristic $\Delta\nu$ value for this particular carboxyl group is 250 cm^{-1} , which qualified the ligand for anisobidentate mode of chelation with the organobismuth moiety [233]. Thus FT-IR data fully supported the proposed structural motifs for the prepared compounds and are also in accordance with the reports published earlier [148, 233].

The FT-IR spectral data for free ligands (**L1-L4**) and target complexes (**26-45**) clearly demonstrated their successful synthesis as per Schemes 2.1-2.3. In free ligand, the IR absorption band for hydroxyl ν (OH) and azomethine ν (C=N) moiety emerged around 3354 and 1636 cm^{-1} , which upon coordination with the respective Zn/Ln metal(s) shifted to 3182-3355 and 1609-1611 cm^{-1} , respectively. The stretching vibration band for phenolic group ν (C-O) appeared around 1274 cm^{-1} , which moved to slightly higher frequency upon coordination in di/trinuclear metal complexes (**26-45**) and appeared in the range of 1272-1330 cm^{-1} , thus clearly manifesting the establishment of Ln-O linkage through the deprotonation of phenolic hydrogen (present in the ligand). Additional support to the formation of the target complexes was provided by the presence of Zn-N and Zn-O absorption bands around 490-606 and 488-491 cm^{-1} , respectively. The IR stretching frequency for ν (Ln-O) 436-437 cm^{-1} , clearly indicated the attachment of rare earth metal in the binding pocket of phenolic oxygen of monometallic zinc complexes via bridging mode. As the previous reports [151, 255] manifested, the current IR data also evidenced

respective 3d/4f metal(s) to ligand bonds through the involvement of azomethine nitrogen and phenolic oxygen of the tetradentate ligand.

3.3. NMR spectroscopic data

The chemical structures for (**1-25**) were further ascertained by their multinuclear NMR spectral data which were recorded in deuterated chloroform as solvent. The chemical shift values explicitly determined magnetically non-equivalent protons present in the synthesized organobismuth derivatives along with their coupling constants. The ^1H NMR data for these compounds revealed the successful coordination of the appropriate carboxylic acid to the metal center by its deprotonation as indicated by the absence of resonance around 11 ppm which was present in the free acids. The resonances for all the aromatic protons were observed in the range of 8.30-7.30 ppm as reported earlier [257]. The ethoxy protons of (**8, 20**) showed quartet and triplet signals for $-\text{CH}_2-$ and $-\text{CH}_3$ groups that resonated in the range of 4.15-4.08 and 1.47-1.43 ppm, respectively [233].

The ^{13}C NMR data for (**1-25**) manifested the presence of all the unique carbons in their structural patterns. The characteristic resonance peak pertaining to $\text{C}=\text{O}$ functionality appears in the range of 174.8-156.2 ppm for the compounds. The methyl carbon of p-tolyl group resonated around 21 ppm for (**13-25**). Thus, the data authenticated attachment of the respective aryl bismuth moiety to the substituted carboxylic acid. The aromatic carbons existed in their usual regions: $\text{C}_{\text{ipso-Bi}}$ (161.5-134.1), $\text{o-CH}_{\text{aromatic}}$ (125.7-134.3), $\text{o-CH}_{\text{aromatic}}$ (130.8-132.1), $\text{p-CH}_{\text{aromatic}}$ (141.8-127.4), $\text{C}_3\text{-OEt}$ (151.7-154.4), $\text{C}_4\text{-OEt}$ (147.7-151.5) [54]. The $-\text{CH}_2$ and $-\text{CH}_3$ carbons of ethoxy group, present in compounds (**8, 20**), appear at 64.5 and 14.8 ppm, respectively [54]. The coupling constants, as mentioned in the experimental section, furnished useful structural information as well as precise location of substituents present on the aromatic ring.

3.4. X-ray crystallographic data

Six of the synthesized compounds (**7, 17, 18, 19, 27** and **45**) were characterized through XRD analysis: $[\text{BiPh}_3(\text{O}_2\text{CC}_6\text{H}_4(2\text{-CH}_3))_2]$ (**7**), $[\text{Bi}(\text{p-toly})_3(\text{O}_2\text{CC}_{10}\text{H}_7)_2]$ (**17**), $[\text{Bi}(\text{p-toly})_3(\text{O}_2\text{CC}_6\text{H}_4(4\text{-Cl}))_2]$ (**18**), $[\text{Bi}(\text{p-toly})_3(\text{O}_2\text{CC}_6\text{H}_4(2\text{-CH}_3))_2]$ (**19**),

[ZnNd(L₁)(NO₃)₃H₂O] (**27**) and [Zn₂Dy(L₄)₂(NO₃)₃H₂O].CH₃CN.H₂O (**45**). The coordination behavior of all the analyzed compounds were found to be isostructural with each other with slight changes in bond lengths and bond angles in organobismuth derivatives. The crystallographic and structural refinement data are summarized in Tables A1-A3. The solid-state molecular structures of the compounds as their ORTEP diagrams are reported in Fig. 3.1-3.6.

3.4.1. *Bis(2-methylbenzoato)triphenylbismuth(V)* (**7**)

The compound (**7**) with chemical formula [BiPh₃(O₂CC₆H₄(2-CH₃))₂] was also analyzed by single crystal XRD technique and its ORTEP diagram is given in Fig. 3.1, whereas the selected bond lengths and bond angles are presented in Table 3.4. The XRD data revealed the existence of five-coordinated bismuth center having distorted trigonal bipyramidal molecular geometry. It is worth-mentioning here that the lability of Bi-O interaction is sensitive to the basicity of the donor species and the reactions involving multifunctional ligands are dependent on conditions. Moreover, flexibility of the ligand backbone may result in structural variability in terms of chelation and bridging. The emerging out five coordinated metal center occupies carboxylates at axial positions and phenyl moiety fits at equatorial positions [25]. The Bi-C bond lengths for phenyl fall in the range of 2.206(4)-2.223(5) with average bond length of 2.247 Å and the data are compatible with the reported values [53, 54, 258]. The bond lengths for Bi1-O1 and Bi1-O3 equals 2.276(4) and 2.292(4) Å, respectively. The XRD data supports IR findings that described monodentate binding behavior for the two carboxylates with the metal center.

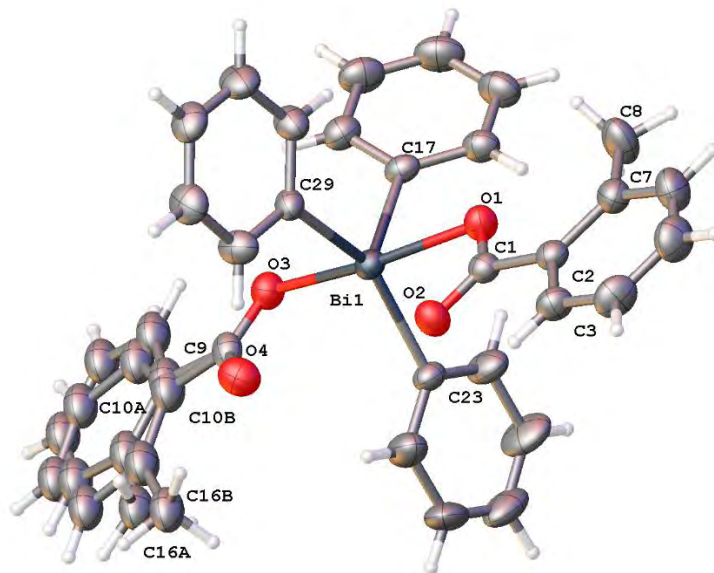


Figure 3.1: ORTEP diagram for (7)

Table-3.1. Selected bond lengths (Å) and bond angles (°) for (7)

7			
Bi1—C29	2.206 (4)	C23—Bi1—O1	91.84° (16)
Bi1—C23	2.210 (4)	C17—Bi1—O1	84.88° (16)
Bi1—C17	2.223 (5)	C29—Bi1—O3	93.01° (16)
Bi1—O1	2.276 (4)	C23—Bi1—O3	89.36° (17)
Bi1—O3	2.292 (4)	C17—Bi1—O3	84.27° (17)
C29—Bi1—C23	147.3° (2)	O1—Bi1—O3	168.91° (13)
C29—Bi1—C17	104.41° (17)	C1—O1—Bi1	105.7° (3)
C23—Bi1—C17	108.23° (18)	C9—O3—Bi1	108.0° (3)
C29—Bi1—O1	91.92° (15)		

3.4.2. *Bis(2-naphthoato)tris(p-tolyl)bismuth(V)* (17)

The selected bond lengths and bond angles for (17) with chemical composition of $[\text{Bi}(\text{p-tol})_3(\text{O}_2\text{CC}_{10}\text{H}_7)_2]$ are delineated in Table 3.2, whereas the ORTEP diagram is presented in Fig. 3.2. The structural parameters of compounds (7 & 17) are isostructural with each other showing slight changes in bond lengths and bond angles. The data revealed the existence of five-coordinated bismuth center, assuming the distorted trigonal bipyramidal molecular geometry, where carboxylate occupies axial position and p-tolyl

group takes in equatorial position. The Bi-C bond lengths for p-tolyl groups are in the range of 2.185(4)-2.209(5) with average bond length of 2.197Å and the XRD data are in accordance with the already reported works [53, 54, 258]. The bond lengths for Bi1-O1 and Bi1-O3 fall at 2.288(3) and 2.293(3)Å, respectively for (17). The XRD data are also corresponds with the FT-IR findings that manifested monodentate binding behavior for the two carboxylates with the metal center.

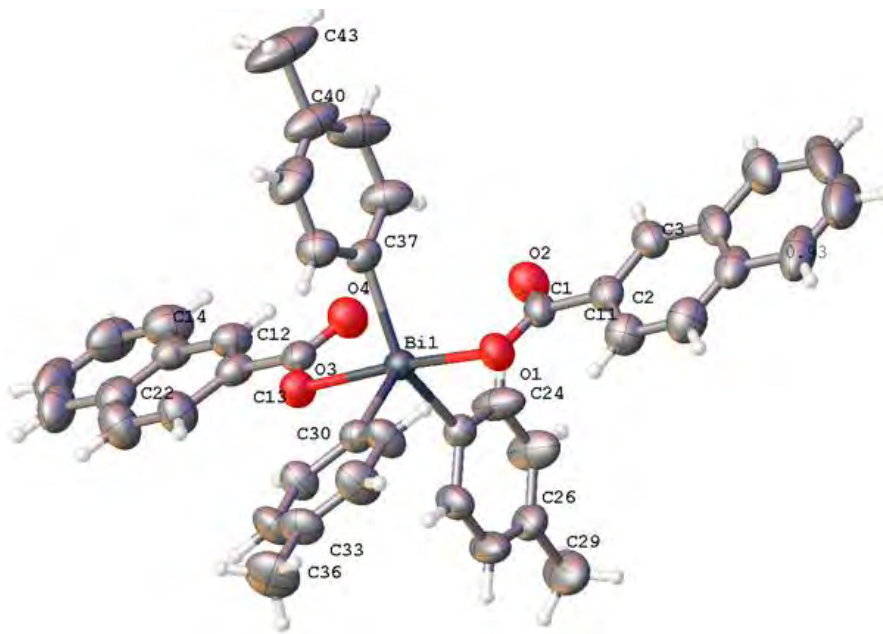


Figure 3.2: ORTEP diagram for (17)

Table-3.2. Selected bond lengths (Å) and bond angles (°) for (17)

17			
Bi1—C37	2.185 (4)	C23—Bi1—O3	89.41° (14)
Bi1—C23	2.202 (4)	C30—Bi1—O3	85.70° (15)
Bi1—C30	2.209 (5)	C37—Bi1—O1	92.42° (14)
Bi1—O1	2.293 (3)	C23—Bi1—O1	92.51° (14)
Bi1—O3	2.288 (3)	C30—Bi1—O1	86.19° (15)
C37—Bi1—C23	142.77° (19)	O3—Bi1—O1	171.87° (12)
C37—Bi1—C30	109.47° (18)	C1—O1—Bi1	107.6° (3)
C23—Bi1—C30	107.67° (17)	C12—O3—Bi1	109.5° (3)
C37—Bi1—O3	90.82 (14)		

3.4.3. *Bis(4-chlorobenzoato)tris(p-tolyl)bismuth(V) (18)*

The ORTEP diagram for **(18)** is delineated as Fig. 3.3 describing that the crystal comprises of two molecules. The selected bond lengths and bond angles regarding the crystal structure are listed in Table 3.3. This compound crystallized with space group $P6_5$ in hexagonal system. One of the moieties of the twinned structure having five coordinated Bi1 center assumed distorted trigonal bipyramidal molecular geometry, whereas the second moiety with Bi2 center hexacoordinated and possessed distorted octahedral geometry where carboxylate captured axial position and p-tolyl group joined in equatorial position. Here, flexibility of the ligand backbone may result in structural variability in terms of chelation and bridging. The Bi1-C bond lengths for p-tolyl are formed in the range of 2.215(15)-2.204(14) with average bond length of 2.210Å, whereas for Bi2-C appears in range 2.843(16)-2.232(13) with average bond length of 2.636Å and the data are compatible with the reported ones. The bond lengths for Bi1-O1 and Bi1-O3 were measured as 2.304(10) and 2.295(10)Å, whereas for Bi2-O5 and Bi2-O7 determined as 2.367(10) and 2.655(10)Å which demonstrated slight elongation that favored the bidentate mode of chelation for the carboxylate moiety.

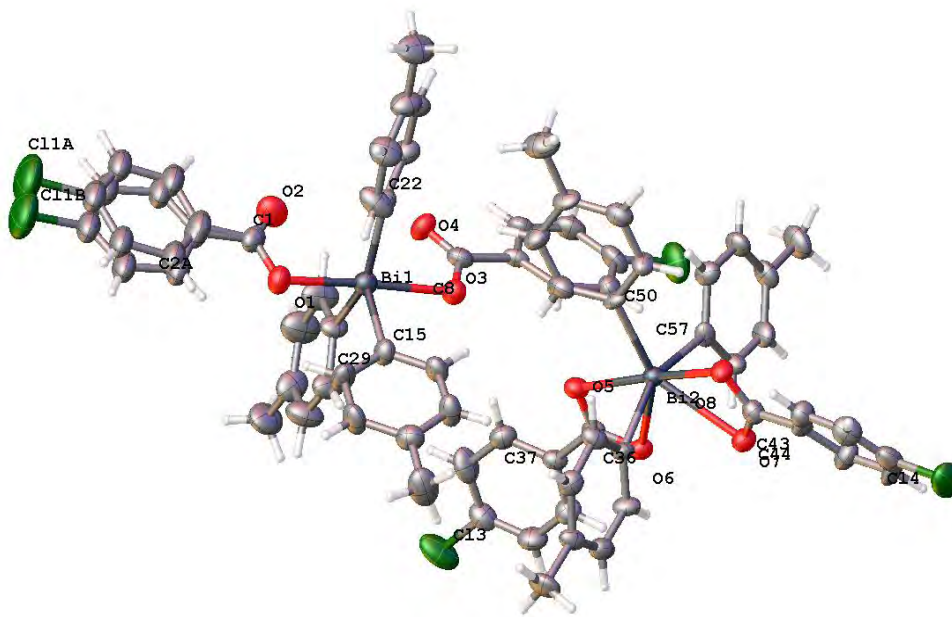


Figure 3.3: ORTEP diagram for **(18)**

Table-3.3. Selected bond lengths (Å) and bond angles (°) for **(18)**

18			
Bi1—C15	2.204 (14)	O1—Bi1—O3	174.3° (4)
Bi1—C22	2.213 (17)	C15—Bi1—O1	87.5° (5)
Bi1—C29	2.215 (15)	C15—Bi1—O3	86.9° (5)
Bi2—C36	2.843 (15)	C15—Bi1—C29	106.4° (5)
Bi2—C43	2.833 (16)	C22—Bi1—O1	89.1° (5)
Bi2—C50	2.232 (13)	C22—Bi1—O3	91.2° (5)
Bi1—O1	2.304 (10)	O8—Bi2—O7	52.5° (3)
Bi1—O3	2.295 (10)	O8—Bi2—C36	154.8° (4)
Bi2—O5	2.367 (10)	O8—Bi2—C43	26.3° (4)
Bi2—O6	2.625 (10)	C50—Bi2—O7	140.4° (5)
Bi2—O7	2.655 (10)	C50—Bi2—O8	88.2° (5)
Bi2—O8	2.313 (9)		

3.4.4. *Bis(2-methylbenzoato)tris(p-tolyl)bismuth(V) (19)*

The ORTEP diagram for **(19)** is shown in Fig. 3.4, and the selected bond lengths and bond angles are presented in Table 3.4. The XRD data for the compound confirmed hexacoordination for bismuth center in addition to a unique anisobidentate interaction of one carboxylate ligand that rendered the molecular geometry as distorted octahedral. The Bi-C bond lengths for p-tolyl groups are found in the range of 2.198(4)-2.218(4) with the average bond length of 2.236Å. The bond lengths for Bi1-O1 and Bi1-O3 in the complex are computed as 2.294(3) and 2.286(3)Å respectively, while the bond length for (Bi1-O2) is ascertained as 2.729(3)Å indicating lengthening of the bond that compels the carboxyl group to coordinate with the bismuth center via anisobidentate manner assuming overall distorted octahedral geometry [233].

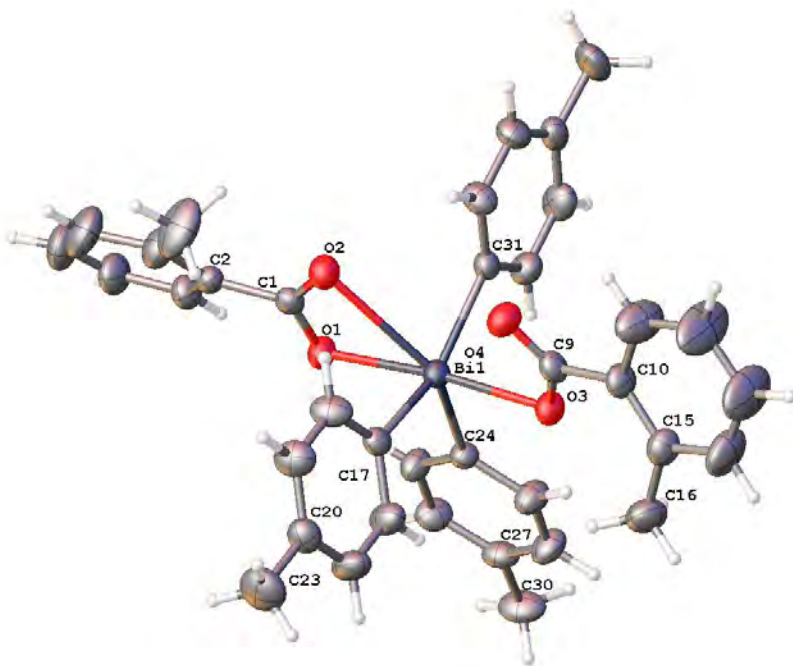


Figure 3.4: ORTEP diagram for **(19)**

Table-3.4. Selected bond lengths (Å) and bond angles (°) for **(19)**

19			
Bi1—C17	2.198 (4)	C17—Bi1—O3	88.50° (14)
Bi1—C31	2.202 (4)	C31—Bi1—O3	90.69° (14)
Bi1—C24	2.218 (4)	C24—Bi1—O3	87.08° (14)
Bi1—O1	2.294 (3)	C17—Bi1—O1	89.49° (14)
Bi1—O2	2.729 (3)	C31—Bi1—O1	93.90° (14)
Bi1—O3	2.286 (3)	C24—Bi1—O1	87.95° (14)
C17—Bi1—C31	150.27° (16)	O3—Bi1—O1	173.92° (10)
C17—Bi1—C24	105.76° (16)	C1—O1—Bi1	103.7° (3)
C31—Bi1—C24	103.88° (15)	C1—O1—Bi1	103.7° (3)

3.4.5. $[ZnNd(L_1)(NO_3)_3H_2O]$ (**27**)

The complex bis(μ^2 -2,2'-(Ethane-1,2-diylbis(nitrilomethylidene))bis(6-methoxyphenolato)tris(nitrato)zinc(II)neodymium(III) (**27**) was also analyzed crystallographically as a representative of dinuclear Zn^{II} - Ln^{III} complexes (**26-35**). The relevant crystallographic data, bond length and bond angles of which are set forth in Tables A3 and 3.5. The asymmetrical unit of the complex is composed of a neutral

[ZnNd(L₁)(NO₃)₃H₂O] moiety as shown in the ORTEP diagram (Fig. 3.5). The heterodinuclear host structure is formulated when one monometallic zinc complex coordinates with one Nd³⁺ ion via bridging mode along with the three bidentate nitrate moieties.

The X-ray structure for (27), completely described the coordination behavior of each metal center and geometric shape of the heteronuclear bimetallic compound. Here Zn(II) and Nd(III) are coordinated through N, O and O, O sites respectively. The Zn(II) center is pentacoordinated having distorted square pyramidal geometry where Zn-O and Zn-N bond lengths lie in the range of 1.987(3)-2.026(3)Å and 2.365(3)-2.046Å respectively. The neodymium center is decacoordinated attached to four oxygen atoms, where Nd-O bond length is between 2.365-2.667Å. Another significant structural feature is the presence of hydrogen bonding that controls a variety of physical properties like catalytic, solubility, etc. The complex involves intermolecular H-bonding, which is delineated in Table 3.9. The intermolecular H-bonding is present between O(11)-H(5A), O(6)-H(5B) and O(11)-H(11) with bond lengths 2.08(6), 1.99(6) and 2.60(6)Å, respectively. The bond angles for these moieties are lies in the range of 163-167°. This intermolecular hydrogen bonding provides extra stability to the synthesized compound.

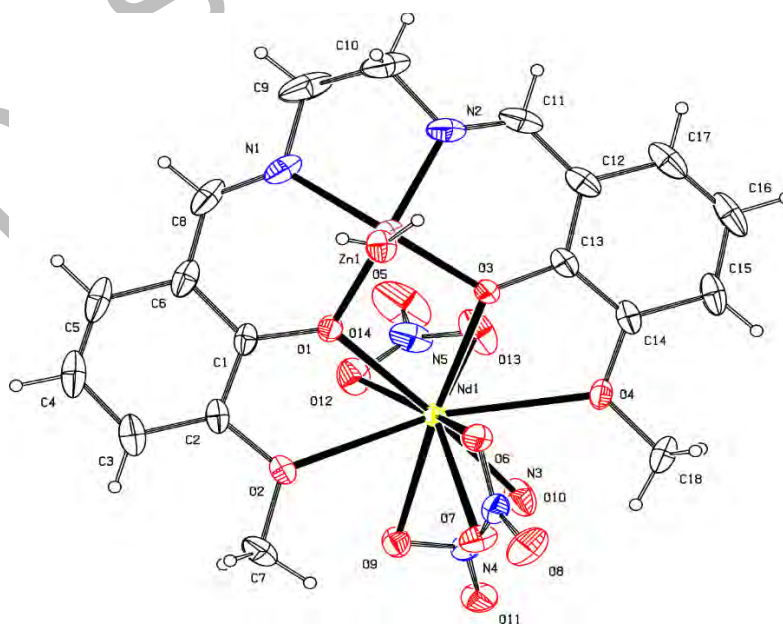


Figure 3.5: ORTEP diagram for (27)

Table-3.5. Selected bond lengths (Å) and bond angles (°) for (27)

27				
Zn1-N1	2.047 (4)	O1-Nd1-O3	64.84° (9)	
Zn1-N2	2.008 (4)	O1-Nd1-O4	124.65° (9)	
Zn2-O1	1.999 (3)	Nd1-O1	2.364 (3)	
Zn2-O3	1.987 (3)	Nd1-O2	2.667 (3)	
Zn1-O5	2.047 (3)	Nd1-O3	2.394 (3)	
O1-Nd1-O2	60.12° (10)	Nd1-O4	2.652 (3)	

Table-3.6. Selected hydrogen bond parameters for (27)

<i>D—H\cdotsA</i>	<i>H\cdotsA</i> (Å)	<i>D—H</i> (Å)	<i>D—H\cdotsA</i> (°)	<i>D\cdotsA</i> (Å)
O5-H5A \cdots O11	2.08 (6)	0.71 (5)	167 (6)	2.779 (5)
O5-H5B \cdots O6	1.99 (6)	0.86 (5)	163 (5)	2.818 (4)
C11-H11 \cdots O11	2.60 (6)	0.93 (5)	165 (5)	3.505 (4)

3.4.6. [Zn₂Dy(L₄)₂(NO₃)₃H₂O].CH₃CN.H₂O (45)

The complex [Zn₂Dy(L₄)₂(NO₃)₃H₂O].CH₃CN.H₂O (**45**) was examined as a representative heterotrimeric complex; Zn^{II}-Ln^{III}-Zn^{II} (**36-45**) using single crystal XRD technique. The crystallographic data, bond lengths and bond angles are mentioned in Tables A3 and 3.7. The asymmetrical unit of the trinuclear compound is composed of a neutral species [Zn₂Dy(L₄)₂(NO₃)₃H₂O], along with acetonitrile and water as solvated molecules (Fig. 3.6). The heterotrimeric host structure is formulated when two ZnL coordinate with one Dy⁺³ ion in bridging mode along with two bidentate nitrate moieties. The Zn(II) and Dy(III) are coordinated to N, O and O, O sites respectively, where Zn(II) center is pentacoordinated having distorted square pyramidal geometry consisting of two N's and two O's, where Zn(1) is ligated with H₂O and Zn(2) is attached to NO₃ in monodentate fashion [81]. The Zn-O and Zn-N bond distances for Zn(1) are [2.013(9), 2.006(9)Å] and [2.044(12), 2.060(10)Å] respectively. The Zn(1)-O(14) bond distance for the water molecule, attached at the apical positions, is 1.991(11)Å. The Zn-O and Zn-N bond distance for Zn(2) are [2.035(9), 2.011(9)Å] and [2.053(13), 2.056(11)Å] respectively. The Zn(2)-O(11A) bond distance for the monodentate nitrate moiety, attached

at the apical position is $2.030(2)^\circ$. The [O-Zn-O] and [N-Zn-N] bond angle around Zn(1) is $82.7(3)$ and $79.6(5)^\circ$, and similarly for Zn(2) these bond angles are $83.2(3)^\circ$ and $80.1(5)^\circ$, respectively. These quantitative parameters clearly display that Zn^{+2} ions in both entities are positioned symmetrically resulting in comparable bond distances and bond angles as reported earlier [138, 259].

Here, the dysprosium center is octacoordinated and ligated to eight oxygen atoms out of which four oxygen atoms, i.e., O_2O_2 are ligated through zinc-incorporated salopn⁻² precursor and rest of the four oxygens have their origin from bidentate nitrate groups that are sandwiched between the zinc precursor. In this way Dy-O bond length for the sandwiched Dy^{+3} ion with the zinc precursor ranges from 2.306-2.316Å, which is shorter as compare to the Dy-O bond length of bidentate nitrate O atoms which lies in range, 2.437-2.517Å, depicting firm binding of Dy^{III} with the Zn salopn core structure [81]. The nitro group along with nitrito functionality, attached to the Zn(2) is disordered over two positions with occupancy ratio of 0.77(2):0.23(2) for each. The significant interaction includes hydrogen bonding, that controls variety of physical properties. The complex **45** involves both intermolecular and intramolecular H-bonding, which is delineated in Table 3.8. The intramolecular H-bonding involves O3-H3A...N8 moiety between O(3)-H(3A) and H(3A)-N(8) having bond length 0.93 and 1.86Å respectively. The intermolecular H-bonding present between O(3) and H(3B) reveal bond length of 0.93Å. The bond angles for these moieties are 159 and 130°, respectively. These inter- and intramolecular hydrogen bonding provide extra stability to the synthesized compound and may control many physico-chemical properties.

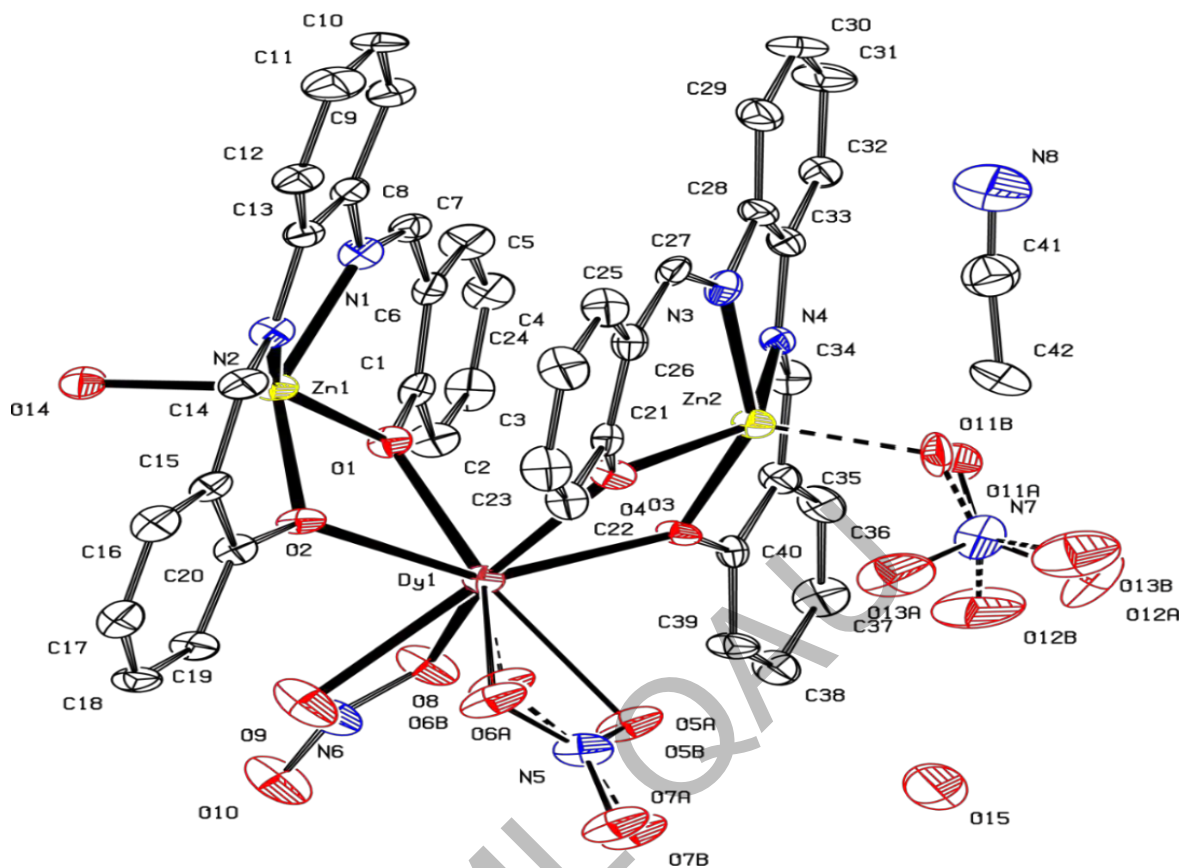


Figure 3.6: ORTEP diagram for **(45)**

Table-3.7 : Selected bond lengths (Å) and bond angles (°) for **(45)**

45			
Zn1-N1	2.044 (13)	N1-Zn1-N2	79.6° (5)
Zn1-N2	2.060 (10)	N3-Zn2-N4	80.1° (5)
Zn2-N3	2.053 (13)	Dy1-O1	2.298 (9)
Zn2-N4	2.058 (11)	Dy1-O2	2.332 (8)
Zn1-O1	2.013 (9)	Dy1-O3	2.292 (9)
Zn1-O2	2.006 (9)	Dy1-O4	2.314 (8)
Zn2-O3	2.035 (9)	Dy1-O5A	2.443 (10)
Zn2-O4	2.011 (9)	Dy1-O6A	2.517 (17)
Zn1-O14	1.991 (10)	Dy1-O8	2.444 (10)
Zn2-O11A	2.030 (3)	Dy1-O9	2.437 (12)
O1-Zn1-O2	82.7° (3)		
O3-Zn2-O4	83.2° (3)		

Table-3.8 : Selected hydrogen bond parameters for (45)

$D-H\cdots A$	$H\cdots A(A^\circ)$	$D-H(A^\circ)$	$D-H\cdots A(A^\circ)$	$D\cdots A(A^\circ)$
O3-H3A \cdots N8	1.86	0.93	159(6)	2.75(2)
O3-H3B \cdots O15	2.00	0.93	130(6)	2.69(19)
O15-H15B \cdots N7	2.54	0.99	158(6)	3.48(2)
C2-H2 \cdots O7	2.40	0.93	146(6)	3.21(2)

3.5. Biological applications

Organobismuth(V) compounds have been considered to be potentially bioactive species due to their reported biocidal properties and low toxicity [13, 158]. They were preliminary screened to find out their biological significance in medicinal research.

3.5.1. Antimicrobial activity

The target complexes (**1-25**) were evaluated *in vitro* to determine their antimicrobial potential against bacterial and fungal strains, utilizing the standard drugs roxithromycin or cefixime and clotrimazole (as the case may be) and the data are given in Tables 3.9 and 3.10. Some compounds show significant activity against certain bacterial strains such as **6** against *S. aureus*, and **12**, **21** and **23** against *K. pneumonia*, having minimum inhibitory concentration of 3.125 $\mu\text{g/mL}$. The compounds **11**, **12** and **23** exhibit good activity against three bacterial strains, namely *S. aureus*, *K. pneumonia* and *E. coli* with MIC value 6.25 $\mu\text{g/mL}$ for each. The antifungal activity profile for **4**, **5**, **7**, **17**, **21** and **22** demonstrated their substantial activity against *A. flavus* with MIC value of 6.25 $\mu\text{g/mL}$ for each. The results demonstrated that antimicrobial activity of the target compounds became enhanced when appropriate carboxylic acids were complexed with the respective triarylbismuth moiety as manifested by their least MIC values (lesser the MIC value for the compound, more it will be effective).

The increased antimicrobial activity of the compounds may be attributed to the involvement of pentavalent bismuth ion and the current data can be interpreted in terms of Tweedy's theory of chelation [260]. The polarity of the metal ion becomes generally

reduced due to chelation because of the partial sharing of positive charge of bismuth with the donor carboxylate moiety. The delocalization of pi electrons on the aromatic ring may also contribute in enhancing the antimicrobial capacity of the compounds when compared with the reported data [25]. The present work demonstrates that the compounds which showed significant MIC value of 6.25 µg/mL, had naphthalene and methyl substituents (electron donating group) in their structural motifs, facilitating the delocalization of π electrons within the system. The delocalization further increases lipophilic character of the complexes that aids in gaining entry into the lipid bilayer of bacterial and fungal cell membranes that ultimately leads to the rise in their antimicrobial properties [261, 262].

Table 3.9. Antibacterial activity data for (1-25)

Number of compounds	MIC(µg/mL)			
	Antibacterial Strains			
	<i>B. subtilis</i>	<i>S. aureus</i>	<i>K. pneumoniae</i>	<i>E. coli</i>
1	12.5	12.5	50	25
2	25	NA	50	25
3	12.5	25	12.5	25
4	12.5	25	50	25
5	12.5	50	25	25
6	12.5	3.125	25	25
7	50	12.5	50	6.25
8	50	50	50	25
9	25	25	25	50
10	25	50	25	25
11	25	25	6.25	12.5
12	25	6.25	3.125	6.25
13	50	50	50	50
14	25	50	50	25
15	50	25	12.5	50
16	12.5	25	50	25
17	12.5	25	25	50
18	12.5	12.5	25	12.5
19	50	25	50	25
20	50	50	50	50
21	25	50	3.125	50
22	25	25	25	12.5
23	25	6.25	3.125	25
24	25	50	12.5	25

25	25	50	NA	25
Ph₃BiBr₂	50	25	25	25
(p-tolyl)₃BiBr₂	25	25	12.5	12.5
Cefixime*	1.11	0.334	0.334	1.11
Roxithromycin*	0.334	0.334	0.334	0.334

* Standard drug, - No activity

Table 3.10. Antifungal activity data for (1-25)

Number of compounds	MIC(μ g/mL)			
	Antifungal Strains			
	<i>A. Flavus</i>	<i>A. Niger</i>	<i>A. Fumigatus</i>	<i>Mucor</i>
1	12.5	50	25	> 50
2	12.5	50	50	> 50
3	12.5	50	25	50
4	6.25	50	25	50
5	6.25	25	12.5	50
6	12.5	50	50	> 50
7	6.25	12.5	12.5	> 50
8	25	25	12.5	> 50
9	25	50	12.5	> 50
10	12.5	12.5	12.5	50
11	12.5	12.5	12.5	25
12	12.5	12.5	12.5	25
13	12.5	50	25	> 50
14	25	50	50	> 50
15	12.5	50	50	> 50
16	12.5	50	50	> 50
17	6.25	50	25	> 50
18	12.5	50	25	> 50
19	25	25	12.5	50
20	25	50	25	> 50
21	6.25	50	50	> 50
22	6.25	25	12.5	50
23	12.5	12.5	12.5	> 50
24	12.5	12.5	12.5	> 50
25	25	50	25	> 50
Ph₃BiBr₂	12.5	12.5	12.5	12.5
(p-tolyl)₃BiBr₂	12.5	12.5	12.5	12.5
Clotrimazole*	10	5	5	2.5

* Standard drug, - No activity

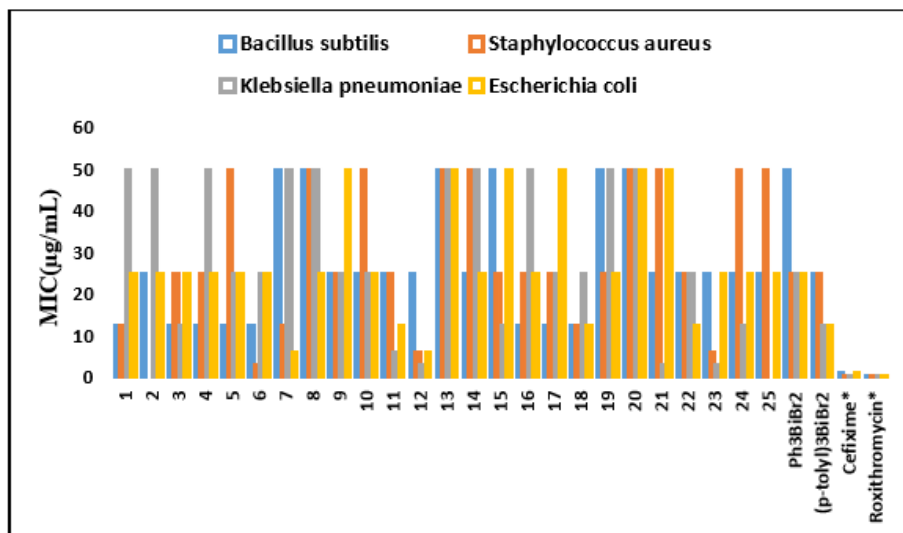


Figure 3.7: Bar graph marking antibacterial activity for (1-25)

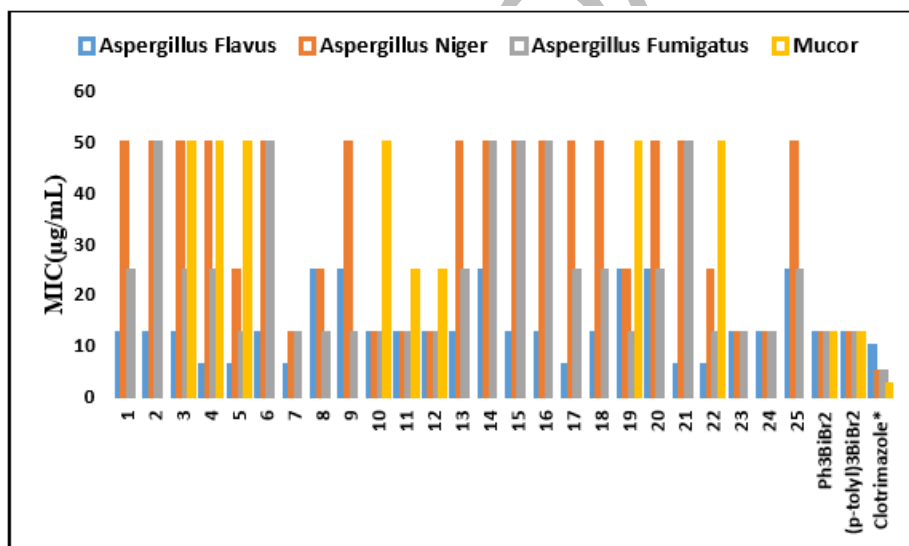


Figure 3.8: Bar graph displaying antifungal activity for (1-25)

3.5.2. Alpha amylase inhibition assay

The compounds (1-25) were also bioassayed for their possible chromogenic alpha amylase inhibition activity. The percentage inhibition of alpha amylase activity was observed at 100 µg/mL, applying acarbose as positive and DMSO as negative control with the data appearing in Table 3.11. It is clear that compounds (2), (13), (14) and (15) exhibit

highest percentage inhibition of 62.36, 45.25, 62.2 and 42.84 respectively, as they contain nitro, iodo and indole moieties in their structural motifs. These values are comparable to the standard drug used here as a reference. The activity of the complexes was also compared with the precursors, $[\text{Ph}_3\text{BiBr}_2]$ and $(\text{p-tolyl})_3\text{BiBr}_2$ and least % age inhibition of -33.54 and -33.71 respectively, were observed for them, but on derivatization with the appropriately substituted carboxylic acids, the percent inhibition got elevated 15 to 60% for the metal complexes [233]. Greater the percentage inhibition value for alpha amylase enzyme, more it will be effective against hyperglycemia or diabetes mellites. The data are presented with the prospect that the prepared compounds may prove themselves as potent candidates in future drug development and delivery processes.

Table 3.11. Alpha amylase inhibition data for (1-25)

Compounds No.	%age Inhibition
1	27.72
2	62.36
3	15.34
4	32.76
5	18.59
6	-4.09
7	31.49
8	11.66
9	21.25
10	27.4
11	35.91
12	8.67
13	45.25
14	62.2
15	42.84
16	-0.63
17	21.1
18	-17.16
19	34.81
20	14.65
21	1.1
22	23.5
23	17.79

24	20.47
25	-12.28
Ph ₃ BiBr ₂	-33.54
(p-toly) ₃ BiBr ₂	-33.71
Acarbose*	69.29

* Standard drug, Concentration = 100 µg/mL in DMSO

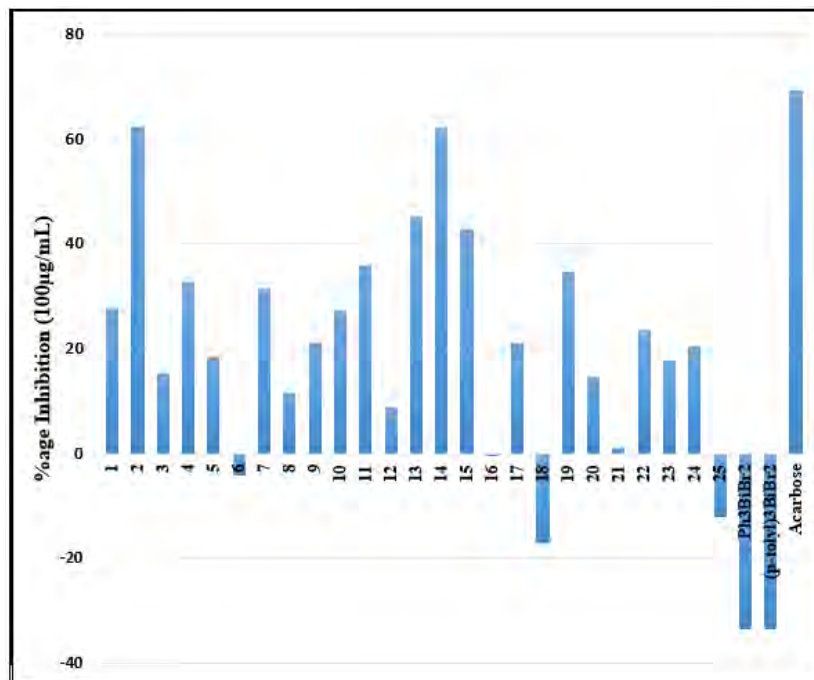


Figure 3.9: Bar graph showing antidiabetic activity for (1-25)

3.5.3. Protein kinase inhibition assay

To evaluate the protein kinase inhibitory potential for (1-25), surfactin and DMSO were employed as positive and negative control, respectively, and the data are presented in Table 3.12. The non-toxic effect of DMSO was verified by the absence of growth inhibition zone. A significant inhibition zone of 30 mm bald phenotype corresponds to (7) which is equivalent to the standard drug (surfactin; 100µg /disc), whereas (4), (9) and (10) show clear zone at 30 mm for each. The zones of inhibition greater than 20 mm bald and clear are attributed to significant activity and cytotoxic nature, respectively, for the compounds under trial. The electron-donating group such as methyl (-CH₃), attached to the carboxylic

moiety [as for (7)], is responsible for this exceptional percentage inhibition of protein kinase enzyme at 100 µg disc loading. The assay involves *Streptomyces* 85E strain to envisage the protein kinase inhibition, as it resembles with the eukaryotic cells that readily provides evidence for anticancer and cytotoxic nature of the synthesized compounds. The protein kinases are involved in phosphorylation of various eukaryotic cells, whereas the protein kinase inhibitors are specifically concerned with in blocking them in order to stop the proliferation of cancerous cells. The kinase inhibition data for some of the organobismuth (V) compounds are encouraging and may prove suitable agents in futuristic drug discovery processes [233].

Table 3.12. Protein kinase inhibition data for (1-25)

Compound No.	Zones of Inhibition	
	Clear Zone (nm)	Bald Zone (nm)
1	20	15
2	15	-
3	25	-
4	30	20
5	25	-
6	-	-
7	-	30
8	22	18
9	30	-
10	30	-
11	15	-
12	20	-
13	20	-
14	22	18
15	-	8
16	20	15
17	20	-
18	-	-
19	-	15
20	-	20
21	15	20
22	25	20
23	-	15
24	15	-
25	20	-
Ph₃BiBr₂	-	20

(p-toly) ₃ BiBr ₂	24	-
Surfactin*	-	30

* Standard drug, - No activity, Concentration = 100µg/disc in DMSO

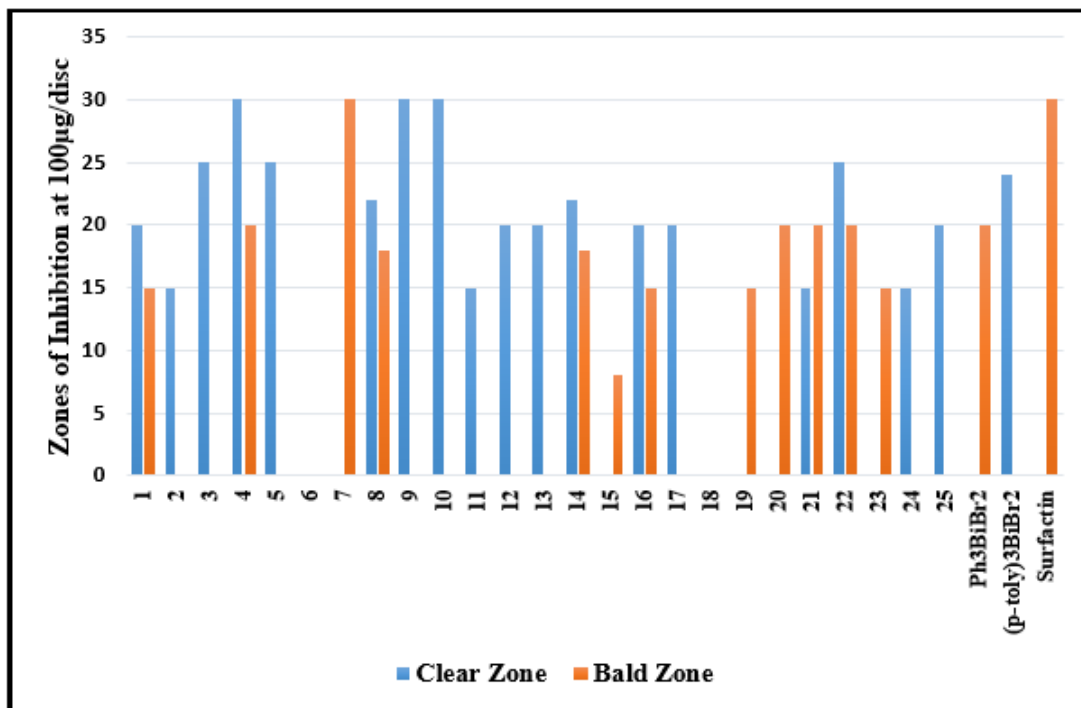


Figure 3.10: Bar graph showing protein kinase inhibition activity for (1-25)

3.5.4. Brine shrimp lethality assay

The brine shrimp lethality assay is a simple, robust and least expensive technique for assessing the toxic/cytotoxic nature of the prepared organobismuth(V) derivatives. This bioassay facilitates to develop a toxicity appraisal for the compounds in comparison to the reference drug (doxorubicin). The results are documented in terms of LD₅₀ values, which refer to the dose required to kill half of the tested population of the biological specie in specific time duration (Table 3.13). The percentage mortality of *Artemia salina* was tested in serial dilutions as 200, 100, 50 and 25 µg/mL. The least LD₅₀ values for (9), (10) and (21) were found to be 3.39, 5.25 and 12.28 µg/mL, respectively, establishing their toxic nature while majority of the compounds were comparatively less toxic having LD₅₀ values ranging from 53.97 to 58.29 µg/mL for (2), (6), (8) and (17). The data suggest that the synthesized compounds are moderately toxic but their biological significance can be

further optimized for future drug discovery processes by altering their structural motifs [263].

Table 3.13. Brine shrimp lethality data for (1-25)

Compd. No	% age Mortality				LD ₅₀ (µg/mL)
	200 (µg/mL)	100 (µg/mL)	50 (µg/mL)	25 (µg/mL)	
1	100	70	60	50	29.31
2	100	70	90	50	53.97
3	100	90	50	30	42.15
4	100	50	40	40	55.94
5	100	80	70	60	18.61
6	100	60	40	30	58.29
7	100	60	50	40	44.45
8	100	60	50	20	56.95
9	100	100	90	90	3.39
10	100	90	80	60	5.25
11	100	70	70	60	17.56
12	100	60	80	30	35.72
13	100	90	50	30	43.15
14	100	40	60	30	28.42
15	100	90	80	40	29.31
16	100	60	60	50	30.43
17	100	60	40	30	58.29
18	100	80	70	60	18.61
19	100	90	80	50	24.77
20	100	90	80	60	19.05
21	100	90	80	70	12.28
22	100	70	80	30	42.54
23	100	80	60	30	40.43
24	100	90	40	30	48.26
25	100	90	60	50	28.42
Ph ₃ BiBr ₂	100	100	90	30	30.30
(p-toly) ₃ BiBr ₂	100	100	90	50	25.01
Doxorubicin*	90	80	60	40	5.93

* Standard drug

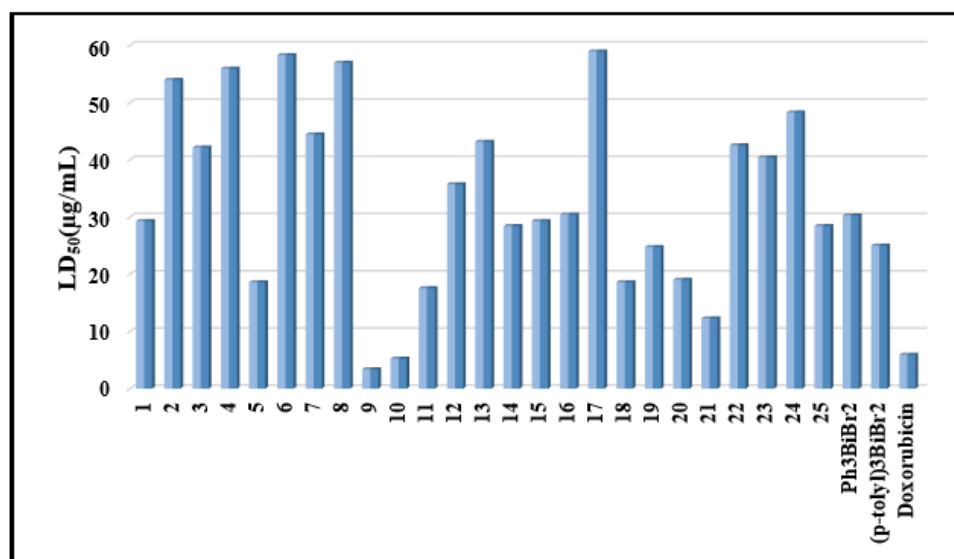


Figure 3.11: Bar graph showing brine shrimp lethality assay for (1-25)

3.5.5. Computational studies

Molecular docking studies were performed using Genetic Optimization for Ligand Docking (GOLD) program [243, 244]. The GOLD implements a genetic algorithm for docking flexible ‘lead’ compounds into the active sites of the selected receptor. The crystal structure of *Helicobacter pylori* urease, human pancreatic alpha amylase, and epidermal growth factor receptor tyrosine kinase were retrieved from RCSB protein data bank (PDB) for molecular docking investigations. The binding sites of the selected proteins were taken from the literature survey [245-247], and for more details consult [248]. The compounds exhibiting greater GOLD fitness score will be considered as having better binding affinity with the receptor [249].

3.5.5.1. *H. pylori* Urease

The molecular docking data for representative compounds, depicted in Table 3.14, suggest that compound (20) exhibits the highest GOLD fitness score of 56 and could serve as a ‘lead’ compound. The active sites of protein that interact directly with the compound include: Asp403, Ala407, His459, Cys559, His560, Arg576, Val558, Met555, Asp554, Glu551, Arg606, Gly605, Gln602, Ile376, Ser601, Val607, and Thr408 (Fig. 3.12). The

binding pattern analysis of the docked complex indicates strong hydrogen bonding between oxygen atoms of the ligand with the Arg606 and Cys559 residues of the receptor. The amide- π stacking interactions play an important role towards improved binding affinity in receptor-ligand complexes [264]. Moreover, the binding orientation analysis shows that multiple interactions like amide- π and alkyl- π , in docked complexes, are taking part in anchoring the ligand within the binding pocket of the protein (Fig. 3.12 and 3.13). For instance, protein residues (Arg606, Val558, Cys559, and Asn406) are stabilizing the complex by forming aromatic interactions with the benzene ring of the ligand. The results of the docking studies imply that prepared compounds are potentially active against *H. pylori* urease which may find place for themselves as potent inhibitors.

Table-3.14. GOLD fitness score against various enzymes* for selected compounds

Compounds No.	GOLD Fitness Score		
	<i>H. pylori</i> Urease*	Tyrosine kinase*	Human pancreatic alpha amylase*
5	40.49	64.09	55.69
7	29.38	46.28	62.65
8	55.99	40.51	57.15
10	41.10	40.72	57.19
17	44.25	41.82	60.91
19	28.45	41.91	58.64
20	56.30	58.85	62.1
22	42.2	17.44	45.79

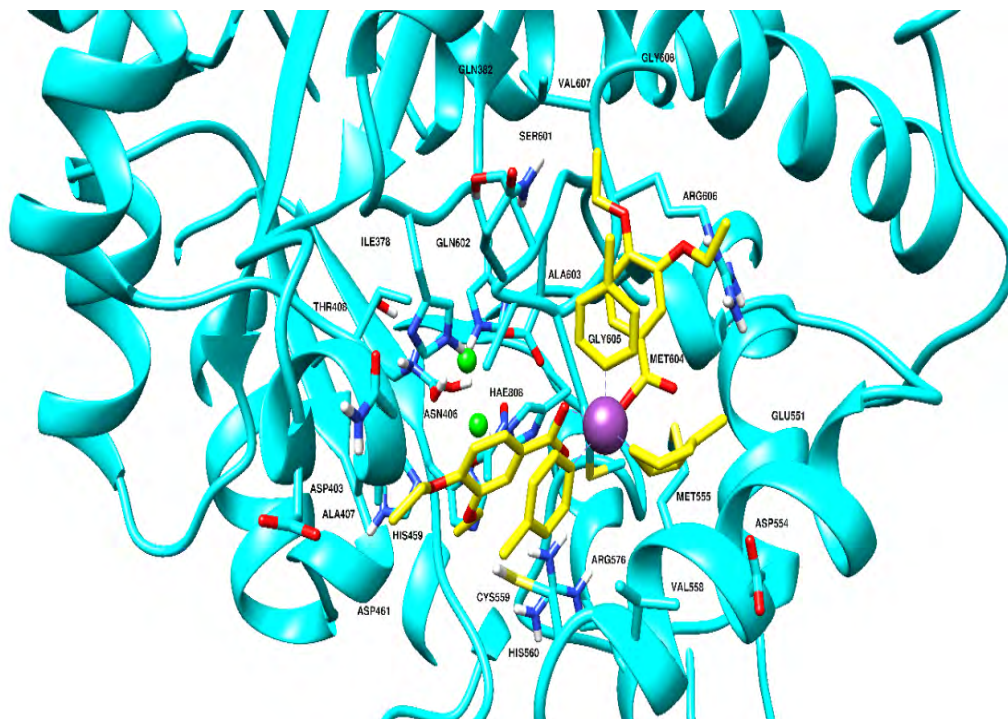


Figure-3.12 : Preferred binding mode for (20) in the active site of *H. pylori* urease

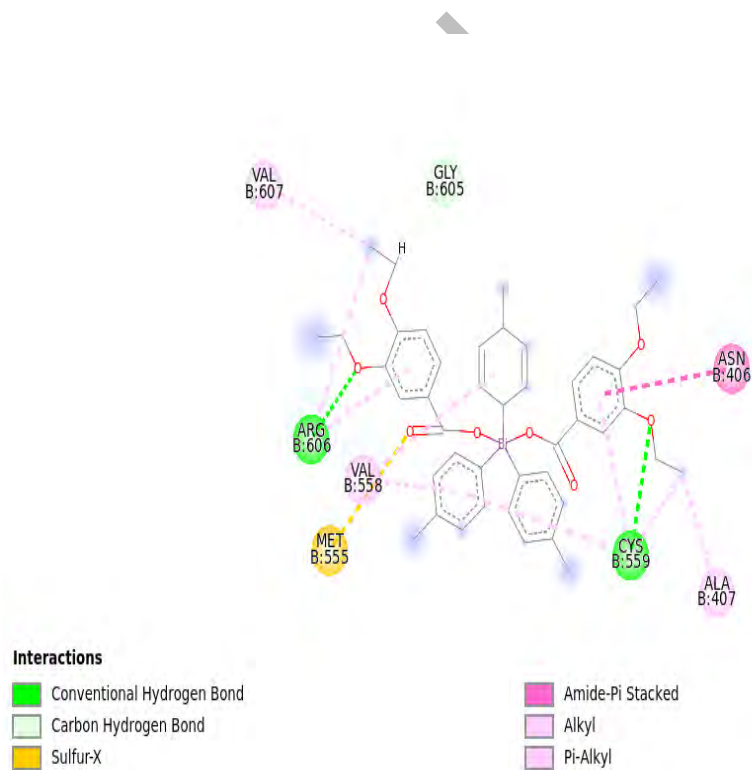


Figure-3.13: The 2-D depiction of docked ‘lead compound’ within the binding pocket of urease protein through DS Visualizer

3.5.5.2. Tyrosine kinase

The molecular docking studies for representative complexes against the receptor tyrosine kinase were conducted and the literature widely hints that kinases influence the onset of cancer by increasing cell proliferation [265]. The data reveal that compound **(5)**, with the GOLD fitness score of 64.09 has the higher binding potential to kinase, whereas rest of the compounds also demonstrate substantial binding affinity with the enzyme structure (Table 3.14). The active site residues of protein that involved in binding with the ligand are: Ala27, Lys180, Pro182, Gly26, Asp160, Asp105, Leu149, Leu104, Asn147, Arg146, Thr159, and Phe28 (Fig. 3.14). The strong hydrogen bonding have been observed between protein residues (Asp160, Asn147, and Arg146) and the oxygen atoms of the ligand (Fig. 3.15). It is worth-mentioning that compounds **(20)** and **(5)** may prove as potential candidates for ‘lead compound’ against the receptor tyrosine kinase in future studies as their *in-silico* binding interactions with the enzyme are also significant.

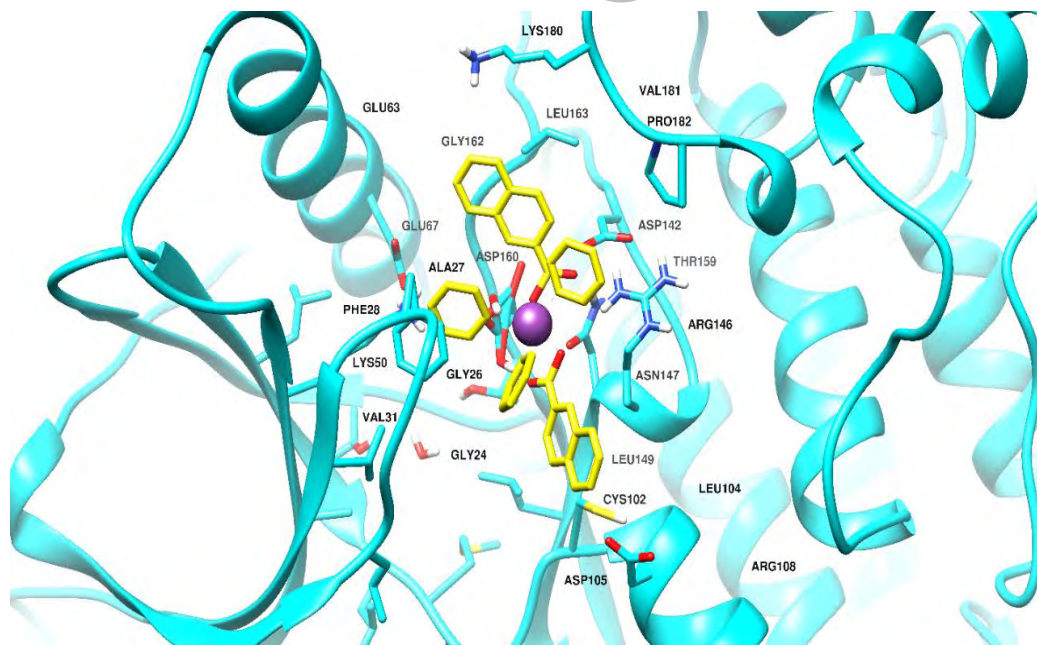


Figure 3.14: Preferred binding mode for **(5)** with the active site of receptor tyrosine kinase

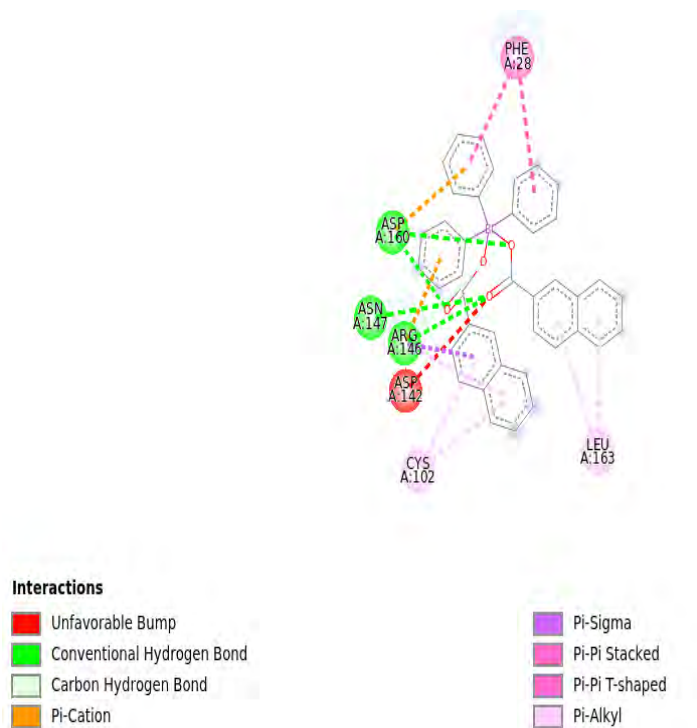


Figure 3.15: The 2-D representation of docked ‘lead’ complex within the binding pocket of tyrosine kinase protein through DS Visualizer

3.5.5.3. *Human pancreatic alpha amylase*

To analyze the amylase inhibitory potential of the synthesized compounds molecular docking tests were performed and the data are grouped in Table 3.14. The maximum GOLD fitness score of 62.65 for (7) suggests its firm affinity to the active site of protein. The GOLD fitness scores for other compounds are also impressive and may be considered for their possible role as amylase inhibitors in future drug discovery processes. The active site residues, participating in receptor-ligand interactions comprise Trp59, Gln63, Thr163, Leu162, Leu165, His201, Ala198, Glu233, Asp300, and Ile235 as illustrated in Fig. 3.16. A strong hydrogen bond is observed between Thr163, and oxygen atom of the carboxylate moiety present in the ligand. The major role of anchoring and stabilizing the ligand within the binding pocket is played by several pi-alkyl and pi-pi interactions of benzene ring of the ligand with the protein residues.

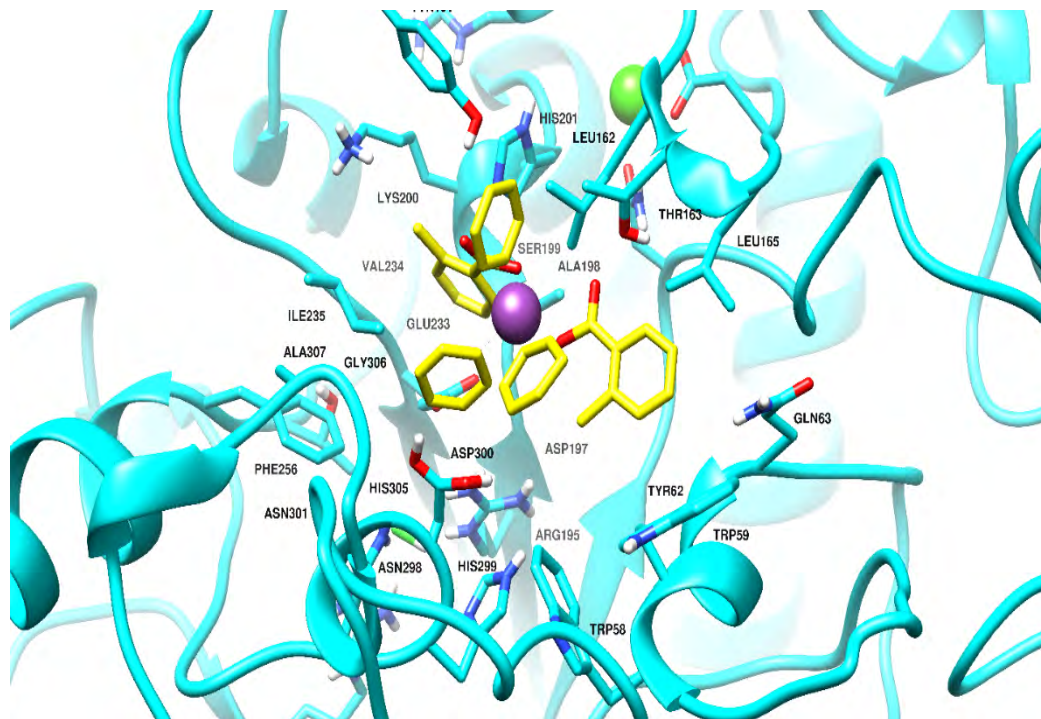


Figure 3.16: Preferred binding modes for (7) in active sites of human pancreatic alpha amylase

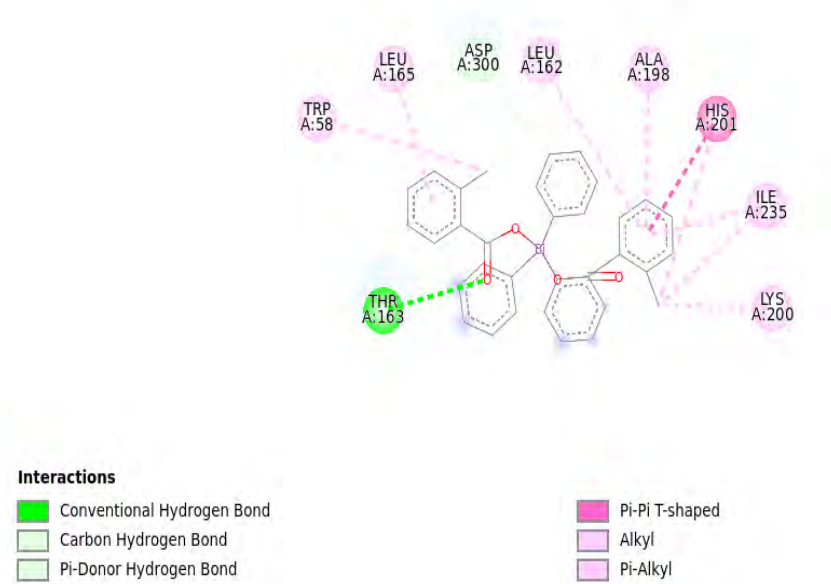


Figure 3.17: The 2-D presentation for (7) showing interactions within the binding pocket of alpha amylase protein through DS Visualizer

3.6. Structure to activity relationship (SAR)

All the synthesized complexes (**1-25**) unfold moderate to good activity against various positive controls. Upon coordination with organobismuth(V) derivatives they show remarkable activity. All these biocidal applications furnish a rational structure-to -activity relationship. To develop a limited structure to activity relationship (SAR), various substituents on different positions of phenyl ring, present in the synthesized compounds (**1-25**), were taken into consideration.

- The compounds (**6, 12, 21** and **23**) contain 4-Cl, 4-Br, 3-CF₃, 3-Br functionalities (having electron-withdrawing effects) show MIC values of 3.125 µg/mL against *K. pneumoniae*.
- Similarly, the data for antifungal activity are also encouraging that may provide guidelines to the researchers working in this field.
- The preliminary screening data for alpha amylase inhibition demonstrate that compounds (**2, 13, 14** and **15**) exhibit highest percentage inhibition of 62.36, 45.25, 62.2 and 42.84 respectively, as they accommodate nitro, iodo and indole moiety in their structural motifs justifying the obtained results at 100 µg/mL disc loading.
- The data for protein kinase inhibition assay showed a significant inhibition zone of 30 mm bald phenotype corresponding to (**7**) which is equivalent to the standard drug (surfactin; 100 µg/disc). The electron-donating group such as methyl (-CH₃) attached to the carboxylic moiety, is responsible for this exceptional percentage inhibition of protein kinase enzyme at 100 µg disc loading.
- The brine shrimp lethality assay data exhibit that fluorinated and chlorinated organobismuth (V) carboxylates (**9, 10** and **21**) have the least LD₅₀ value of 3.39, 5.25 and 12.28 µg/mL, respectively, making them most toxic among all the synthesized complexes.

Thus, it is inferred from the presented data that a compromise will have to be made between activity and toxicity of such compounds so as to render them amenable to future drug delivery system, and for that some adjustments/alterations, like physicochemical

nature of the complexing agents, nature/length of alkyl chain of substituted moiety and hydrophobicity have to be taken into account.

3.7. Non-biological applications

There is currently some growing attention in the synthesis of salen-based bi-compartmental azomethine ligands with 3d and 4f nucleus leading to the simultaneous incorporation of magnetic and photophysical properties [81, 82]. Owing to this fact, the synthesized metal complexes were explored for magnetic and photoluminescence domains and the results are discussed in subsequent sections.

3.7.1. Photoluminescence data

Lanthanide complexes with salen and salopn type of compartmental Schiff base ligands exhibit exceptional photophysical properties owing to their ligand-dependent luminescence sensitization and long emission lifetimes. Keeping the preceding in view, the photoluminescence studies were performed for ligands (**L1**, **L3** and **L4**), mononuclear zinc precursor [Zn(salopn)H₂O] (**ZnL4**), dinuclear (**26**, **37**) and trinuclear complexes (**43**, **45**) to determine the ability of the ligand to act as an efficient sensitizer upon coordination with lanthanide metals. Detailed account is given for representative trinuclear complexes. In all cases they were studied in methanol as a solvent applying excitation source of 306 nm. The UV visible spectra of **L4** set out four intense absorption band at λ_{\max} = 202, 226, 270 and 331 nm. The two former bands at < 230 nm are responsible for spin-allowed singlet π - π^* transition for phenyl and phenolic ring, while third and fourth bands are attributable to C=N π - π^* transition and ligand intramolecular charge transfer transitions respectively. Upon excitation at λ_{\max} = 306 nm, **L4** exhibits a comparatively broad emission band having emission wavelength λ_{em} = 455 nm [81].

The absorption spectra of trinuclear Zn^{II}-Ln^{III}-Zn^{II} complexes (**43**, **45**) depict that one of the latter bands disappears upon coordination with 3d/4f metals, whereas the other three bands show slight red shift in the target complexes in contrast to ligand. All complexes (**ZnL4**, **43** and **45**) manifest metal-centered charge-transfer luminescence in UV region around 385-390 nm due to π - π^* transition. This results in the appearance of emission band

for Dy^{III} (⁴F_{9/2} → ⁶H_{15/2}) and Sm^{III} (⁴G_{5/2} → ⁶H_{5/2}) in the visible region at 458 and 469 nm respectively [81]. After excitation at 306 nm, the PL kinetics was measured at various wavelengths (Table 3.15). The measured PL kinetics of the samples is shown in Fig. 3.20 and their corresponding average PL lifetimes are evaluated by using exponential decay models.

Table 3.15: Photoluminescence parameters for the selected compounds

Compound codes	Absorption wavelength (λ_{em})	Emission wavelength (λ_{em})	Average PL Lifetime (τ)
	(nm)	(nm)	(ns)
L ₁	263	470	3.28
L ₃	317	449	2.72
L ₄	331	455	3.85
ZnL ₄	289	460	3.48
26	307	451	2.90
37	351	452	3.93
43	389	458	4.02
45	392	469	3.74

Excitation source at $\lambda_{max}=306nm$

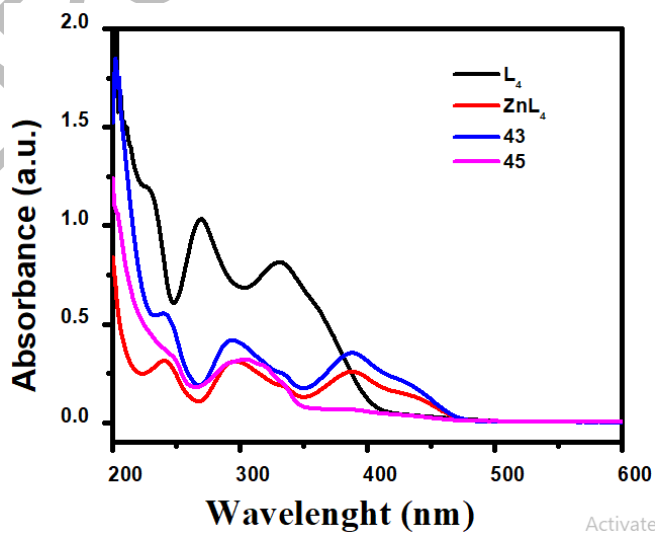


Figure 3.18. UV-vis spectra for L₄, ZnL₄, 43 and 45

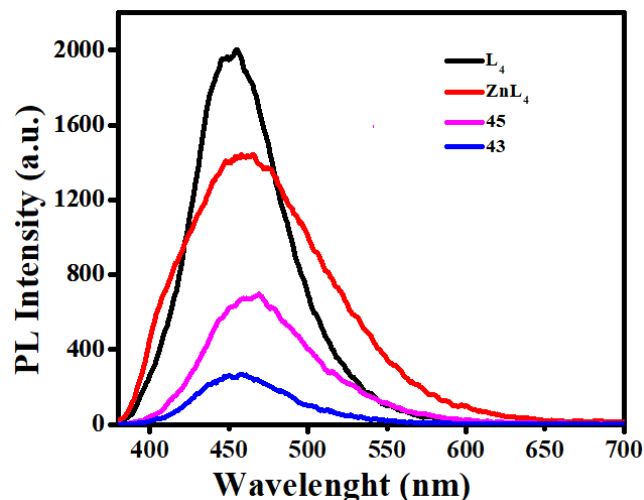


Figure 3.19. Steady-state photoluminescence spectra for L_4 , ZnL_4 , 43 and 45 [in methanol (2×10^{-5} M)]

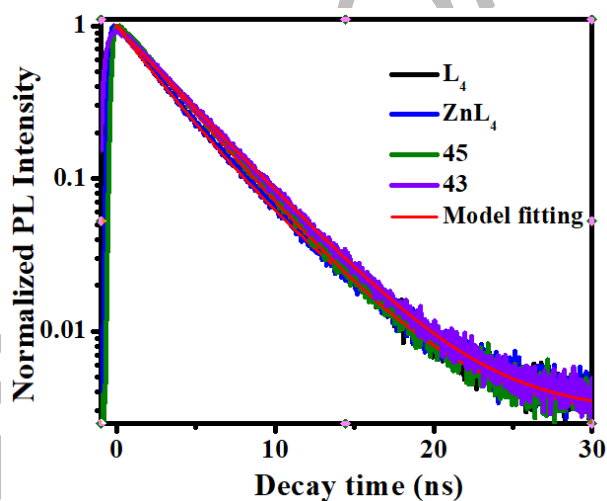


Figure 3.20 Time-resolved photoluminescence spectra for L_4 , ZnL_4 , 43 and 45 [in methanol (2×10^{-5} M)]

3.7.2. Magnetic susceptibility data

The direct current magnetic susceptibility of the synthesized heterodinuclear (26-30) and trinuclear (41-45) 3d/4f metal complexes were performed at 291K under the applied magnetic field owing to the fact that they exhibit paramagnetic behavior over wide range of temperatures. The room temperature $\chi_m T$ values for certain lanthanide-based

compounds: La (**26, 41**), Nd (**27, 42**), Sm (**28, 43**), Gd (**29, 44**) and Dy (**30, 45**) are similar to the calculated magnetic susceptibility values for the ground state of Ln(III) ion as listed in Table 3.19 [82, 266], whereas the ground states of Nd^{III} ($4f^3$, $S = 3/2$, $J = 9/2$, $g_J = 8/11$, $^4I_{9/2}$), Sm^{III} ($4f^5$, $S = 5/2$, $J = 5/2$, $g_J = 2/7$, $^6H_{5/2}$), Gd^{III} ($4f^7$, $S = 7/2$, $J = 7/2$, $g_J = 2$, $^8S_{7/2}$) and Dy^{III} ($4f^9$, $S = 5/2$, $J = 15/2$, $g_J = 4/3$, $^6H_{15/2}$) are responsible for these $\chi_m T$ values in free-ion approximation [82]. The data revealed that the calculated effective magnetic moment (μ_{eff}) values [1.20, 4.10, 2.15, 8.36 and 11.05 μ_B for La (**41**), Nd (**42**), Sm (**43**), Gd (**44**) and Dy (**45**)] are in good agreement with the reported μ_{eff} values i.e., 0, 3.89, 1.76, 7.93, 10.42 μ_B (Table 3.16). The data suggested that bi-compartmental phenylene-bridged ligand did not affect the unpaired electrons of paramagnetic lanthanide metals but might have augmented their magnetic properties at a wide range of temperature.

The comparative assessment of magnetic susceptibility $\chi_m T$ is made on the basis of literature with respect to nuclearity (i.e., di-, tri-, tetra-, penta- and hexanuclear). The data explicitly depict that synthesized complexes have followed increasing trend concerning to unpaired electrons which correlates to their high single ion magnetic moment range due to their strong response against external magnetic field. In general, the Ln^{III} containing complexes have large energy difference between the ground and first excited states. However, compound (**43**) with Sm^{III} metal has not followed the said trend at room temperature because the ground state ($^4G_{5/2}$) and the first excited state ($^6H_{7/2}$) are not well separated (lie close to each other), so they are thermally populated even at room temperature that leads to the exceptionally low $\chi_m T$ value, i.e., 0.58 emu mol⁻¹ K at 300K [82, 267]. While Dy^{III} incorporated heterotrimeric complex showed exceptionally high values for $\chi_m T$ and μ_{eff} at 15.37 emu mol⁻¹ K and 11.05, respectively. The presented data provide an impetus to outline magnetically strong materials with the advantage of magnetic interactions between Ln^{III} and Zn^{II} ions in a heterometallic d-f system.

Table 3.16. A comparative study of magnetic susceptibility data for some selected compounds ^(a,b)

Comp. codes	Compounds	Gram susceptibility	Magnetic susceptibility	Effective magnetic moment
		χ_g (emu g ⁻¹)	$\chi_m \cdot T$ (emu mol ⁻¹ K)	μ_{eff} (μ_B)
26	[ZnLa(L ₁)(NO ₃) ₃ H ₂ O]	0.19×10 ⁻⁶	0.18	1.22
27	[ZnNd(L ₁)(NO ₃) ₃ H ₂ O]	5.39×10 ⁻⁶	1.30	3.22
28	[ZnSm(L ₁)(NO ₃) ₃ H ₂ O]	1.25×10 ⁻⁶	0.419	1.82
29	[ZnGd(L ₁)(NO ₃) ₃ H ₂ O]	38.5×10 ⁻⁶	8.60	8.27
30	[ZnDy(L ₁)(NO ₃) ₃ H ₂ O]	55.7×10 ⁻⁶	12.45	9.95
41	[Zn ₂ La(L ₄) ₂ (NO ₃) ₃ H ₂ O].CH ₃ CN.H ₂ O	0.10×10 ⁻⁶	0.18	1.20
42	[Zn ₂ Nd(L ₄) ₂ (NO ₃) ₃ H ₂ O].CH ₃ CN.H ₂ O	5.73×10 ⁻⁶	2.12	4.10
43	[Zn ₂ Sm(L ₄) ₂ (NO ₃) ₃ H ₂ O].CH ₃ CN.H ₂ O	1.2×10 ⁻⁶	0.58	2.15
44	[Zn ₂ Gd(L ₄) ₂ (NO ₃) ₃ H ₂ O].CH ₃ CN.H ₂ O	24.8×10 ⁻⁶	8.80	8.36
45	[Zn ₂ Dy(L ₄) ₂ (NO ₃) ₃ H ₂ O].CH ₃ CN.H ₂ O	43.4×10 ⁻⁶	15.37	11.05

^a L₁ = N,N'-bis(2-hydroxy-3-methoxysalicylidene)ethylene-1,2-diamine

^b L₄ = N,N'-bis(2-hydroxy-salicylidene)phenylene-1,2-diamine

References

- [1] F. Thomas, B. Bialek, R. Hensel, Medical use of bismuth: the two sides of the coin, *Journal of Clinical Toxicology*, 3 (2011) 495.
- [2] P. J. Sadler, Inorganic chemistry and drug design, *Advances in Inorganic Chemistry*, Elsevier, (1991) 1-48.
- [3] D. M. Keogan, D. M. Griffith, Current and potential applications of bismuth-based drugs, *Molecules*, 19 (2014) 15258-15297.
- [4] J. Kyle, P. Breuer, K. Bunney, R. Pleysier, P. May, Review of trace toxic elements (Pb, Cd, Hg, As, Sb, Bi, Se, Te) and their deportment in gold processing. Part 1: mineralogy, aqueous chemistry and oxicity, *Hydrometallurgy*, 107 (2011) 91-100.
- [5] J. Kyle, P. Breuer, K. Bunney, R. Pleysier, Review of trace toxic elements (Pb, Cd, Hg, As, Sb, Bi, Se, Te) and their deportment in gold processing: Part II: Deportment in gold ore processing by cyanidation, *Hydrometallurgy*, 111 (2012) 10-21.
- [6] J. M. Bothwell, S. W. Krabbe, R. S. Mohan, Applications of bismuth(III) compounds in organic synthesis, *Chemical Society Reviews*, 40 (2011) 4649-4707.
- [7] R. Mohan, N. Leonard, L. Wieland, Applications of bismuth(III) compounds in organic synthesis, *Tetrahedron*, 58 (2002) 8373-8397.
- [8] N. C. Norman, *Chemistry of arsenic, antimony and bismuth*, Springer Science & Business Media, 1997.
- [9] A. Slikkerveer, F. A. de Wolff, Pharmacokinetics and toxicity of bismuth compounds, *Medical Toxicology and Adverse Drug Experience*, 4 (1989) 303-323.
- [10] J. R. Lambert, Pharmacology of bismuth-containing compounds, *Reviews of Infectious Diseases*, 13 (1991) S691-S695.

- [11] H. Sun, L. Zhang, K. Y. Szeto, Bismuth in medicine, *Metal Ions in Biological Systems*, 41 (2004) 333-378.
- [12] R. G. Grávalos, Seven-day 'rescue' therapy after *Helicobacter pylori* treatment failure: omeprazole, bismuth, tetracycline and metronidazole vs. ranitidine bismuth citrate, tetracycline and metronidazole, *Alimentary Pharmacology & Therapeutics*, 13 (1999) 1311-1316.
- [13] R. Mohan, Green bismuth, *Nature Chemistry*, 2 (2010) 336-336.
- [14] G. Baxter, Settling the stomach, *Chemistry in Britain*, 28 (1992) 445-448.
- [15] N. Burford, S. Vanzantten, L. Agocs, L. Best, T. Cameron, B. Yhard, J. Curtis, Anti-*Helicobacter-Pylori* properties of new bismuth compounds, in: *Gastroenterology*, Wb Saunders Co Independence Square West Curtis Center, Ste 300, Philadelphia ..., (1994) A59-A59.
- [16] E. Asato, K. Katsura, M. Mikuriya, U. Turpeinen, I. Mutikainen, J. Reedijk, Synthesis, structure, and spectroscopic properties of bismuth citrate compounds and the bismuth-containing ulcer-healing agent colloidal bismuth subcitrate (CBS). 4. Crystal structure and solution behavior of a unique dodecanuclear cluster $(\text{NH}_4)_{12}[\text{Bi}_{12}\text{O}_8(\text{cit})_8](\text{H}_2\text{O})_{10}$, *Inorganic Chemistry*, 34 (1995) 2447-2454.
- [17] X. Wang, X. Zhang, J. Lin, J. Chen, Q. Xu, Z. Guo, DNA-binding property and antitumor activity of bismuth(III) complex with 1, 4, 7, 10-tetrakis (2-pyridylmethyl)-1, 4, 7, 10-tetraazacyclododecane, *Dalton Transactions*, (2003) 2379-2380.
- [18] P. Köpf-Maier, T. Klapötke, Antitumor activity of some organometallic bismuth(III) thiolates, *Inorganica Chimica acta*, 152 (1988) 49-52.
- [19] X. W. Zhang, J. Xia, H. W. Yan, S. L. Luo, S. F. Yin, C. T. Au, W. Y. Wong, Synthesis, structure, and in vitro antiproliferative activity of cyclic hypervalent organobismuth(III) chlorides and their triphenylgermylpropionate derivatives, *Journal of Organometallic Chemistry*, 694 (2009) 3019-3026.

- [20] D. L. Van Caekenberghe, J. Breysens, In vitro synergistic activity between bismuth subcitrate and various antimicrobial agents against *Campylobacter pyloridis* (*C. pylori*), *Antimicrobial Agents and Chemotherapy*, 31 (1987) 1429-1430.
- [21] J.S. Solanki, U. Tripathi, A. Bhardwaj, T. Thapak, Synthesis, spectral study and antimicrobial activity of bismuth(III) 3(2'-hydroxyphenyl)-5-(4-substitutedphenyl) pyrazolates, *Journal of Coordination Chemistry*, 61 (2008) 4025-4032.
- [22] D. Bandyopadhyay, S. Mukherjee, J. C. Granados, J. D. Short, B. K. Banik, Ultrasound-assisted bismuth nitrate-induced green synthesis of novel pyrrole derivatives and their biological evaluation as anticancer agents, *European Journal of Medicinal Chemistry*, 50 (2012) 209-215.
- [23] R. Ouyang, Y. Yang, X. Tong, K. Feng, Y. Yang, H. Tao, X. Zhang, T. Zong, P. Cao, F. Xiong, *Journal of Inorganic Biochemistry*, 168 (2017) 18-26.
- [24] L. Cui, C. Bi, Y. Fan, X. Li, X. Meng, N. Zhang, Z. Zhang, Synthesis, crystal structures, DNA interaction and anticancer activity of organobismuth(V) complexes, *Inorganica Chimica Acta*, 437 (2015) 41-46.
- [25] A. Islam, J. G. Da Silva, F. M. Berbet, S. M. Da Silva, B. L. Rodrigues, H. Beraldo, M. N. Melo, F. Frézard, C. Demicheli, Novel triphenylantimony(V) and triphenylbismuth(V) complexes with benzoic acid derivatives: structural characterization, in vitro antileishmanial and antibacterial activities and cytotoxicity against macrophages, *Molecules*, 19 (2014) 6009-6030.
- [26] M. N. Rocha, P. M. Nogueira, C. Demicheli, L. G. de Oliveira, M. M. da Silva, F. Frézard, M. N. Melo, R. P. Soares, Cytotoxicity and in vitro antileishmanial activity of antimony(V), Bismuth(V), and Tin(IV) complexes of lapachol, *Bioinorganic Chemistry and Applications*, 2013 (2013).
- [27] P. J. Sadler, H. Li, H. Sun, Coordination chemistry of metals in medicine: target sites for bismuth, *Coordination Chemistry Reviews*, 185 (1999) 689-709.

- [28] H. Menge, B. Brosius, A. Lang, M. Gregor, Bismuth absorption from the stomach and small intestine, *Gastroenterology*, 102 (1992) 2192.
- [29] N. Yang, H. Sun, Biocoordination chemistry of bismuth: Recent advances, *Coordination Chemistry Reviews*, 251 (2007) 2354-2366.
- [30] S. Mahbul Hasan, A. Chowdhury, C. A. Keya, Urease: The Ultimate Therapeutic Target for *Helicobacter pylori*, *Gastroenterol Hepatol*, 23 (2001) 1175-1181.
- [31] F. Lazarini, Redetermination of the structure of bismuth(III) nitrate pentahydrate, $\text{Bi}(\text{NO}_3)_3 \cdot 5\text{H}_2\text{O}$, *Acta Crystallographica Section C: Crystal Structure Communications*, 41 (1985) 1144-1145.
- [32] R.G. Pearson, Hard and soft acids and bases, *Journal of the American Chemical Society*, 85 (1963) 3533-3539.
- [33] J. Supniewski, R. Adams, Organic Bismuth Compounds. I. Preparation of Tricarboxy-Triphenylbismuth Dichlorides and Certain Nitro-Triaryl Bismuth Compounds, *Journal of the American Chemical Society*, 48 (1926) 507-517.
- [34] P. C. Andrews, G. B. Deacon, W. R. Jackson, M. Maguire, N. M. Scott, B. W. Skelton, A. H. White, Solvent-free synthesis of bismuth thiolates and carboxylates, *Journal of the Chemical Society, Dalton Transactions*, (2002) 4634-4638.
- [35] V. Stavila, J. C. Fettinger, K. H. Whitmire, Synthesis and characterization of new phenylbis(salicylato)bismuth(III) complexes, *Organometallics*, 26 (2007) 3321-3328.
- [36] P. C. Andrews, R. L. Ferrero, P. C. Junk, I. Kumar, Q. Luu, K. Nguyen, J. W. Taylor, Bismuth(III) complexes derived from non-steroidal anti-inflammatory drugs and their activity against *Helicobacter pylori*, *Dalton Transactions*, 39 (2010) 2861-2868.
- [37] P. C. Andrews, G. B. Deacon, P. C. Junk, I. Kumar, J. G. MacLellan, Synthesis, ethanolysis, and hydrolysis of bismuth(III) ortho-nitrobenzoate complexes en route to a pearl necklace-like polymer of Bi_{10} oxo-clusters, *Organometallics*, 28 (2009) 3999-4008.

- [38] M. Busse, E. Border, P. C. Junk, R. L. Ferrero, P. C. Andrews, Bismuth(III) complexes derived from α -amino acids: the impact of hydrolysis and oxido-cluster formation on their activity against *Helicobacter pylori*, *Dalton Transactions*, 43 (2014) 17980-17990.
- [39] P. C. Andrews, G. B. Deacon, P. C. Junk, I. Kumar, M. Silberstein, Synthetic and structural comparisons of bismuth(III) carboxylates synthesised under solvent-free and reflux conditions, *Dalton Transactions*, (2006) 4852-4858.
- [40] O. Anjaneyulu, T. Prasad, K. K. Swamy, Coordinatively polymeric and monomeric bismuth(III) complexes with pyridine carboxylic acids, *Dalton Transactions*, 39 (2010) 1935-1940.
- [41] O. Anjaneyulu, K. K. Swamy, Studies on bismuth carboxylates-synthesis and characterization of a new structural form of bismuth(III) dipicolinate, *Journal of Chemical Sciences*, 123 (2011) 131-137.
- [42] O. Anjaneyulu, D. Maddileti, K. K. Swamy, Structural motifs in phenylbismuth heterocyclic carboxylates-secondary interactions leading to oligomers, *Dalton Transactions*, 41 (2012) 1004-1012.
- [43] I. Kumar, P. Bhattacharya, K. H. Whitmire, Structural diversity in phenylbismuth(III)bis(carboxylate) complexes, *Journal of Organometallic Chemistry*, 794 (2015) 153-167.
- [44] S. Andleeb, Intiaz-ud-Din., Recent progress in designing the synthetic strategies for bismuth based complexes, *Journal of Organometallic Chemistry*, 898 (2019) 120871.
- [45] S. Sivasekar, K. Ramalingam, C. Rizzoli, N. Alexander, Synthesis, structural, Continuous Shape Measure and bond valence sum characterization of bismuth(III) complexes of substituted dithiocarbamates and their solvothermal decomposition, *Inorganica Chimica Acta*, 419 (2014) 82-88.
- [46] S. Tamilvanan, G. Gurumoorthy, S. Thirumaran, S. Ciattini, Synthesis, characterization, cytotoxicity and antimicrobial studies on Bi(III) dithiocarbamate

complexes containing furfuryl group and their use for the preparation of Bi₂O₃ nanoparticles, *Polyhedron*, 121 (2017) 70-79.

[47] I. Ozturk, C. N. Banti, N. Kourkoumelis, M. J. Manos, A. J. Tasiopoulos, A. Owczarzak, M. Kubicki, S. K. Hadjikakou, Synthesis, characterization and biological activity of antimony(III) or bismuth(III) chloride complexes with dithiocarbamate ligands derived from thiuram degradation, *Polyhedron*, 67 (2014) 89-103.

[48] K. R. Chaudhari, A. P. Wadawale, V. K. Jain, N. Yadav, R. Bohra, Monoorganobismuth(III) thiocarboxylates: Synthesis, characterization and crystal structures of [PhBi (SOCR)₂](R= Ph or Me), National Institute Of Science Communication and Policy Research (2010).

[49] P. C. Andrews, R. L. Ferrero, C. M. Forsyth, P. C. Junk, J. G. Maclellan, R. M. Peiris, Bismuth(III) saccharinate and thiosaccharinate complexes and the effect of ligand substitution on their activity against *Helicobacter pylori*, *Organometallics*, 30 (2011) 6283-6291.

[50] M. X. Li, L. Z. Zhang, M. Yang, J. Y. Niu, J. Zhou, Synthesis, crystal structures, in vitro biological evaluation of zinc(II) and bismuth(III) complexes of 2-acetylpyrazine N (4)-phenylthiosemicarbazone, *Bioorganic & Medicinal Chemistry Letters*, 22 (2012) 2418-2423.

[51] I. P. Ferreira, E. D. Piló, A. A. Recio-Despaigne, J. G. Da Silva, J. P. Ramos, L. B. Marques, P. H. Prazeres, J. A. Takahashi, E. M. Souza-Fagundes, W. Rocha, Bismuth(III) complexes with 2-acetylpyridine and 2-benzoylpyridine-derived hydrazones: Antimicrobial and cytotoxic activities and effects on the clonogenic survival of human solid tumor cells, *Bioorganic Medicinal Chemistry*, 24 (2016) 2988-2998.

[52] K. S. Ferraz, N. F. Silva, J. G. da Silva, L. F. de Miranda, C. F. Romeiro, E. M. Souza-Fagundes, I. C. Mendes, H. Beraldo, Investigation on the pharmacological profile of 2,6-diacetylpyridinebis(benzoylhydrazone) derivatives and their antimony(III) and bismuth(III) complexes, *European Journal of Medicinal Chemistry*, 53 (2012) 98-106.

- [53] Y. C. Ong, V. L. Blair, L. Kedzierski, K. L. Tuck, P. C. Andrews, Stability and toxicity of tris-tolylbismuth(V) dicarboxylates and their biological activity towards *Leishmania major*, *Dalton Transactions*, 44 (2015) 18215-18226.
- [54] Y. C. Ong, V. L. Blair, L. Kedzierski, P. C. Andrews, Stability and toxicity of heteroleptic organometallic Bi(V) complexes towards *Leishmania major*, *Dalton Transactions*, 43 (2014) 12904-12916.
- [55] I. Kumar, P. Bhattacharya, K. H. Whitmire, Facile one-pot synthesis of triphenylbismuth(V)bis(carboxylate) complexes, *Organometallics*, 33 (2014) 2906-2909.
- [56] V. Sharutin, O. Sharutina, Synthesis and structure of triphenylbismuth bis (pentachlorobenzoate), *Russian Journal of Inorganic Chemistry*, 59 (2014) 558-560.
- [57] V. Sharutin, I. Egorova, M. Kazakov, O. Sharutina, Synthesis and structure of triphenylbismuth bis (2-phenylaminobenzoate), *Russian Journal of Inorganic Chemistry*, 54 (2009) 1095-1098.
- [58] V. Sharutin, O. Sharutina, V. Senchurin, Synthesis and structure of tri-m-tolylbismuth dicarboxylates, *Russian Journal of Inorganic Chemistry*, 58 (2013) 1470-1474.
- [59] X. Y. Zhang, R. X. Wu, C. F. Bi, X. Zhang, Y. H. Fan, A new organobismuth(V) complex with fluorobenzoic ligands: Synthesis, crystal structure, photodegradation properties, *Inorganica Chimica Acta*, 483 (2018) 129-135.
- [60] H. Sun, *Biological chemistry of arsenic, antimony and bismuth*, John Wiley & Sons, 2010.
- [61] R. Ge, H. Sun, *Bioinorganic chemistry of bismuth and antimony: target sites of metallodrugs*, *Accounts of Chemical Research*, 40 (2007) 267-274.
- [62] A. Luqman, V. L. Blair, A. M. Bond, P. C. Andrews, Formation of bismuth(V) thiolates: protolysis and oxidation of triphenylbismuth(III) with heterocyclic thiols, *Angewandte Chemie International Edition*, 52 (2013) 7247-7251.

- [63] L. S. Cui, J. R. Meng, Y. L. Gan, Y. C. Li, Synthesis and structure of an organobismuth(V) dithiocarbamate polymer $[\text{PhBiS}_2\text{CN}(\text{CH}_3)_2\text{Cl}]^n$ and its use as a high-efficiency photocatalysis for organic dyes degradation, *Inorganic and Nano-Metal Chemistry*, 47 (2017) 1537-1541.
- [64] W. Y. Bi, X. Q. Lü, W. L. Chai, J. R. Song, W. Y. Wong, W. K. Wong, R. A. Jones, Construction and NIR luminescent property of hetero-bimetallic Zn-Nd complexes from two chiral salen-type Schiff-base ligands, *Journal of Molecular Structure*, 891 (2008) 450-455.
- [65] W. Y. Bi, X. Q. Lü, W. L. Chai, W. J. Jin, J. R. Song, W. K. Wong, Synthesis, structure and near-infrared (NIR) luminescence of three solvent-induced pseudo-polymorphic complexes from a bimetallic Zn-Nd Schiff-base molecular unit, *Inorganic Chemistry Communications*, 11 (2008) 1316-1319.
- [66] P. P. Chakrabarty, S. Saha, K. Sen, A. D. Jana, D. Dey, D. Schollmeyer, S. García-Granda, Unexplored analytics of some novel 3d-4f heterometallic Schiff base complexes, *RSC Advances*, 4 (2014) 40794-40802.
- [67] M. Bottrill, L. Kwok, N.J. Long, Lanthanides in magnetic resonance imaging, *Chemical Society Reviews*, 35 (2006) 557-571.
- [68] S. Aime, D. D. Castelli, S. G. Crich, E. Gianolio, E. Terreno, Pushing the sensitivity envelope of lanthanide-based magnetic resonance imaging (MRI) contrast agents for molecular imaging applications, *Accounts of Chemical Research*, 42 (2009) 822-831.
- [69] A. J. Tasiopoulos, T. A. O'Brien, K. A. Abboud, G. Christou, Mixed Transition-Metal-lanthanide complexes at higher oxidation states: heteronuclear $\text{Ce}^{\text{IV}}-\text{Mn}^{\text{IV}}$ clusters, *Angewandte Chemie International Edition*, 43 (2004) 345-349.
- [70] Y. Ning, M. Zhu, J. L. Zhang, Near-infrared (NIR) lanthanide molecular probes for bioimaging and biosensing, *Coordination Chemistry Reviews*, 399 (2019) 213028.

- [71] W. Feng, Y. Zhang, Z. Zhang, X. Lu, H. Liu, G. Shi, D. Zou, J. Song, D. Fan, W. K. Wong, Anion-induced self-assembly of luminescent and magnetic homoleptic cyclic tetranuclear $\text{Ln}_4(\text{Salen})_4$ and $\text{Ln}_4(\text{Salen})_2$ complexes ($\text{Ln} = \text{Nd}, \text{Yb}, \text{Er}, \text{or Gd}$), *Inorganic chemistry*, 51 (2012) 11377-11386.
- [72] C. D. M. Donegá, S. A. Junior, G. F. De Sá, Europium (III) mixed complexes with β -diketones and o-phenanthroline-N-oxide as promising light-conversion molecular devices, *Chemical Communications*, (1996) 1199-1200.
- [73] J. Yang, Q. Yue, G.-D. Li, J. J. Cao, G. H. Li, J. S. Chen, Structures, photoluminescence, up-conversion, and magnetism of 2-D and 3-D rare-earth coordination polymers with multicarboxylate linkages, *Inorganic Chemistry*, 45 (2006) 2857-2865.
- [74] L. Ding, W. Jin, Z. Chu, L. Chen, X. Lü, G. Yuan, J. Song, D. Fan, F. Bao, Bulk solvent-free melt ring-opening polymerization (ROP) of L-lactide catalyzed by Ni(II) and Ni(II)-Ln(III) complexes based on the acyclic Salen-type Schiff-base ligand, *Inorganic Chemistry Communications*, 14 (2011) 1274-1278.
- [75] W. Y. Bi, X. Q. Lü, W. L. Chai, J. R. Song, W. K. Wong, X. P. Yang, R. A. Jones, Effect of heavy-atom (Br) at the phenyl rings of Schiff-base ligands on the NIR luminescence of their bimetallic Zn-Nd complexes, *Zeitschrift für Anorganische und Allgemeine Chemie*, 634 (2008) 1795-1800.
- [76] K. Kuriki, Y. Koike, Y. Okamoto, Plastic optical fiber lasers and amplifiers containing lanthanide complexes, *Chemical Reviews*, 102 (2002) 2347-2356.
- [77] J. Kido, Y. Okamoto, Organo lanthanide metal complexes for electroluminescent materials, *Chemical Reviews*, 102 (2002) 2357-2368.
- [78] S. Faulkner, L. S. Natrajan, W. S. Perry, D. Sykes, Sensitised luminescence in lanthanide containing arrays and d-f hybrids, *Dalton Transactions*, (2009) 3890-3899.
- [79] S. Faulkner, S. J. Pope, B. P. Burton-Pye, Lanthanide complexes for luminescence imaging applications, *Applied Spectroscopy Reviews*, 40 (2005) 1-31.

- [80] W. Feng, Y. Hui, T. Wei, X. Lü, J. Song, Z. Chen, S. Zhao, W. K. Wong, R.A. Jones, Anion-induced near-infrared (NIR) luminescent Zn₂Nd and ZnNd complexes based on the pure Salen-type Schiff-base ligand, *Inorganic Chemistry Communications*, 14 (2011) 75-78.
- [81] J.P. Costes, S. Titos-Padilla, I. Oyarzabal, T. Gupta, C. Duhayon, G. Rajaraman, E. Colacio, Analysis of the Role of Peripheral Ligands Coordinated to ZnII in Enhancing the Energy Barrier in Luminescent Linear Trinuclear Zn-Dy-Zn Single-Molecule Magnets, *Chemistry—A European Journal*, 21 (2015) 15785-15796.
- [82] T.D. Pasatoiu, C. Tiseanu, A. M. Madalan, B. Jurca, C. Duhayon, J.P. Sutter, M. Andruh, Study of the luminescent and magnetic properties of a series of heterodinuclear [Zn^{II}Ln^{III}] complexes, *Inorganic Chemistry*, 50 (2011) 5879-5889.
- [83] P.G. Lacroix, Second-order optical nonlinearities in coordination chemistry: The case of bis (salicylaldiminato) metal Schiff base complexes, *European Journal of Inorganic Chemistry*, 2001 (2001) 339-348.
- [84] M. J. O'donnell, The enantioselective synthesis of α -amino acids by phase-transfer catalysis with achiral Schiff base esters, *Accounts of Chemical Research*, 37 (2004) 506-517.
- [85] K. Gupta, A. K. Sutar, Catalytic activities of Schiff base transition metal complexes, *Coordination Chemistry Reviews*, 252 (2008) 1420-1450.
- [86] E. Hadjoudis, I. M. Mavridis, Photochromism and thermochromism of Schiff bases in the solid state: structural aspects, *Chemical Society Reviews*, 33 (2004) 579-588.
- [87] L. Canali, D. C. Sherrington, Utilisation of homogeneous and supported chiral metal (salen) complexes in asymmetric catalysis, *Chemical Society Reviews*, 28 (1999) 85-93.
- [88] D. A. Atwood, M. J. Harvey, Group 13 compounds incorporating salen ligands, *Chemical Reviews*, 101 (2001) 37-52.

- [89] P. G. Cozzi, Metal-Salen Schiff base complexes in catalysis: practical aspects, *Chemical Society Reviews*, 33 (2004) 410-421.
- [90] L. Li, P. Cai, Y. Deng, L. Yang, X. He, L. Pu, D. Wu, J. Liu, H. Xiang, X. Zhou, Water-soluble porphyrin-based logic gates, *Journal of Porphyrins and Phthalocyanines*, 16 (2012) 72-76.
- [91] H. Xiang, L. Zhou, Y. Feng, J. Cheng, D. Wu, X. Zhou, Tunable fluorescent/phosphorescent platinum(II) porphyrin-fluorene copolymers for ratiometric dual emissive oxygen sensing, *Inorganic Chemistry*, 51 (2012) 5208-5212.
- [92] L.T. Yang, D. Wu, H.-F. Xiang, Synthesis, Structure and Optical Properties of a Zinc (II) Tetrakis (Phenylbutadiny) Porphyrin, *Heterocycles: an International Journal for Reviews and Communications in Heterocyclic Chemistry*, 85 (2012) 1987-1996.
- [93] M. Andruh, Compartmental Schiff-base ligands-a rich library of tectons in designing magnetic and luminescent materials, *Chemical Communications*, 47 (2011) 3025-3042.
- [94] A. W. Kleij, Zinc-centred salen complexes: Versatile and accessible supramolecular building motifs, *Dalton Transactions*, (2009) 4635-4639.
- [95] G. Consiglio, S. Failla, I.P. Oliveri, R. Purrello, Controlling the molecular aggregation. An amphiphilic Schiff-base zinc(II) complex as supramolecular fluorescent probe, *Dalton Transactions*, (2009) 10426-10428.
- [96] S. J. Wezenberg, E. C. Escudero-Adán, J. Benet-Buchholz, A. W. Kleij, Anion-templated formation of supramolecular multinuclear assemblies, *Chemistry—A European Journal*, 15 (2009) 5695-5700.
- [97] I. P. Oliveri, S. Failla, G. Malandrino, New molecular architectures by aggregation of tailored zinc (II) Schiff-base complexes, *New Journal of Chemistry*, 35 (2011) 2826-2831.
- [98] M. Hosseini, Z. Vaezi, M. R. Ganjali, F. Faridbod, S. D. Abkenar, K. Alizadeh, M. Salavati-Niasari, Fluorescence “turn-on” chemosensor for the selective detection of zinc

ion based on Schiff-base derivative, *Spectrochimica Acta Part A: Molecular and Biomolecular Spectroscopy*, 75 (2010) 978-982.

[99] Y. Xu, J. Meng, L. Meng, Y. Dong, Y. Cheng, C. Zhu, A highly selective fluorescence-based polymer sensor incorporating an (R, R)-salen moiety for Zn²⁺ detection, *Chemistry–A European Journal*, 16 (2010) 12898-12903.

[100] S. Wang, G. Men, L. Zhao, Q. Hou, S. Jiang, Binaphthyl-derived salicylidene Schiff base for dual-channel sensing of Cu, Zn cations and integrated molecular logic gates, *Sensors and Actuators B: Chemical*, 145 (2010) 826-831.

[101] E. Lamour, S. Routier, J. L. Bernier, J. P. Catteau, C. Bailly, H. Vezin, Oxidation of Cu^{II} to Cu^{III}, Free Radical Production, and DNA Cleavage by Hydroxy-salen–Copper Complexes. Isomeric Effects Studied by ESR and Electrochemistry, *Journal of the American Chemical Society*, 121 (1999) 1862-1869.

[102] P. Wu, D. L. Ma, C. H. Leung, S. C. Yan, N. Zhu, R. Abagyan, C. M. Che, Stabilization of G-Quadruplex DNA with Platinum(II) Schiff Base Complexes: Luminescent Probe and Down-Regulation of c-myc Oncogene Expression, *Chemistry–A European Journal*, 15 (2009) 13008-13021.

[103] Y. Hai, J. J. Chen, P. Zhao, H. Lv, Y. Yu, P. Xu, J. L. Zhang, Luminescent zinc salen complexes as single and two-photon fluorescence subcellular imaging probes, *Chemical Communications*, 47 (2011) 2435-2437.

[104] J. Jing, J. J. Chen, Y. Hai, J. Zhan, P. Xu, J. L. Zhang, Rational design of ZnSalen as a single and two photon activatable fluorophore in living cells, *Chemical Science*, 3 (2012) 3315-3320.

[105] K. Y. Hwang, M. H. Lee, H. Jang, Y. Sung, J. S. Lee, S. H. Kim, Y. Do, Aluminium–salen luminophores as new hole-blocking materials for phosphorescent OLEDs, *Dalton Transactions*, (2008) 1818-1820.

- [106] J. O. Huh, M. H. Lee, H. Jang, K. Y. Hwang, J. S. Lee, S. H. Kim, Y. Do, A Novel Solution-Processible Heterodinuclear Al^(III)/Ir^(III) Complex for Host–Dopant Assembly OLEDs, *Inorganic Chemistry*, 47 (2008) 6566-6568.
- [107] K. Y. Hwang, H. Kim, Y. S. Lee, M. H. Lee, Y. Do, Synthesis and Properties of Salen–Aluminum Complexes as a Novel Class of Color-Tunable Luminophores, *Chemistry–A European Journal*, 15 (2009) 6478-6487.
- [108] Q. Hou, L. Zhao, H. Zhang, Y. Wang, S. Jiang, Synthesis and luminescent properties of two Schiff-base boron complexes, *Journal of Luminescence*, 126 (2007) 447-451.
- [109] Y. Zhou, J. W. Kim, R. Nandhakumar, M. J. Kim, E. Cho, Y.S. Kim, Y. H. Jang, C. Lee, S. Han, K. M. Kim, Novel binaphthyl-containing bi-nuclear boron complex with low concentration quenching effect for efficient organic light-emitting diodes, *Chemical Communications*, 46 (2010) 6512-6514.
- [110] Y. Zhou, J. W. Kim, M. J. Kim, W. J. Son, S. J. Han, H. N. Kim, S. Han, Y. Kim, C. Lee, S. J. Kim, Novel bi-nuclear boron complex with pyrene ligand: red-light emitting as well as electron transporting material in organic light-emitting diodes, *Organic Letters*, 12 (2010) 1272-1275.
- [111] C. M. Che, S. C. Chan, H. F. Xiang, M. C. Chan, Y. Liu, Y. Wang, Tetradentate Schiff base platinum(II) complexes as new class of phosphorescent materials for high-efficiency and white-light electroluminescent devices, *Chemical Communications*, (2004) 1484-1485.
- [112] H. F. Xiang, S. C. Chan, C. M. Che, P. Lai, P. C. Chui, High-efficiency electrophosphorescent organic light-emitting devices based on Schiff base platinum(II) complexes, in: *Organic Light-Emitting Materials and Devices VIII*, International Society for Optics and Photonics, 2004, pp. 296-303.

- [113] H. F. Xiang, S. C. Chan, K. K. Y. Wu, C. M. Che, P. Lai, High-efficiency red electrophosphorescence based on neutral bis (pyrrole)-diimine platinum (II) complex, *Chemical Communications*, (2005) 1408-1410.
- [114] P. Wang, Z. Hong, Z. Xie, S. Tong, O. Wong, C.-S. Lee, N. Wong, L. Hung, S. Lee, A bis-salicylaldiminato Schiff base and its zinc complex as new highly fluorescent red dopants for high performance organic electroluminescence devices, *Chemical communications*, (2003) 1664-1665.
- [115] Y. Hamada, T. Sano, M. Fujita, T. Fujii, Y. Nishio, K. Shibata, Blue electroluminescence in thin films of azomethin-zinc complexes, *Japanese Journal of Applied Physics*, 32 (1993) L511.
- [116] A. Vashchenko, L. Lepnev, A. Vitukhnovskii, O. Kotova, S. Eliseeva, N. Kuz'mina, Photo-and electroluminescent properties of zinc (II) complexes with tetradentate Schiff bases, derivatives of salicylic aldehyde, *Optics and Spectroscopy*, 108 (2010) 463-465.
- [117] K. H. Chang, C. C. Huang, Y. H. Liu, Y. H. Hu, P. T. Chou, Y. C. Lin, Synthesis of photo-luminescent Zn(II) Schiff base complexes and its derivative containing Pd(II) moiety, *Dalton Transactions*, (2004) 1731-1738.
- [118] Y. Dong, J. Li, X. Jiang, F. Song, Y. Cheng, C. Zhu, Na⁺ triggered fluorescence sensors for Mg²⁺ detection based on a coumarin salen moiety, *Organic Letters*, 13 (2011) 2252-2255.
- [119] L. Zhou, P. Cai, Y. Feng, J. Cheng, H. Xiang, J. Liu, D. Wu, X. Zhou, Synthesis and photophysical properties of water-soluble sulfonato-Salen-type Schiff bases and their applications of fluorescence sensors for Cu²⁺ in water and living cells, *Analytica Chimica Acta*, 735 (2012) 96-106.
- [120] C. Gou, S. H. Qin, H. Q. Wu, Y. Wang, J. Luo, X. Y. Liu, A highly selective chemosensor for Cu²⁺ and Al³⁺ in two different ways based on Salicylaldehyde Schiff, *Inorganic Chemistry Communications*, 14 (2011) 1622-1625.

- [121] M. Hosseini, M. R. Ganjali, S. D. Abkenar, B. Veismohammadi, S. Riahl, P. Norouzi, M. Salavati-Niasari, Highly selective ratiometric fluorescent sensor for La(III) ion based on a new Schiff's base, *Analytical Letters*, 42 (2009) 1029-1040.
- [122] L. Zhou, Y. Feng, J. Cheng, N. Sun, X. Zhou, H. Xiang, Simple, selective, and sensitive colorimetric and ratiometric fluorescence/phosphorescence probes for platinum (II) based on salen-type Schiff bases, *RSC Advances*, 2 (2012) 10529-10536.
- [123] X. Y. Li, Q. P. Kang, L. Z. Liu, J. C. Ma, W. K. Dong, Trinuclear Co(II) and mononuclear Ni(II) Salamo-type bisoxime coordination compounds, *Crystals*, 8 (2018) 43.
- [124] R. Mazzoni, F. Roncaglia, L. Rigamonti, When the Metal Makes the Difference: Template Syntheses of Tridentate and Tetradentate Salen-Type Schiff Base Ligands and Related Complexes, *Crystals*, 11 (2021) 483.
- [125] Y. D. Peng, X. Y. Li, Q. P. Kang, G. X. An, Y. Zhang, W. K. Dong, Synthesis and fluorescence properties of asymmetrical Salamo-type tetranuclear zinc(II) complex, *Crystals*, 8 (2018) 107.
- [126] C. Marvel, N. Tarköy, Heat Stability Studies on Chelates from Schiff Bases of Salicylaldehyde Derivatives I, *Journal of the American Chemical Society*, 79 (1957) 6000-6002.
- [127] C. Marvel, N. Tarköy, Heat stability studies on chelates from schiff bases of salicylaldehyde derivatives. II, *Journal of the American Chemical Society*, 80 (1958) 832-835.
- [128] G. Manecke, W. Wille, Preparation and properties of chelate-forming monomeric and polymeric Schiff-base derived from salicylaldehyde and 2.5-Dihydroxyterephthalaldehyde, *Makromolekulare Chemie*, 133 (1970) 61.
- [129] G. Manecke, W. Wille, G. Kossmehl, Preparation and properties of monomeric and polymeric Schiff-Bases derived from salicylaldehyde and 2.5-Dihydroxyterephthalaldehyde. 2. Electrical Conductivity, *Makromolekulare Chemie*, 160 (1972) 111-116.

- [130] S.M. Elbert, M. Mastalerz, Metal Salen-and Salphen-Containing Organic Polymers: Synthesis and Applications, *Organic Materials*, 2 (2020) 182-203.
- [131] W. K. Lo, W. K. Wong, J. Guo, W. Y. Wong, K. F. Li, K. W. Cheah, Synthesis, structures and luminescent properties of new heterobimetallic Zn-4f Schiff base complexes, *Inorganica Chimica Acta*, 357 (2004) 4510-4521.
- [132] W. K. Lo, W. K. Wong, W. Y. Wong, J. Guo, K. T. Yeung, Y. K. Cheng, X. Yang, R. A. Jones, Heterobimetallic Zn(II)-Ln(III) phenylene-bridged Schiff base complexes, computational studies, and evidence for singlet energy transfer as the main pathway in the sensitization of near-infrared Nd³⁺ luminescence, *Inorganic Chemistry*, 45 (2006) 9315-9325.
- [133] W. K. Wong, X. Yang, R. A. Jones, J. H. Rivers, V. Lynch, W. K. Lo, D. Xiao, M. M. Oye, A. L. Holmes, Multinuclear luminescent Schiff-base Zn-Nd sandwich complexes, *Inorganic Chemistry*, 45 (2006) 4340-4345.
- [134] W. K. Wong, H. Liang, W. Y. Wong, Z. Cai, K.-F. Li, K.-W. Cheah, Synthesis and near-infrared luminescence of 3d-4f bi-metallic Schiff base complexes, *New Journal of Chemistry*, 26 (2002) 275-278.
- [135] W. Y. Bi, X. Q. Lü, W. L. Chai, T. Wei, J. R. Song, S. S. Zhao, W. K. Wong, Unsymmetrical exo-dentate ligand for further self-assembly with the Zn-Nd Salen-type Schiff-base ligands, *Inorganic Chemistry Communications*, 12 (2009) 267-271.
- [136] W. X. Feng, Y. N. Hui, G. X. Shi, D. Zou, X. Q. Lü, J. R. Song, D. D. Fan, W. K. Wong, R. A. Jones, Synthesis, structure and near-infrared (NIR) luminescence of series of Zn₂Ln (Ln= Nd, Yb or Er) complexes based on the Salen-type Schiff-base ligand with the flexible linker, *Inorganic Chemistry Communications*, 20 (2012) 33-36.
- [137] G. X. Shi, W. X. Feng, D. Zou, X. Q. Lü, Z. Zhang, Y. Zhang, D. D. Fan, S. S. Zhao, W. K. Wong, R. A. Jones, Hetero-binuclear near-infrared (NIR) luminescent ZnLn (Ln=

Nd, Yb or Er) complexes self-assembled from the benzimidazole-based ligand, *Inorganic Chemistry Communications*, 22 (2012) 126-130.

[138] Y. Zhang, W. Feng, H. Liu, Z. Zhang, X. Lü, J. Song, D. Fan, W. K. Wong, R. A. Jones, Photo-luminescent hetero-trinuclear Zn_2Ln ($Ln = Nd, Yb, Er$ or Gd) complexes based on the binuclear Zn_2L precursor, *Inorganic Chemistry Communications*, 24 (2012) 148-152.

[139] Z. Zhang, W. Feng, P. Su, L. Liu, X. Lü, J. Song, D. Fan, W. K. Wong, R. A. Jones, C. Su, Near-infrared (NIR) luminescent $Zn(II)$ - $Ln(III)$ -containing ($Ln = Nd, Yb$ or Er) Wolf Type II metallopolymer hybrid materials, *Synthetic Metals*, 199 (2015) 128-138.

[140] G. Wilkinson, F. G. A. Stone, E. W. Abel, *Comprehensive organometallic chemistry*, Pergamon Press, 1982.

[141] S. J. Parikh, J. Chorover, FT-IR spectroscopic study of biogenic Mn-oxide formation by *Pseudomonas putida* GB-1, *Journal of Geomicrobiology*, 22 (2005) 207-218.

[142] R. M. Silverstein, *Infrared spectrometry, Spectrometric identification of organic compounds*, (1974).

[143] S. Minzanova, V. Mironov, A. Vyshtakalyuk, O. Tsepaeva, L. Mironova, I. Ryzhkina, L. Murtazina, A. Gubaidullin, Complexes of pectin polysaccharide with acetylsalicylic acid, in: *Doklady Chemistry*, Springer, 2013, pp. 230-233.

[144] E. Helen Pricilla Bai, S. Vairam, Hydrazine Complexes of Lanthanides with 3-Acetoxy and 4-Acetoxybenzoic Acids: Spectroscopic, Thermal, and XRD Studies, *Journal of Chemistry*, 2013 (2013).

[145] S. Chandrasekhar, H. V. Kumar, The reaction of aspirin with base, *Tetrahedron Letters*, 52 (2011) 3561-3564.

[146] P. Raj, A. Saxena, K. Singhal, A. Ranjan, Synthesis and some reactions of tris (pentafluorophenyl) antimony compounds, *Polyhedron*, 4 (1985) 251-258.

- [147] K. Singhal, N.K. Verma, Preparation and Characterization of Some New Tris (p-fluorophenyl) Bismuth(III) and Bismuth(V) Halides and Pseudohalides.
- [148] G. Deacon, R. Phillips, Relationships between the carbon-oxygen stretching frequencies of carboxylato complexes and the type of carboxylate coordination, *Coordination Chemistry Reviews*, 33 (1980) 227-250.
- [149] S. Abdel-Latif, H. Hassib, Y. Issa, Studies on some salicylaldehyde Schiff base derivatives and their complexes with Cr(III), Mn(II), Fe(III), Ni(II) and Cu(II), *Spectrochimica Acta Part A: Molecular and Biomolecular Spectroscopy*, 67 (2007) 950-957.
- [150] A.P. Mishra, R. Mishra, R. Jain, S. Gupta, Synthesis of new VO(II), Co(II), Ni(II) and Cu(II) complexes with Isatin-3-chloro-4-floroaniline and 2-pyridinecarboxylidene-4-aminoantipyrine and their antimicrobial studies, *Mycobiology*, 40 (2012) 20-26.
- [151] T. Fatima, Imtiaz-ud-Din., A. Akbar, M.S. Anwar, M.N. Tahir, Six new dinuclear Schiff base complexes of Cu(II)/Ln(III) system: Synthesis, characterization and magnetic studies, *Journal of Molecular Structure*, 1184 (2019) 462-467.
- [152] H. Barucki, S. J. Coles, J. F. Costello, T. Gelbrich, M. B. Hursthouse, Characterising secondary bonding interactions within triaryl organoantimony(V) and organobismuth(V) complexes, *Journal of the Chemical Society, Dalton Transactions*, (2000) 2319-2325.
- [153] G. Goyat, A. Malik, K. Vikas, S. Garg, Synthesis, Characterization and Biological Activities of Tellurium(IV) Complexes of Bidentate Schiff Base Derived from 5-Chlorosalicylaldehyde and 3-Aminopyridine, *International Journal of Scientific Research in Science, Engineering and Technology*, 4 (2018) 763-769.
- [154] M. Pervaiz, M. Yousaf, M. Sagir, M. Mushtaq, M. Naz, S. Ullah, R. Mushtaq, Synthesis and characterization of bimetallic post transition complexes for antimicrobial activity, *Synthesis and Reactivity in Inorganic, Metal-Organic, and Nano-Metal Chemistry*, 45 (2015) 546-552.

- [155] A. L. Albright, J. M. White, Determination of absolute configuration using single crystal X-ray diffraction, in: *Metabolomics tools for natural product discovery*, Springer, 2013, pp. 149-162.
- [156] K. R. Seddon, Pseudo polymorph: a polemic, *Crystal Growth & Design*, 4 (2004) 1087-1087.
- [157] G. G. Briand, N. Burford, Bismuth compounds and preparations with biological or medicinal relevance, *Chemical Reviews*, 99 (1999) 2601-2658.
- [158] H. Sun, H. Li, P. J. Sadler, The biological and medicinal chemistry of bismuth, *Chemische Berichte*, 130 (1997) 669-681.
- [159] K. Goh, N. Parasakthi, S. Peh, N. Wong, Y. Lo, S. Puthuchery, Helicobacter pylori infection and non-ulcer dyspepsia: the effect of treatment with colloidal bismuth subcitrate, *Scandinavian Journal of Gastroenterology*, 26 (1991) 1123-1131.
- [160] P. Malfertheiner, F. Bazzoli, J. C. Delchier, K. Celiński, M. Giguère, M. Rivière, F. Mégraud, P. S. Group, Helicobacter pylori eradication with a capsule containing bismuth subcitrate potassium, metronidazole, and tetracycline given with omeprazole versus clarithromycin-based triple therapy: a randomised, open-label, non-inferiority, phase 3 trial, *The Lancet*, 377 (2011) 905-913.
- [161] G.E.G. Felga, F.M. Silva, R.C. Barbuti, T. Navarro-Rodriguez, S. Zaterka, J.N. Eisig, Quadruple therapy with furazolidone for retreatment in patients with peptic ulcer disease, *World journal of gastroenterology: WJG*, 14 (2008) 6224.
- [162] P.C. Andrews, G.B. Deacon, C.M. Forsyth, P.C. Junk, I. Kumar, M. Maguire, Towards a structural understanding of the anti-ulcer and anti-gastritis drug bismuth subsalicylate, *Angewandte Chemie*, 118 (2006) 5766-5770.
- [163] J. Gilster, K. Bacon, K. Marlink, B. Sheppard, C. Deveney, M. Rutten, Bismuth subsalicylate increases intracellular Ca^{2+} , MAP-kinase activity, and cell proliferation in

normal human gastric mucous epithelial cells, *Digestive Diseases and Sciences*, 49 (2004) 370-378.

[164] P. T. Reynolds, K. C. Abalos, J. Hopp, M. E. Williams, Bismuth toxicity: a rare cause of neurologic dysfunction, (2012).

[165] P. C. Andrews, M. Busse, G. B. Deacon, R. L. Ferrero, P. C. Junk, J. G. MacLellan, A. Vom, Remarkable in vitro bactericidal activity of bismuth(III) sulfonates against *Helicobacter pylori*, *Dalton Transactions*, 41 (2012) 11798-11806.

[166] P. C. Andrews, M. Busse, G. B. Deacon, R. L. Ferrero, P. C. Junk, K. K. Huynh, I. Kumar, J. G. MacLellan, Structural and solution studies of phenylbismuth(III) sulfonate complexes and their activity against *Helicobacter pylori*, *Dalton Transactions*, 39 (2010) 9633-9641.

[167] P. C. Andrews, G. B. Deacon, R. L. Ferrero, P. C. Junk, A. Karrar, I. Kumar, J. G. MacLellan, Bismuth(III) 5-sulfosalicylate complexes: structure, solubility and activity against *Helicobacter pylori*, *Dalton Transactions*, (2009) 6377-6384.

[168] P. C. Andrews, V. L. Blair, R. L. Ferrero, P. C. Junk, L. Kedzierski, R. M. Peiris, Bismuth(III) β -thioxoketonates as antibiotics against *Helicobacter pylori* and as anti-leishmanial agents, *Dalton Transactions*, 43 (2014) 1279-1291.

[169] S. Andleeb, Imtiaz-ud-Din., M. K. Rauf, S. S. Azam, A. Badshah, H. Sadaf, A. Raheel, M. N. Tahir, S. Raza, *RSC Advances*, 6 (2016) 79651-79661.

[170] R. Chen, G. Cheng, M. H. So, J. Wu, Z. Lu, C. M. Che, H. Sun, Bismuth subcarbonate nanoparticles fabricated by water-in-oil microemulsion-assisted hydrothermal process exhibit anti-*Helicobacter pylori* properties, *Materials Research Bulletin*, 45 (2010) 654-658.

[171] R. Chen, M. H. So, J. Yang, F. Deng, C. M. Che, H. Sun, Fabrication of bismuth subcarbonate nanotube arrays from bismuth citrate, *Chemical Communications*, (2006) 2265-2267.

- [172] A. Mendis, B. Marshall, H. Sun, *Biological Chemistry of Arsenic, Antimony and Bismuth*, (2011).
- [173] E. Torres-Guerrero, M. Quintanilla-Cedillo, J. Ruiz-Esmenjaud, R. Arenas, *Leishmaniasis: a review*. *F1000Res* 6: 750, in, 2017.
- [174] Y. Chai, S. Yan, I.L. Wong, L.M. Chow, H. Sun, Complexation of antimony Sb(V) with guanosine 5'-monophosphate and guanosine 5'-diphospho-D-mannose: Formation of both mono-and bis-adducts, *Journal of Inorganic Biochemistry*, 99 (2005) 2257-2263.
- [175] B. A. Fowler, D. W. Sullivan Jr, M. J. Sexton, Bismuth, in: *Handbook on the Toxicology of Metals*, Elsevier, 2015, pp. 655-666.
- [176] C. A. Tylenda, D. W. Sullivan Jr, B. A. Fowler, Antimony, in: *Handbook on the Toxicology of Metals*, Elsevier, 2015, pp. 565-579.
- [177] A. Pathak, V. L. Blair, R. L. Ferrero, P. C. Junk, R. F. Tabor, P. C. Andrews, Synthesis and structural characterisation of bismuth(III) hydroxamates and their activity against *Helicobacter pylori*, *Dalton Transactions*, 44 (2015) 16903-16913.
- [178] Y. C. Ong, L. Kedzierski, P. C. Andrews, Do bismuth complexes hold promise as antileishmanial drugs?, *Future Medicinal Chemistry*, 10 (2018) 1721-1733.
- [179] P. C. Andrews, R. Frank, P. C. Junk, L. Kedzierski, I. Kumar, J. G. MacLellan, Anti-Leishmanial activity of homo-and heteroleptic bismuth(III) carboxylates, *Journal of Inorganic Biochemistry*, 105 (2011) 454-461.
- [180] A. Loh, Y. C. Ong, V. L. Blair, L. Kedzierski, P. C. Andrews, Bismuth(III) α -hydroxy carboxylates: highly selective toxicity of glycolates towards *Leishmania major*, *JBIC Journal of Biological Inorganic Chemistry*, 20 (2015) 1193-1203.
- [181] E. H. Lizarazo-Jaimes, R. L. Monte-Neto, P. G. Reis, N. G. Fernandes, N. L. Speziali, M. N. Melo, F. Frézard, C. Demicheli, Improved antileishmanial activity of Dppz through

complexation with antimony(III) and bismuth(III): Investigation of the role of the metal, *Molecules*, 17 (2012) 12622-12635.

[182] M. L. Gomes, G. DeFreitas-Silva, P. G. dos Reis, M. N. Melo, F. Frézard, C. Demicheli, Y. M. Idemori, Synthesis and characterization of bismuth(III) and antimony(V) porphyrins: High antileishmanial activity against antimony-resistant parasite, *JBIC Journal of Biological Inorganic Chemistry*, 20 (2015) 771-779.

[183] A. Luqman, V. L. Blair, R. Brammananth, P. K. Crellin, R. L. Coppel, L. Kedzierski, P. C. Andrews, Homoleptic and Heteroleptic Bismuth(III) Thiazole–Thiolates and the Influence of Ring Substitution on Their Antibacterial and Antileishmanial Activity, *European Journal of Inorganic Chemistry*, 2015 (2015) 725-733.

[184] P. C. Andrews, P. C. Junk, L. Kedzierski, R. M. Peiris, Anti-leishmanial activity of novel homo- and heteroleptic bismuth(III) thiocarboxylates, *Australian Journal of Chemistry*, 66 (2013) 1297-1305.

[185] A. Chaudhary, A. Singh, Synthesis, characterization, and evaluation of antimicrobial and antifertility efficacy of heterobimetallic complexes of copper(II), *Journal of Chemistry*, 2017 (2017).

[186] A. A. Osowole, O. B. Agbaje, B. O. Ojo, Synthesis, characterization and antibacterial properties of some heteroleptic metal(II) complexes of paracetamol and vanillin, *Asian Journal of Pharmaceutical and Clinical Research*, 7 (2014) 145-149.

[187] K. Prajapati, P. Prajapati, M. Brahmabhatt, J. Vora, a Review: Lanthanide Complexes and Their Biological Importance, *Res J Life Sci Bioinformatics, Journal of Pharmaceutical Chemistry & Chemical Science*, 4 (2018) 803-813.

[188] T. A. Hanna, The role of bismuth in the SOHIO process, *Coordination Chemistry Reviews*, 248 (2004) 429-440.

[189] D. Mendoza-Espinosa, T. A. Hanna, Heterobimetallic Bismuth(III)/Molybdenum(VI) and Antimony(III)/Molybdenum(VI) Calix[5]arene

Complexes. Progress toward Modeling the SOHIO Catalyst, *Inorganic Chemistry*, 48 (2009) 7452-7456.

[190] S. Roggan, C. Limberg, Molecular molybdenum/bismuth compounds, *Inorganica Chimica Acta*, 359 (2006) 4698-4722.

[191] Z. Jin, Z. Zhang, J. Xiu, H. Song, T. Gatti, Z. He, A critical review on bismuth and antimony halide based perovskites and their derivatives for photovoltaic applications: recent advances and challenges, *Journal of Materials Chemistry A*, 8 (2020) 16166-16188.

[192] R. Retoux, F. Studer, C. Michel, B. Raveau, A. Fontaine, E. Dartyge, Valence state for bismuth in the superconducting bismuth cuprates, *Physical Review B*, 41 (1990) 193.

[193] K. Ueda, T. Bohno, K. Takita, K. Mukae, T. Uede, I. Itoh, M. Mimura, N. Uno, T. Tanaka, Design and testing of a pair of current leads using bismuth compound superconductor, *IEEE Transactions on Applied Superconductivity*, 3 (1993) 400-403.

[194] A. W. Sleight, Superconductive barium-lead-bismuth oxides, in, Google Patents, 1976.

[195] J. L. Rehspringer, J. Bursik, D. Niznansky, A. Klarikova, Characterisation of bismuth-doped yttrium iron garnet layers prepared by sol-gel process, *Journal of Magnetism and Magnetic Materials*, 211 (2000) 291-295.

[196] A. B. J. Kharrat, S. Moussa, N. Moutiaa, K. Khirouni, W. Boujelben, Structural, electrical and dielectric properties of Bi-doped $\text{Pr}_{0.8-x}\text{Bi}_x\text{Sr}_{0.2}\text{MnO}_3$ manganite oxides prepared by sol-gel process, *Journal of Alloys and Compounds*, 724 (2017) 389-399.

[197] X. Du, Y. Xu, H. Ma, J. Wang, X. Li, Synthesis and characterization of bismuth titanate by an aqueous sol-gel method, *Journal of the American Ceramic Society*, 90 (2007) 1382-1385.

- [198] S. Stepanov, I. Sokolov, Adaptive interferometers using photorefractive crystals, in: 1989 Second International Conference on Holographic Systems, Components and Applications, IET, 1989, pp. 95-100.
- [199] W. Horn, I. Földvari, C. Denz, Holographic data storage in photorefractive bismuth tellurite, *Journal of Physics D: Applied Physics*, 41 (2008) 224006.
- [200] A. Pisarevsky, Volatile bismuth complexes-precursors for high-Tc superconducting films manufacturing via chemical vapor deposition, in: AIP Conference Proceedings, American Institute of Physics, 1992, pp. 231-240.
- [201] F. Hintermaier, B. Hendrix, J. Roeder, P. Van Buskirk, T. H. Baum, Method for the selective deposition of bismuth based ferroelectric thin films by chemical vapor deposition, in, Google Patents, 2000.
- [202] M. Ihara, T. Kimura, H. Yamawaki, K. Ikeda, High-Tc BiSrCaCuO superconductor grown by CVD technique, *IEEE Transactions on Magnetics*, 25 (1989) 2470-2473.
- [203] M. Mehring, S. Paalasmaa, M. Schürmann, Structural Relationships in High-Nuclearity Heterobimetallic Bismuth-Oxo Clusters, *European Journal of Inorganic Chemistry*, 2005 (2005) 4891-4901.
- [204] M. Mehring, D. Mansfeld, S. Paalasmaa, M. Schürmann, Polynuclear Bismuth-Oxo Clusters: Insight into the Formation Process of a Metal Oxide, *Chemistry-A European Journal*, 12 (2006) 1767-1781.
- [205] J. Pell, W. Davis, H. Zur Loye, Bismuth Alkoxides. The First Structurally-Characterized Bismuth-Transition Metal Heterobimetallic Alkoxide: $[\text{BiCl}_3\text{OV}(\text{OC}_2\text{H}_4\text{OCH}_3)_3]_2$, *Inorganic Chemistry*, 35 (1996) 5754-5755.
- [206] H.J. Breunig, Bismuth Compounds, *Kirk-Othmer Encyclopedia of Chemical Technology*, (2000).

- [207] L. Balazs, H.J. Breunig, E. Lork, A. Soran, C. Silvestru, Isomers of a Dibismuthane, $R_2Bi-BiR_2$ [$R= 2,6-(Me_2NCH_2)-2-C_6H_3$], and Unusual Reactions with Oxygen: Formation of $[R_2Bi]_2 (O_2)$ and $R' R''Bi$ [$R' = 2-(Me_2NCH_2)-6-\{Me_2N(O)CH_2\} C_6H_3$; $R'' = 2-(Me_2NCH_2)-6-\{O(O)C\}C_6H_3$], *Inorganic Chemistry*, 45 (2006) 2341-2346.
- [208] A. Kuczkowski, S. Schulz, M. Nieger, Reactions of Et_4Bi_2 with tBu_3M ($M= Al, Ga$)-Synthesis of Complexes with a Bidentate Dibismuthane Ligand, *Angewandte Chemie International Edition*, 40 (2001) 4222-4225.
- [209] N. Tokitoh, Y. Arai, R. Okazaki, S. Nagase, Synthesis and characterization of a stable dibismuthene: Evidence for a Bi-Bi double bond, *Science*, 277 (1997) 78-80.
- [210] N.J. Hardman, B. Twamley, P. P. Power, $(2,6-Mes_2H_3C_6)_2BiH$, a Stable, Molecular Hydride of a Main Group Element of the Sixth Period, and Its Conversion to the Dibismuthene $(2,6-Mes_2H_3C_6)Bi-Bi(2,6-Mes_2C_6H_3)$, *Angewandte Chemie International Edition*, 39 (2000) 2771-2773.
- [211] T. Arnauld, D. H. Barton, E. Doris, The chemistry of pentavalent organobismuth reagents. New preparative methods for aryl bismuth(V) carboxylates and sulfonates, *Tetrahedron Letters*, 38 (1997) 365-366.
- [212] C. Train, T. Nuida, R. Gheorghe, M. Gruselle, S. I. Ohkoshi, Large magnetization-induced second harmonic generation in an enantiopure chiral magnet, *Journal of the American Chemical Society*, 131 (2009) 16838-16843.
- [213] C. Train, M. Gruselle, M. Verdaguer, The fruitful introduction of chirality and control of absolute configurations in molecular magnets, *Chemical Society Reviews*, 40 (2011) 3297-3312.
- [214] E. Coronado, P. Day, Magnetic molecular conductors, *Chemical reviews*, 104 (2004) 5419-5448.

- [215] S. I. Ohkoshi, H. Tokoro, T. Matsuda, H. Takahashi, H. Irie, K. Hashimoto, Coexistence of ferroelectricity and ferromagnetism in a rubidium manganese hexacyanoferrate, *Angewandte Chemie*, 119 (2007) 3302-3305.
- [216] E. Chelebaeva, J. Larionova, Y. Guari, R.A. Sa Ferreira, L.D. Carlos, F.A. Almeida Paz, A. Trifonov, C. Guérin, A luminescent and magnetic cyano-bridged Tb³⁺- Mo⁵⁺ coordination polymer: toward multifunctional materials, *Inorganic chemistry*, 47 (2008) 775-777.
- [217] F. Pointillart, O. Cador, B. Le Guennic, L. Ouahab, Uncommon lanthanide ions in purely 4f Single Molecule Magnets, *Coordination Chemistry Reviews*, 346 (2017) 150-175.
- [218] L. Ungur, L.F. Chibotaru, Strategies toward high-temperature lanthanide-based single-molecule magnets, *Inorganic Chemistry*, 55 (2016) 10043-10056.
- [219] Y. Bi, X. T. Wang, W. Liao, X. Wang, R. Deng, H. Zhang, S. Gao, Thiocalix [4] arene-Supported planar Ln₄ (Ln= Tb^{III}, Dy^{III}) clusters: toward luminescent and magnetic bifunctional materials, *Inorganic Chemistry*, 48 (2009) 11743-11747.
- [220] C. S. Liu, M. Du, E. C. Sañudo, J. Echeverria, M. Hu, Q. Zhang, L. M. Zhou, S. M. Fang, A luminescent linear trinuclear Dy(III) complex exhibiting slow magnetic relaxation of single ion origin, *Dalton Transactions*, 40 (2011) 9366-9369.
- [221] D. K. Cao, Y. W. Gu, J. Q. Feng, Z. S. Cai, M. D. Ward, Mononuclear lanthanide complexes incorporating an anthracene group: structural modification, slow magnetic relaxation and multicomponent fluorescence emissions in Dy compounds, *Dalton Transactions*, 42 (2013) 11436-11444.
- [222] M. A. Palacios, S. T. Padilla, J. Ruiz, J. M. Herrera, S. J. Pope, E. K. Brechin, E. Colacio, Bifunctional Zn^{II}Ln^{III} dinuclear complexes combining field induced SMM behavior and luminescence: Enhanced NIR lanthanide emission by 9-anthracene carboxylate bridging ligands, *Inorganic Chemistry*, 53 (2014) 1465-1474.

- [223] J.P. Costes, S. T. Padilla, I. Oyarzabal, T. Gupta, C. Duhayon, G. Rajaraman, E. Colacio, Effect of ligand substitution around the DyIII on the SMM properties of dual-luminescent Zn-Dy and Zn-Dy-Zn complexes with large anisotropy energy barriers: a combined theoretical and experimental magnetostructural study, *Inorganic Chemistry*, 55 (2016) 4428-4440.
- [224] P. H. Guo, J. L. Liu, J. H. Jia, J. Wang, F. S. Guo, Y. C. Chen, W. Q. Lin, J. D. Leng, D. H. Bao, X. D. Zhang, Multifunctional Dy(III) Cluster Exhibiting White-Emitting, Ferroelectric and Single-Molecule Magnet Behavior, *Chemistry–A European Journal*, 19 (2013) 8769-8773.
- [225] S. Shintoyo, K. Murakami, T. Fujinami, N. Matsumoto, N. Mochida, T. Ishida, Y. Sunatsuki, M. Watanabe, M. Tsuchimoto, J. Mrozinski, Crystal field splitting of the ground state of terbium(III) and dysprosium(III) complexes with a triimidazolyl tripod ligand and an acetate determined by magnetic analysis and luminescence, *Inorganic Chemistry*, 53 (2014) 10359-10369.
- [226] C. A. Barta, S. R. Bayly, P. W. Read, B. O. Patrick, R. C. Thompson, C. Orvig, Molecular architectures for trimetallic d/f/d complexes: Structural and magnetic properties of a LnNi₂ core, *Inorganic Chemistry*, 47 (2008) 2280-2293.
- [227] J. Ruiz, G. Lorusso, M. Evangelisti, E. K. Brechin, S. J. Pope, E. Colacio, Closely-related Zn^{II}-Ln^{III} complexes (Ln^{III}= Gd, Yb) with either magnetic refrigerant or luminescent single-molecule magnet properties, *Inorganic Chemistry*, 53 (2014) 3586-3594.
- [228] C. E. Burrow, T. J. Burchell, P. H. Lin, F. Habib, W. Wernsdorfer, R. Clérac, M. Murugesu, Salen-based [Zn₂Ln₃] complexes with fluorescence and single-molecule-magnet properties, *Inorganic Chemistry*, 48 (2009) 8051-8053.
- [229] K. Griffiths, J. Mayans, M. A. Shipman, G. J. Tizzard, S. J. Coles, B. A. Blight, A. Escuer, G. E. Kostakis, Four new families of polynuclear Zn-Ln coordination clusters.

Synthetic, topological, magnetic, and luminescent aspects, *Crystal Growth & Design*, 17 (2017) 1524-1538.

[230] X. Lü, W. Bi, W. Chai, J. Song, J. Meng, W. Y. Wong, W. K. Wong, R. A. Jones, Tetranuclear NIR luminescent Schiff-base Zn-Nd complexes, *New Journal of Chemistry*, 32 (2008) 127-131.

[231] S. Zhao, X. Lü, A. Hou, W. Y. Wong, W. K. Wong, X. Yang, R. A. Jones, Heteronuclear trimetallic and 1D polymeric 3d-4f Schiff base complexes with OCN^- and SCN^- ligands, *Dalton Transactions*, (2009) 9595-9602.

[232] X. P. Yang, R. A. Jones, W. K. Wong, V. Lynch, M. M. Oye, A. L. Holmes, Design and synthesis of a near infra-red luminescent hexanuclear Zn-Nd prism, *Chemical Communications*, (2006) 1836-1838.

[233] S. Andleeb, Imtiaz-ud-Din, M.K. Rauf, S. S. Azam, I. U. Haq, M. N. Tahir, S. Ahmad, Bioactive heteroleptic bismuth(V) complexes: synthesis, structural analysis and binding pattern validation, *Applied Organometallic Chemistry*, 33 (2019) e5061.

[234] A. B. Pangborn, M. A. Giardello, R. H. Grubbs, R. K. Rosen, F. J. Timmers, Safe and convenient procedure for solvent purification, *Organometallics*, 15 (1996) 1518-1520.

[235] A. Bruker, A. Bruker, Inc., 5465 East Cheryl Parkway, Madison, WI, 53711 (2007).

[236] G. Sheldrick, SHELXS-97 *Acta Crystallogr, Sect. A*, 46 (1990) 467.

[237] T. Fatima, Imtiaz-ud-Din, A. Akbar, M. S. Anwar, M. N. Tahir, Six new dinuclear Schiff base complexes of Cu(II)/Ln(III) system: Synthesis, characterization and magnetic studies, *Journal of Molecular Structure*, 1184 (2019) 462-467.

[238] T. Fatima, Imtiaz-ud-Din, M. K. Rauf, M. S. Anwar, A. Raheel, M. N. Tahir, M. Ashfaq, Synthesis, characterization and magnetic studies for a series of compounds having a trinuclear bimetallic $\text{Cu}_2(\text{II})/\text{Ln}(\text{III})$ system, *Polyhedron*, 186 (2020) 114605.

- [239] H.A. Mannan, I. Ahmed, I. Hussain, M. Jamil, B. Miza, Antibacterial activity and brine shrimp toxicity of *Artemisia dubia* extract, *Pakistan Journal of Botany*, 44 (2012) 1487-1490.
- [240] M. Ahmed, H. Fatima, M. Qasim, B. Gul, Polarity directed optimization of phytochemical and in vitro biological potential of an indigenous folklore: *Quercus dilatata* Lindl. ex Royle, *BMC Complement Altern. Med.*, 17 (2017) 386.
- [241] S.S. Zahra, M. Ahmed, M. Qasim, B. Gul, M. Zia, B. Mirza, I.-u. Haq, Polarity based characterization of biologically active extracts of *Ajuga bracteosa* Wall. ex Benth. and RP-HPLC analysis, *BMC Complementary and Alternative Medicine*, 17 (2017) 1-16.
- [242] H. Fatima, K. Khan, M. Zia, T. Ur Rehman, B. Mirza, I. U. Haq, Extraction optimization of medicinally important metabolites from *Datura innoxia* Mill.: an in vitro biological and phytochemical investigation, *BMC Complementary and Alternative Medicine*, 15 (2015) 376.
- [243] S. Wajid Abbasi, S. Sikander Azam, Structural Characterization of Alpha-methylacyl-CoA Racemase: Comparative Structural Modeling, Molecular Docking and Dynamic Simulations Studies, *Current Cancer Drug Targets*, 15 (2015) 822-835.
- [244] S. S. Azam, A. Abro, F. Tanvir, N. Parvaiz, Identification of unique binding site and molecular docking studies for structurally diverse inhibitors, *Medicinal Chemistry Research*, 23 (2014) 3765-3783.
- [245] J. Stamos, M. X. Sliwowski, C. Eigenbrot, Structure of the epidermal growth factor receptor kinase domain alone and in complex with a 4-anilinoquinazoline inhibitor, *Journal of Biological Chemistry*, 277 (2002) 46265-46272.
- [246] A. B. Casey, C. E. Canal, Classics in chemical neuroscience: aripiprazole, *ACS Chemical Neuroscience*, 8 (2017) 1135-1146.

- [247] N. C. Ha, S. T. Oh, J. Y. Sung, K. A. Cha, M. H. Lee, B. H. Oh, Supramolecular assembly and acid resistance of *Helicobacter pylori* urease, *Nature Structural Biology*, 8 (2001) 505-509.
- [248] J. H. Lii, N. L. Allinger, Directional hydrogen bonding in the MM3 force field: II, *Journal of Computational Chemistry*, 19 (1998) 1001-1016.
- [249] S. T. Baby, S. Sharma, S. Enaganti, P. R. Cherian, Molecular docking and pharmacophore studies of heterocyclic compounds as Heat shock protein 90 (Hsp90) Inhibitors, *Bioinformation*, 12 (2016) 149.
- [250] S. Saeed, A. Iqbal, A. Iqbal, Photoinduced charge carrier dynamics in a ZnSe quantum dot-attached CdTe system, *Proceedings of the Royal Society A*, 476 (2020) 20190616.
- [251] Z. Siddique, J. L. Payne, J. T. Irvine, L. K. Jagadamma, Z. Akhter, I. D. Samuel, A. Iqbal, Effect of halide-mixing on tolerance factor and charge-carrier dynamics in (CH₃NH₃PbBr_{3-x}Cl_x) perovskites powders, *Journal of Materials Science: Materials in Electronics*, 31 (2020) 19415-19428.
- [252] D. Evans, A new type of magnetic balance, *Journal of Physics E: Scientific Instruments*, 7 (1974) 247.
- [253] A. Zafar, Imtiaz-ud-Din, S. Ahmed, D. K. Bucar, M. N. Tahir, R. Palgrave, *New Journal of Chemistry*, (2021).
- [254] G. A. Bain, J. F. Berry, Diamagnetic corrections and Pascal's constants, *Journal of Chemical Education*, 85 (2008) 532.
- [255] T. Fatima, Imtiaz-ud-Din, M. K. Rauf, M. S. Anwar, A. Raheel, M. N. Tahir, M. Ashfaq, Synthesis, characterization and magnetic studies for a series of compounds having a trinuclear bimetallic Cu₂(II)/Ln(III) system, *Polyhedron*, 186 (2020) 114605.

- [256] J. O. Adeyemi, D. C. Onwudiwe, Organotin(IV) dithiocarbamate complexes: Chemistry and biological activity, *Molecules*, 23 (2018) 2571.
- [257] A. Raheel, Imtiaz-ud-Din, S. Andleeb, S. Ramadan, M. N. Tahir, Synthesis and structural characterization of new bioactive ligands and their Bi(III) derivatives, *Applied Organometallic Chemistry*, 31 (2017) e3632.
- [258] V. Sharutin, I. Egorova, O. Sharutina, T. Ivanenko, Y. V. Gatilov, N. Adonin, V. Starichenko, Synthesis and structure of triphenylbismuth bis (fluorobenzoates), *Russian Journal of Coordination Chemistry*, 29 (2003) 462-467.
- [259] Z. Wang, W. Feng, P. Su, H. Liu, Z. Zhang, Y. Zhang, T. Miao, X. Lü, D. Fang, W.-K. Wong, Hetero-trinuclear near-infrared (NIR) luminescent $ZnLn_2$ ($Ln = Nd, Yb$ or Er) complexes based on monomer ZnL Schiff-base precursor and o-vanillin, *Inorganic Chemistry Communications*, 36 (2013) 11-13.
- [260] N. Dharmaraj, P. Viswanathamurthi, K. Natarajan, Ruthenium(II) complexes containing bidentate Schiff bases and their antifungal activity, *Transition Metal Chemistry*, 26 (2001) 105-109.
- [261] A. A. Al-Amiery, A. A. H. Kadhum, A. B. Mohamad, Antifungal and antioxidant activities of pyrrolidone thiosemicarbazone complexes, *Bioinorganic Chemistry and Applications*, 2012 (2012).
- [262] R. Nagarajan, S. I. Mehtaa, S. R. Naik, W. Fabry, Preparation and activity of some novel organo-metallic complexes against *Helicobacter pylori*, *Arzneimittelforschung*, 49 (1999) 951-954.
- [263] M. Mehmood, Imtiaz-ud-Din, M.N. Tahir, I. U. Haq, S. S. Zahra, Synthetic stratagem, characterization and biocidal applications of triorganotin(IV) complexes derived from hydrazide/hydrazone analogues, *Inorganica Chimica Acta*, 486 (2019) 387-394.

- [264] R. F. de Freitas, M. Schapira, A systematic analysis of atomic protein–ligand interactions in the PDB, *Medchemcomm*, 8 (2017) 1970-1981.
- [265] S. Gross, R. Rahal, N. Stransky, C. Lengauer, K. P. Hoeflich, Targeting cancer with kinase inhibitors, *The Journal of clinical investigation*, 125 (2015) 1780-1789.
- [266] J. Ruiz, G. Lorusso, M. Evangelisti, E. K. Brechin, S. J. Pope, E. Colacio, Closely-related $Zn^{II}_2Ln^{III}_2$ complexes ($Ln^{III} = Gd, Yb$) with either magnetic refrigerant or luminescent single-molecule magnet properties, *Inorganic Chemistry*, 53 (2014) 3586-3594.
- [267] M. Andruh, E. Bakalbassis, O. Kahn, J. C. Trombe, P. Porcher, Structure, spectroscopic and magnetic properties of rare earth metal(III) derivatives with the 2-formyl-4-methyl-6-(N-(2-pyridylethyl)formimidoyl) phenol ligand, *Inorganic Chemistry*, 32 (1993) 1616-1622.

Conclusions

Twenty five new bioactive triarylbi­smuth(V) carboxylates (**1-25**) and twenty new heteronuclear 3d/4f metal complexes (**26-45**) were successfully synthesized and characterized by FT-IR, NMR spectroscopy as well as single crystal X-ray diffraction analysis. The X-ray structure for **19** indicated anisobidentate nature of carboxylate functionality that ultimately yielded rare hexa-coordinated bismuth compound, whereas, in case of **7**, **17** and **18**, carboxylates ligated in monodentate fashion. The X-ray diffraction data for **45** revealed that Zn(II) is encapsulated between two amine and two phenolate donors, became a preorganized moiety used to sandwich the Dy(III) ion between the four phenolate oxygens, forming stable 3d/4f/3d complex. The data show good to significant antibacterial and antifungal activity for some of the synthesized compounds with MIC ranging from 50-3.125 $\mu\text{g/mL}$, whereas complex **2** displays exceptional percentage alpha amylase inhibition of 62.36 $\mu\text{g/mL}$. The GOLD fitness scores for **5**, **7** and **20** against EGFR tyrosine kinase, human pancreatic alpha amylase and H. pylori urease are 64.09, 62.65 and 56.30 respectively, which placed them as “lead compounds” in their respective biological domains. Moreover, the preliminary screening data manifest that tritolylbismuth derivatives behave as potent enzyme inhibitors whereas, triphenylbismuth carboxylates as antimicrobial agents, however further evaluation needs to be carried out to arrive at conclusion in future research projects. The data obtained from the computational and experimental investigations propose that the organobismuth carboxylates exhibit promising biocidal activity that could provide a clue to the development of even more potent antimicrobial agents besides improving their anti-diabetic, anti-cancer, and gastrointestinal properties by altering/modifying their structural motifs. The room temperature $\chi_m T$ and μ_{eff} values for the complexes were found in the ranges of 0.18-15.37 $\text{emu}\cdot\text{mole}^{-1}\cdot\text{K}$ and 1.20-11.05 μ_B , respectively. The magnetic susceptibility studies of these compounds confirmed their paramagnetic nature. The recent approach will provide an impetus to outline magnetically strong photoluminescent materials with the advantage of magnetic interactions between Ln^{III} ions in a heterometallic d-f system.

Future Plan

Present study provide extensive research on main group, transition metal complexes, we still think that we have able to add few drops of knowledge in the pool of scientific research, and still more work is needed in this domain. Following are few suggestion that we will considered in future:

- 1) Some more organobismuth(V) complexes are aimed to be prepared by altering phenyl and tolyl moieties with electron withdrawing groups i.e., $-CF_3$ and $-F$ moieties, in order to widen their scope in biological domain.
- 2) Some more compounds are needed to be synthesized having bismuth incorporated bi-compartmental Schiff base moieties by optimizing reaction conditions.
- 3) Heterodi-/trinuclear 3d/4f complex showed exceptional magnetic properties, keeping this in mind we may investigate their magnetic susceptibilities at variable temperatures, in order to evaluate their SMM behavior.

List of Publications

1. **Mehmood, M.**, Imtiaz-ud-Din, Abbas, S., Azam, Zahra, S. S., Tahir, M. N., Pervaiz, N., & A. Tameez-ud-Din, (2020). Bioactive heteroleptic Bismuth(V) carboxylates: synthetic Stratagem, characterization and binding pattern validation. *Journal of Organometallic Chemistry*, 921, 121357.
2. **Mehmood, M.**, Imtiaz-ud-Din, Zafar, A., Iqbal, A., Mukhtar, M., & Tahir, M. N. (2022). Molecular architecture, characterization, and applications of homoleptic heteronuclear 3d/4f metals' complexes derived from bi-compartmental Schiff-base. *Journal of Molecular Structure*, 134547.
3. Abbas, S, Imtiaz-ud-Din, **Mehmood, M**, Rauf, M. K., Azam, Zahra, S. S., Haq, I. U, Tahir, M. N., & Pervaiz, N. (2021). Synthesis, structural characterization, and molecular docking studies of bioactive bismuth(III) complexes with substituted hydrazones. *Journal of Molecular Structure*, 1230, 129870.
4. **Mehmood, M**, Imtiaz-ud-Din, Tahir, M. N., Haq, I. U, & Zahra, S. S. (2019). Synthetic stratagem, characterization and biocidal applications of triorganotin(IV) complexes derived from hydrazide/hydrazone analogues. *Inorganica Chimica Acta*, 486, 387-394.
5. **Mehmood, M**, Imtiaz-ud-Din, Raheel, A, Haq, I. U., & Tahir, M. N. (2020). Preparation, structural elucidation and biocidal applications of trimethyltin(IV) complexes derived from substituted carboxylic acids. *Heliyon*, 6(10), e05156.
6. Abbas, S, Imtiaz-ud-Din, **Mehmood, M**, Raheel, A., Ayub, R, Zahid, M, & Tahir, M. N. (2021). Synthesis and Structural Characterization of Bioactive Ferrocenyl Substituted Hydrazones. *Russian Journal of Coordination Chemistry*, 47(12), 891-902.

Appendix

Table-A1. Crystallographic data and refinement details for (7, 17)

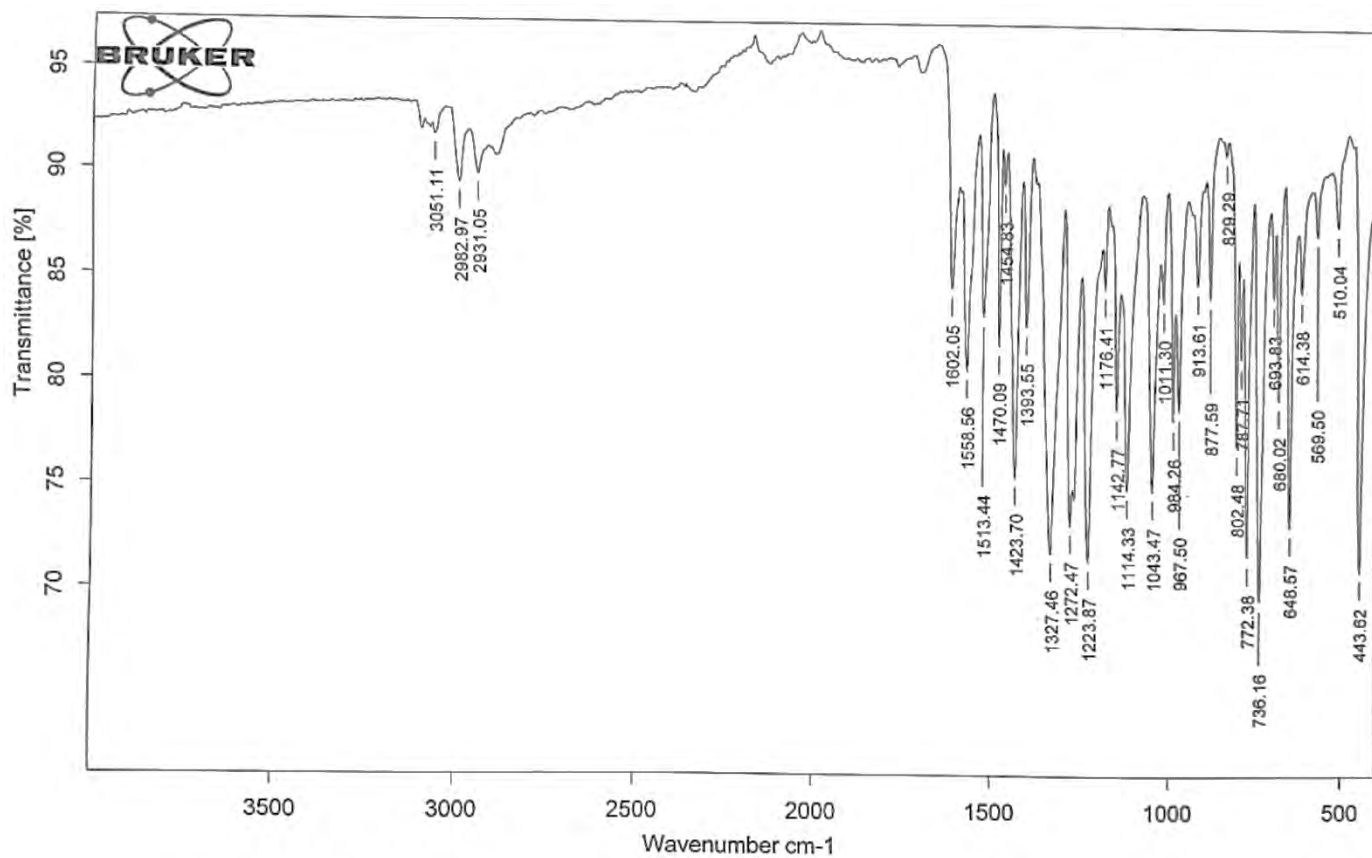
Identification Codes	7	17
Empirical formula	C ₃₄ H ₂₉ O ₄ Bi	C ₄₃ H ₃₅ O ₄ Bi
Formula weight	710.55	824.69
Crystal system	Triclinic	Monoclinic
Temperature/K	296(2)	296(2)
Space group	P-1	P2 ₁ /n
α/°	99.948(4)	90
β/°	103.612(4)	100.520(3)
γ/°	102.951(5)	90
a/Å	8.7736(16)	12.9031(9)
b/Å	10.672(2)	12.2299(9)
c/Å	16.635(3)	22.6797(18)
Z	2	4
F(000)	696.0	1632.0
Volume/Å³	1432.9(4)	3518.8(5)
μ/mm⁻¹	6.189	5.052
Crystal size/mm³	0.400×0.320×0.160	0.420×0.230×0.180
2θ range for data collection/°	5.29 - 56.344	4.9-53.9
Index ranges	-11 ≤ h ≤ 11, -14 ≤ k ≤ 14, -16 ≤ l ≤ 21	-16 ≤ h ≤ 15, -14 ≤ k ≤ 15, -28 ≤ l ≤ 26
Independent reflections	6711	7671
Reflections collected	18133	23550
Goodness of Fit	1.022	0.968
R_{int}	6.189	0.0571
Final R indexes [I ≥ 2σ (I)]	R ₁ = 0.0365, wR ₂ = 0.0878	R ₁ = 0.0354, wR ₂ = 0.0685
Final R indexes [all data]	R ₁ = 0.0476, wR ₂ = 0.0931	R ₁ = 0.0643, wR ₂ = 0.0787

Table-A2. Crystallographic data and refinement details for **(18, 19)**

Identification Codes	18	19
Empirical formula	C ₃₅ H ₂₉ Cl ₂ O ₄ Bi	C ₃₇ H ₃₅ O ₄ Bi
Formula weight	793.46	752.63
Crystal system	Hexagonal	Monoclinic
Temperature/K	296(2)	296(2)
Space group	<i>P</i> 6 ₅	<i>P</i> 2 ₁ / <i>c</i>
$\alpha/^\circ$	90	90
$\beta/^\circ$	90	105.089(9)
$\gamma/^\circ$	120	90
a/Å	33.7638(18)	14.412(3)
b/Å	33.7638(18)	10.6492(19)
c/Å	10.9050 (6)	22.286(3)
Z	12	4
F(000)	4656.0	1488.0
Volume/Å³	10766.1(13)	3302.5(11)
μ/mm^{-1}	5.094	5.375
2θ range for data collection/°	4.446 - 55.786	4.816 - 55.92
Index ranges	- 44 ≤ h ≤ 44, - 44 ≤ k ≤ 28, - 11 ≤ l ≤ 14	-18 ≤ h ≤ 18, -14 ≤ k ≤ 12, -29 ≤ l ≤ 27
Independent reflections	15405	7879
Reflections collected	46035	22673
Goodness of Fit	0.924	1.014
R_{int}	0.0971	0.0528
Final R indexes [all data]	R ₁ = 0.1304, wR ₂ = 0.1228	R ₁ = 0.0628, wR ₂ = 0.0807
Final R indexes [I ≥ 2σ (I)]	R ₁ = 0.0524, wR ₂ = 0.0988	R ₁ = 0.0349, wR ₂ = 0.0708

Table-A3: Crystallographic data and refinement details for (27, 45)

Identification Codes	27	45
Empirical formula	C ₁₈ H ₂₀ N ₅ O ₁₄ ZnNd	C ₄₂ H ₃₅ N ₈ O ₁₅ Zn ₂ Dy
Formula weight	740.00	1185.02
Crystal system	Monoclinic	Triclinic
Temperature/K	296(2)	296(2)
Space group	P2 ₁ /c	<i>P</i> -1
α/°	90	95.670 (9)
β/°	105.86(10)	103.536 (8)
γ/°	90	116.472 (6)
a/Å	9.17(4)	11.334 (3)
b/Å	19.24(9)	11.958 (3)
c/Å	15.04(8)	18.936 (6)
F(000)	1460.0	1178.0
Volume/Å³	2555.1(2)	2171.8 (10)
μ/mm⁻¹	3.027	2.88
Crystal size/mm³	0.38×0.26×0.2	0.38×0.34×0.22
Z	4	2
2θ range for data collection/°	5.078 to 55.808	2.274 to 55.58
Index ranges	-11 ≤ h ≤ 12, -21 ≤ k ≤ 25, -19 ≤ l ≤ 19	-14 ≤ h ≤ 14, -15 ≤ k ≤ 15, -24 ≤ l ≤ 24
Independent reflections	6069 [R _{sigma} = 0.0391]	9299 [R _{sigma} = 0.1607]
Goodness of Fit	1.043	1.125
Reflections collected	26713	9299
Final R indexes [I ≥ 2σ (I)]	R ₁ = 0.0343, wR ₂ = 0.0815	R ₁ = 0.1009, wR ₂ = 0.2425
Final R indexes [all data]	R ₁ = 0.0441, wR ₂ = 0.0888	R ₁ = 0.1685, wR ₂ = 0.2801



Sample Name: PC 8

DR

Figure 3.21 FT-IR spectrum for (8)

DR.IMTIAZ-UD-DIN/MEHWISH/PC8_13CNMR_CDCL3



Current Data Parameters
NAME PC8_13CNMR_CDCL3
EXPNO 1
PROCNO 1

F2 - Acquisition Parameters
Date_ 20181204
Time_ 12.08
INSTRUM spect
PROBHD 5 mm BBO BB-1H
PULPROG zgpg30
TD 35968
SOLVENT CDCL3
NS 512
DS 0
SWH 17985.611 Hz
FIDRES 0.500045 Hz
AQ 0.9999604 sec
RG 6502
LW 27.800 usec
DE 6.00 usec
TE 292.5 K
D1 2.00000000 sec
d11 0.03000000 sec
DELTA 1.89999998 sec
TD0 1

===== CHANNEL f1 =====
NUC1 13C
P1 6.00 usec
PL1 -5.00 dB
SFO1 75.4752953 MHz

===== CHANNEL f2 =====
CPDPRG2 waltz16
NUC2 1H
PCPD2 80.00 usec
PL2 2.00 dB
PL12 20.98 dB
PL13 20.00 dB
SFO2 300.1312005 MHz

F2 - Processing parameters
SI 32768
SF 75.4677450 MHz
WDW EM
SSB 0
LB 1.00 Hz
GB 0
PC 1.40

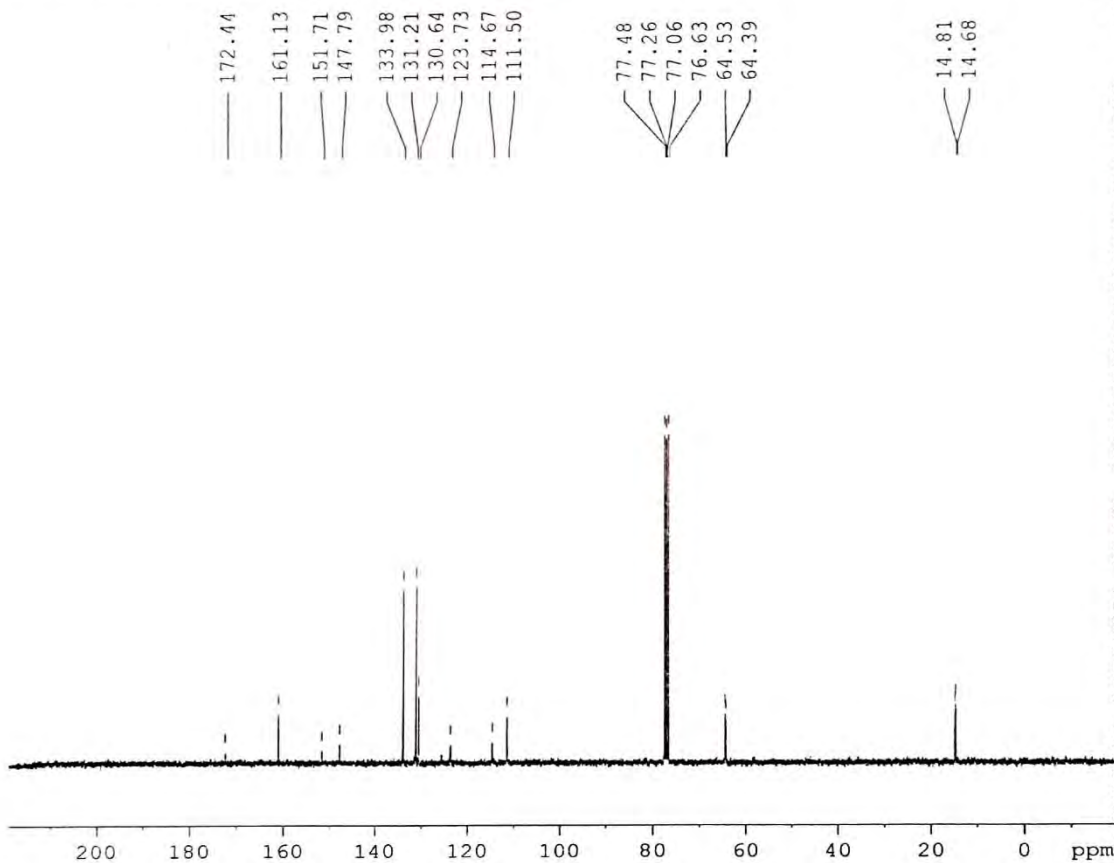
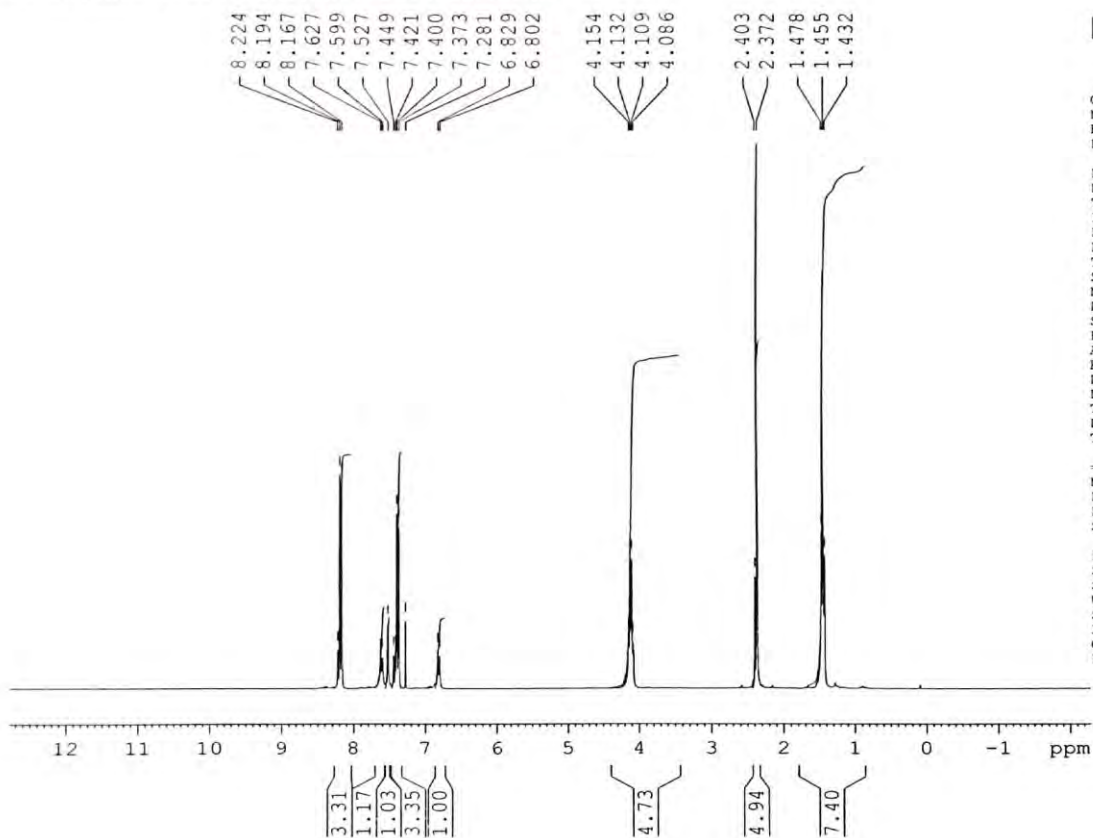


Figure 3.22 ¹³C NMR spectrum for (8)

DR.IMTIAZ-UD-DIN/MEHWISH/TC8_1HNMR_CDCL3



Current Data Parameters
NAME TC8_1HNMR_CDCL3
EXPNO 1
PROCNO 1

F2 - Acquisition Parameters
Date_ 20190726
Time 14.56
INSTRUM spect
PROBHD 5 mm BBO BB-1H
PULPROG zg30
TD 65536
SOLVENT CDCL3
NS 8
DS 0
SWH 6172.839 Hz
FIDRES 0.094190 Hz
AQ 5.3084660 sec
RG 143.7
DW 81.000 usec
DE 6.00 usec
TE 292.9 K
D1 1.00000000 sec
TDO 1

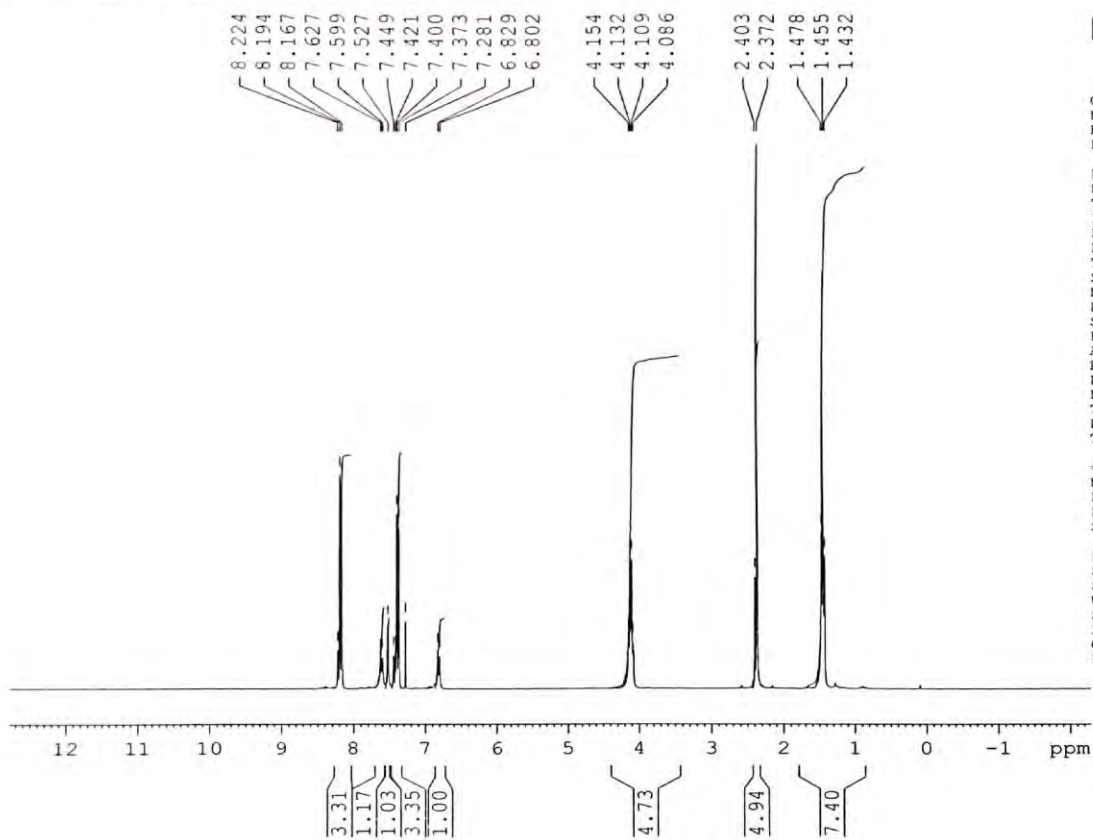
----- CHANNEL f1 -----
NUC1 1H
P1 9.00 usec
PL1 2.00 dB
SFO1 300.1318534 MHz

F2 - Processing parameters
SI 32768
SF 300.1300000 MHz
WDW EM
SSB 0
LB 0.30 Hz
GB 0
PC 1.00



Figure 3.23 ¹³CNMR spectrum for (8)

DR.IMTIAZ-UD-DIN/MEHWISH/TC8_1HNMR_CDCL3



Current Data Parameters
NAME TC8_1HNMR_CDCL3
EXPNO 1
PROCNO 1

F2 - Acquisition Parameters
Date_ 20190726
Time 14.56
INSTRUM spect
PROBHD 5 mm BBO BB-1H
PULPROG zg30
TD 65536
SOLVENT CDCL3
NS 8
DS 0
SWH 6172.839 Hz
FIDRES 0.094190 Hz
AQ 5.3084660 sec
RG 143.7
DW 81.000 usec
DE 6.00 usec
TE 292.9 K
D1 1.00000000 sec
TD0 1

===== CHANNEL f1 =====
NUC1 1H
P1 9.00 usec
PL1 2.00 dB
SFO1 300.1318534 MHz

F2 - Processing parameters
SI 32768
SF 300.1300000 MHz
WDW EM
SSB 0
LB 0.30 Hz
GB 0
PC 1.00



Figure 3.24 ¹H NMR spectrum for (20)

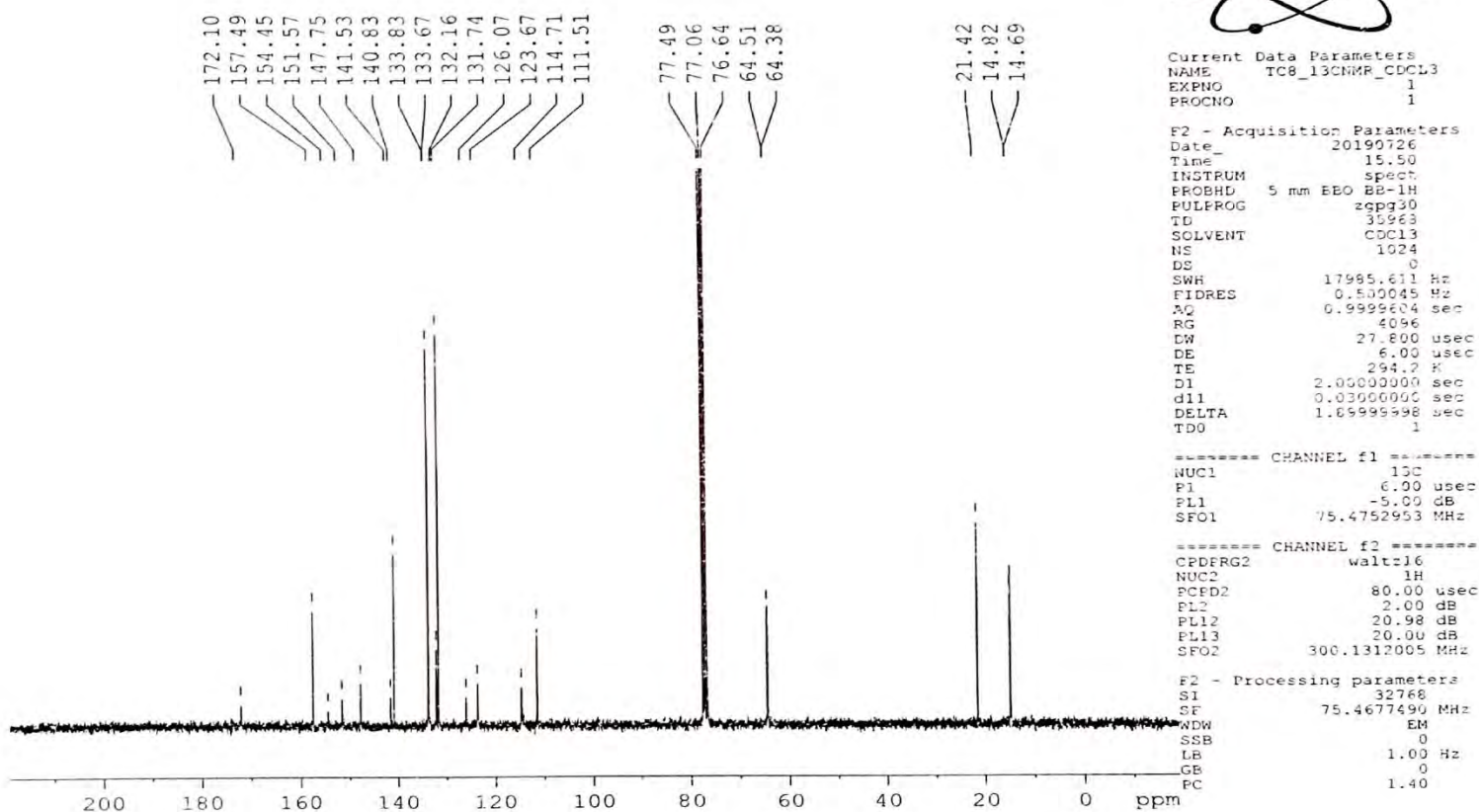
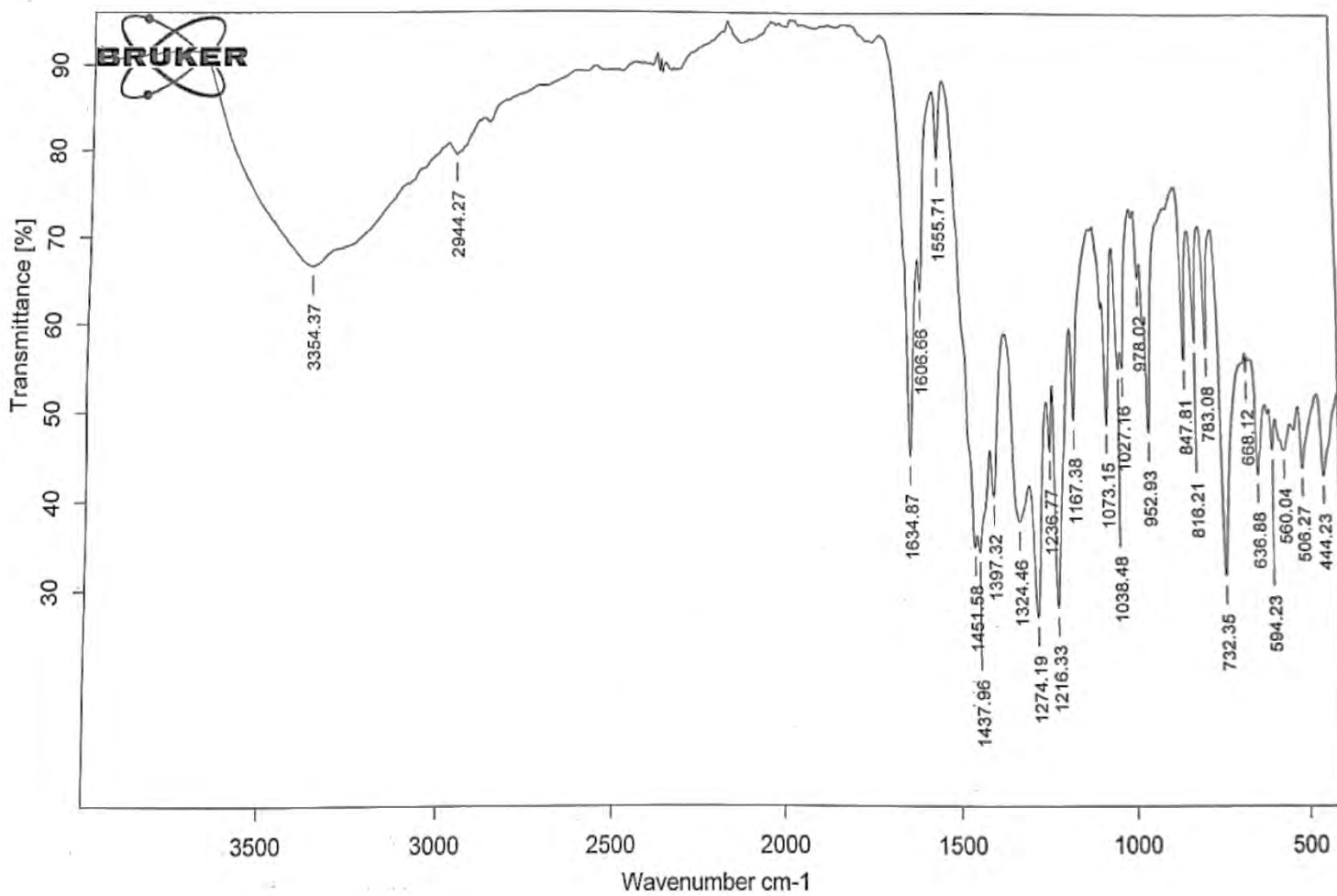
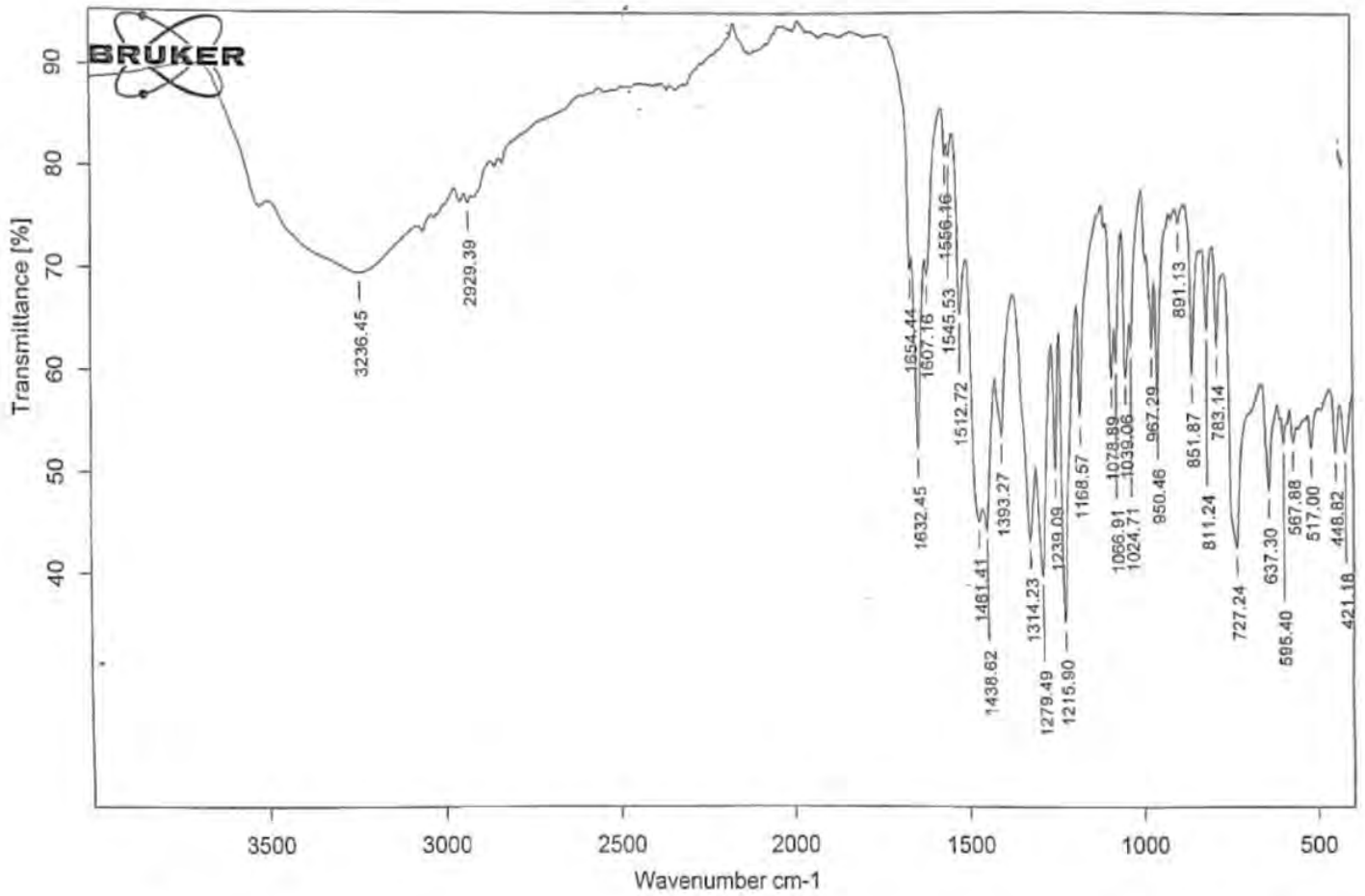


Figure 3.25 ¹³CNMR spectrum for (20)



Sample Name: 5

Figure 3.26 FT-IR spectrum for (L4)



Sample Name: 3

Figure 3.27 FT-IR spectrum for (30)

Turnitin Originality Report

Synthetic Stratagem, Characterization and Potential Applications of Main group/Heteronuclear Transition Metal Complexes derived from N, O containing Ligands by Mehwish Mehmood .

From CL QAU (DRSML)

- Processed on 18-May-2022 08:29 PKT
- ID: 1838817202
- Word Count: 22498

Similarity Index

13%

Similarity by Source

Internet Sources:

7%

Publications:

11%

Student Papers:

2%

sources:

1

1% match (publications)

[Wen-Kui Dong, Jian-Chun Ma, Li-Chun Zhu, Yin-Xia Sun, Sunday Folaranmi Akogun, Yang Zhang. "A Series of Heteromultinuclear Zinc\(II\)–Lanthanide\(III\) Complexes Based on 3-MeOsalamo: Syntheses, Structural Characterizations, and Luminescent Properties", Crystal Growth & Design, 2016](#)

2

1% match (publications)

[Sohaila Andleeb, Imtiaz-ud-Din, Muhammad Khawar Rauf, Syed Sikander Azam et al. "Bioactive Heteroleptic Bismuth\(V\) Complexes: Synthesis, Structural Analysis and Binding Pattern Validation", Applied Organometallic Chemistry, 2019](#)

3

1% match (Internet from 11-Mar-2022)

<http://mzuir.inflibnet.ac.in/bitstream/123456789/1103/1/JAYANTA%20DOWARAH,%20Chem.pdf>

4

< 1% match (Internet from 11-Oct-2020)

<https://bmccomplementmedtherapies.biomedcentral.com/articles/10.1186/s12906-017-1951-5>

5

< 1% match (Internet from 06-Feb-2020)

<https://bmccomplementmedtherapies.biomedcentral.com/articles/10.1186/s12906-017-1894-x>

6

< 1% match (student papers from 02-Apr-2018)

[Submitted to Higher Education Commission Pakistan on 2018-04-02](#)

7

< 1% match (student papers from 22-Jan-2013)

[Submitted to Higher Education Commission Pakistan on 2013-01-22](#)